SANDIA REPORT

SAND98–1719
Unlimited Release
Printed August 1998

Development of the SEAtrace™ Barrier Verification and Validation Technology Final Report

Sandra Dalvit Dunn, William Lowry, Robert Walsh, D. V. Rao, Cecelia Williams

Prepared by
Sandia National Laboratories
Albuquerque, New Mexico 87185 and Livermore, California 94550

Sandia is a multiprogram laboratory operated by Sandia Corporation, a Lockheed Martin Company, for the United States Department of Energy under Contract DE-AC04-94AL85000.

Sandia National Laboratories

Issued by Sandia National Laboratories, operated for the United States Department of Energy by Sandia Corporation.

Available to DOE and DOE contractors from
Office of Scientific and Technical Information
P.O. Box 62
Oak Ridge, TN 37831

Prices available from (615) 576-8401, FTS 626-8401

Available to the public from
National Technical Information Service
U.S. Department of Commerce
5285 Port Royal Rd
Springfield, VA 22161

NTIS price codes
Printed copy: A07
Microfiche copy: A01

DISCLAIMER

Portions of this document may be illegible in electronic image products. Images are produced from the best available original document.

SAND98-1719
Unlimited Release
Printed August 1998

DEVELOPMENT OF THE SEAtrace™ BARRIER VERIFICATION AND VALIDATION TECHNOLOGY FINAL REPORT

Sandra Dalvit Dunn, William Lowry, Robert Walsh, and D.V. Rao
Science and Engineering Associates
3205 Richards Lane, Suite A
Santa Fe, NM 87505

Cecelia Williams
Underground Storage Technology Department
Sandia National Laboratories
P.O. Box 5800
Albuquerque, NM 87185-0706

ABSTRACT

In-situ barrier emplacement techniques and materials for the containment of high-risk contaminants in soils are currently being developed by the Department of Energy (DOE). These include slurry walls, grout barriers, cryogenic barriers, and other forms of impermeable barriers. Because of their relatively high cost, the barriers are intended to be used in cases where the risk is too great to remove the contaminants, the contaminants are too difficult to remove with current technologies, or the potential movement of the contaminants to the water table is so high that immediate action needs to be taken to reduce health risks. Consequently, barriers are primarily intended for use in high-risk sites where few viable alternatives exist to stop the movement of contaminants in the near term. Assessing the integrity of the barrier once it is emplaced, and during its anticipated life, is a very difficult but necessary requirement. Existing surface-based and borehole geophysical techniques do not provide the degree of resolution required to assure the formation of an integral in-situ barrier.

Science and Engineering Associates, Inc., (SEA) and Sandia National Laboratories (SNL) have developed a quantitative subsurface barrier assessment system using gaseous tracers in support of the Subsurface Contaminants Focus Area barrier technology program. Called SEAtrace™, this system integrates an autonomous, multi-point soil vapor sampling and analysis system with a global optimization modeling methodology to locate and size barrier breaches in real time. SEAtrace™ is applicable to impermeable barrier emplacements above the water table. It provides a conservative assessment of barrier integrity after emplacement, as well as a long term integrity monitoring function.

The methodology for the global optimization code was completed and a prototype code written using simplifying assumptions. Preliminary modeling work to validate the code assumptions were performed using the T2VOC numerical code. A multi-point field sampling system was built to take soil gas samples and analyze for tracer gas concentration. The tracer concentration histories were used in the global optimization code to locate and size barrier breaches. SEAtrace™ was consistently able to detect and locate leaks, even under very adverse conditions. The system was able to locate the leak to within 0.75 m of the actual value, and was able to determine the size of the leak to within 0.15 m.

ACKNOWLEDGEMENTS

The SEAtrace development and field scale demonstrations were funded by the Office of Science and Technology (OST) under U.S. Department of Energy (U.S. DOE) contract number DE-AC04-94AL85000.

The authors wish to acknowledge the contributions made by the following individuals in support of this work:

Scott McMullen (DOE/Savannah River Site) for his confidence in the SEAtrace project and his vision in facilitating continued funding for development, demonstration, and deployment.

Tom Colina and Jerry Stockton (Science and Engineering Associates, Inc.) and for their laboratory and field support.

Bruce Reavis and Gerald Reynolds (Sandia National Laboratories) for their field support from site preparation, sampling, and site reclamation.

Patti Comiskey, Dianne Padilla, and Nedra Raney (Sandia National Laboratories) for their contracting, administrative, and secretarial support.

And finally to Jennifer Nelson and George Allen (Sandia National Laboratories) for their staunch support of the project and their efforts to secure funding to take an idea from development to deployment.

Intentionally Left Blank

CONTENTS

Figures

Tables

Intentionally Left Blank

I. INTRODUCTION

In-situ barrier materials and designs are being developed for containment of high-risk contamination as an alternative to immediate removal or remediation. Injected grouts, waxes, polymers, slurries, and freezing of soil moisture are barrier techniques currently under development and/or being demonstrated. The intent of these designs is to prevent the movement of contaminants in either the liquid or vapor phase, essentially buying time until remediation can be implemented or until the contaminant depletes naturally. Quantifying the integrity of in-situ barriers is difficult, but important. A very small breach in a barrier can leak significant amounts of contaminant into the surrounding medium. The need exists for a minimally intrusive, yet quantifiable, method for assessment of a barrier's integrity after emplacement, and monitoring of the barrier's performance over its lifetime.

While surface-based and borehole geophysical techniques such as seismic and electromagnetic surveys, can detect the presence of emplaced barrier materials, their resolution is typically inadequate for leak detection. Nuclear borehole logging is capable of greater resolution, but because of its limited penetration would require an excessive number of boreholes in close proximity to the barrier, rendering it impractical for barrier assessment (Jeiser, H., 1994). Tracer measurements, on the other hand, have been suggested as a viable assessment technique given the state of the gas analysis art (Jeiser, H., 1994 and Betsill, J. D. and Gruebel, 1995). The challenge with the use of gaseous tracers is to develop a system which automatically assesses barrier integrity in real time, to avoid time consuming and expensive numerical back-calculations.

Science and Engineering Associates, Inc. (SEA) and Sandia National Laboratories (SNL) have developed a methodology to locate and size leaks in subsurface barriers. A simple subscale field experiment was used to validate that methodology. The result of this work is the SEAtrace™ system.

The SEAtrace™ system uses gaseous tracer injection, in-field real-time monitoring, and real time data analysis to evaluate barrier integrity in the unsaturated zone. The design has the following features:

- The approach is conservative in that it measures vapor leaks in a containment system whose greatest risk is posed by liquid leaks;
- It is applicable to any impermeable barrier emplacement technology in the unsaturated zone;
- The methodology will quantify both the leak location and size;
- It uses readily available, non-toxic, inexpensive, nonhazardous gaseous tracers;
- The vapor injection and sampling points can be emplaced by direct push techniques (such as Geoprobes) or the rapid ResonantSonic™ technique, avoiding excessive drilling costs and secondary waste generation;

- The methodology for unfolding the soil gas analysis data uses a rigorous global optimization technique which accommodates uncertainties in the measured concentration histories and site characteristics;
- The system can also provide long term monitoring of contaminant soil gases for surveillance of the containment system's performance over time.

This report documents the initial development of the SEAtrace™ system and presents results of the a proof-of-concept field experiment.

II. DESCRIPTION OF THE SEAtrace™ SYSTEM

The SEAtrace™ barrier monitoring system is based on the transport process of binary gaseous diffusion in porous media. Diffusion is an attractive process to utilize for leak detection because the tracer concentration histories measured at locations distant from the source are highly sensitive to both the size of the breach and the distance from the leak source. This sensitivity allows an effective global optimization modeling methodology to be applied to recorded concentration histories at several points around the barrier. The technique, known as simulated annealing, iterates to a leak geometry and location by minimizing errors in the transport calculations. It is a rigorous generalized methodology which can accommodate real world uncertainties.

A schematic of a SEAtrace™ system installation is shown in Figure 1 and an operational flow chart is given in Figure 2. SEAtrace™ can be divided into two distinct functional components: the monitoring system and the analysis code.

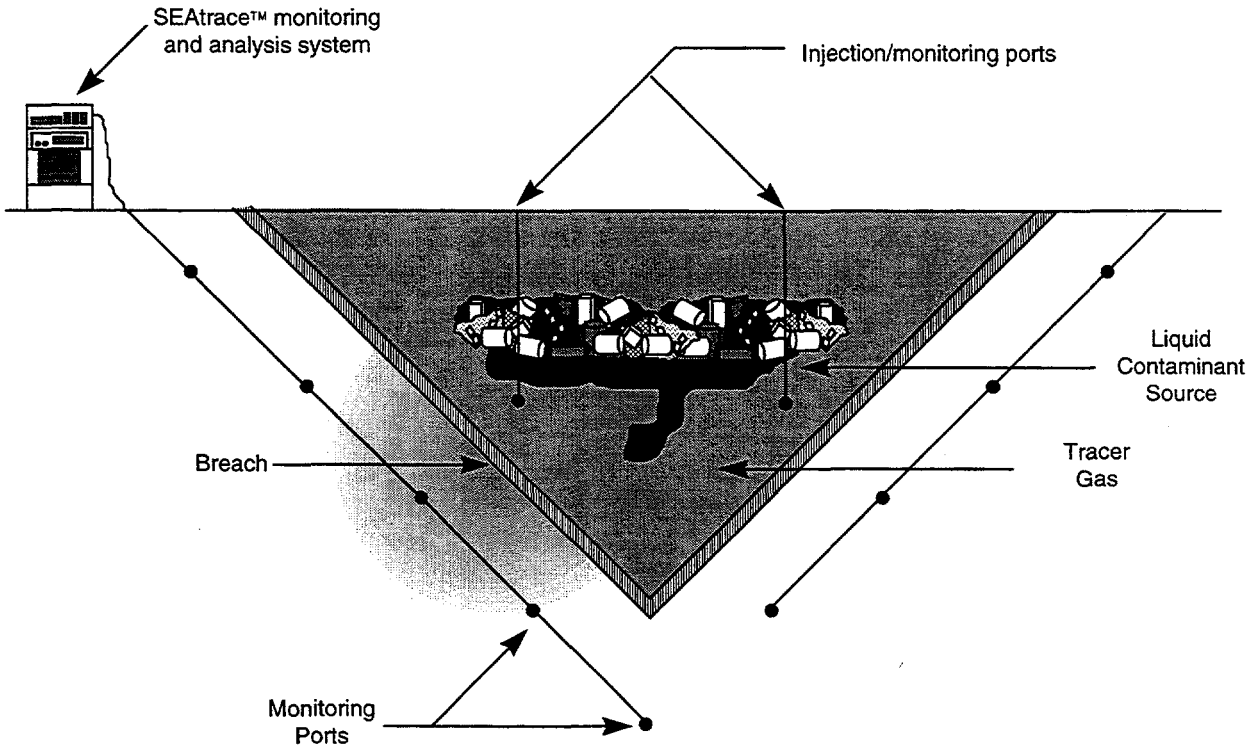

Figure 1. Barrier Test Configuration.

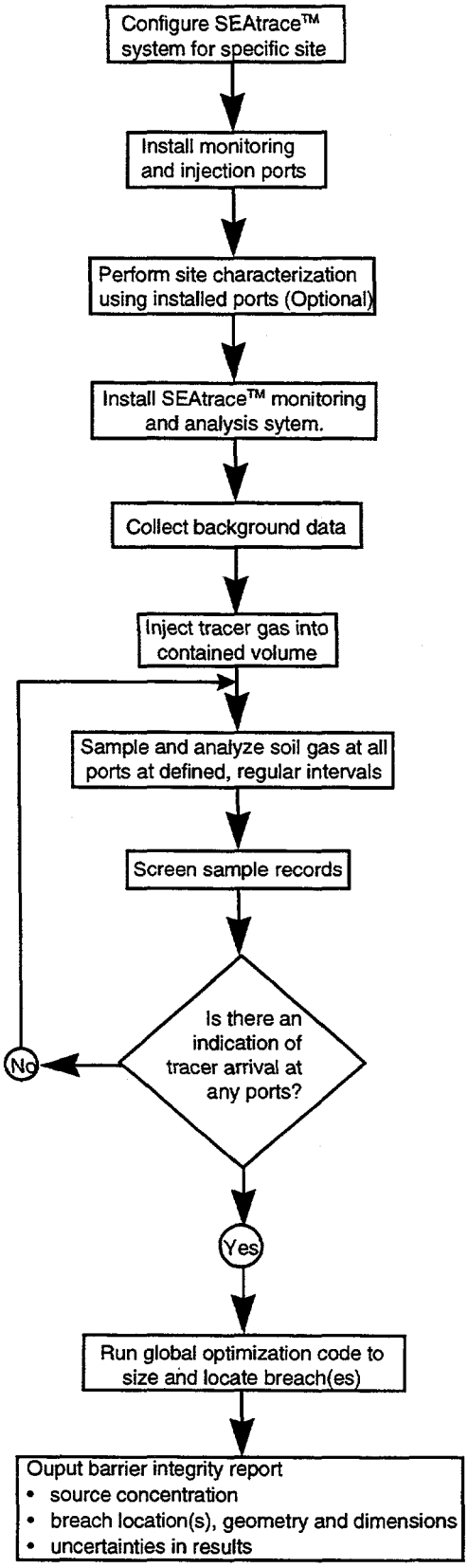

Figure 2. SEAtrace™ barrier integrity monitoring system operational flow.

II.A. Monitoring System

The monitoring system includes all monitoring and injection ports, a sampling manifold, the gas analyzer, and the data acquisition system (Figure 1).

One or more tracer gas injection ports are installed inside the contained volume. These ports are used initially to inject the trace gas into the volume and later, to measure the tracer gas source concentration.

Multiple gas sampling ports are located outside the barrier which are used to monitor for any tracer gas which diffuses into the surrounding medium. The spacing and configuration of these ports are critical to the effectiveness and cost of the monitoring system. Site-specific parameters (geology, anticipated source concentration, barrier construction and geometry, properties of the tracer gas, etc.) will determine the optimum port locations. However, initial estimates have shown that for typical vadose zone conditions, ports spaced on a 1- to 2-m grid between 0.5 to 1 m from the barrier adequately detect a breach anywhere on the barrier.

Installation of the ports can be accomplished by a direct push emplacement tool. If the barrier is shallow (3 to 6 m deep), a manually operated system would suffice, such as the KVA vapor point system. As the emplacement depth increases or the geology becomes more resistive to vapor point emplacements, a truck-mounted system (such as a Geoprobe unit) would be required. For more difficult emplacements, cone penetrometer or ResonantSonic™ emplacements would be suitable.

The data acquisition and analysis system is a stand-alone field unit based on the SEA MultiScan™ autonomous soil gas analysis system (Figure 3). The system reliably monitors up to 32 soil gas vapor lines and provides compositional analysis of up to five analytes in real-time using a photoacoustic gas analyzer. The photoacoustic analyzer is well suited to the analysis of the tracer gas which will commonly be used with the SEAtrace™ system, sulfur hexafluoride (SF_6). Less than half a liter of soil gas is required for each analysis, and a dynamic range of 3 to 5 orders of magnitude is maintained for most compounds. Three to seven minutes is required for each sample, depending on the length and size of the tubing between the monitoring system and the port, and the number of analytes being analyzed. Six- or twelve-hour scanning intervals are typically used. The system is capable of unattended operation for long periods (weeks to several months). Details of the data acquisition system are given in Appendix A.

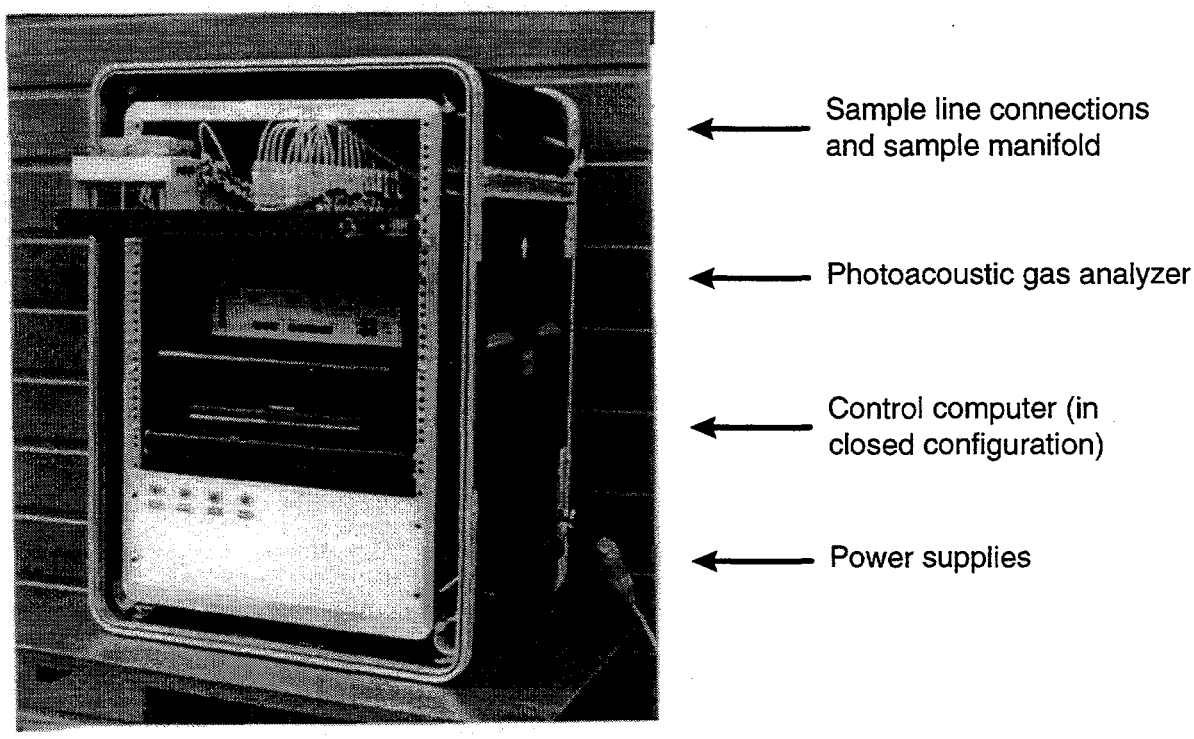

Figure 3. Multipoint tracer gas monitoring system. The photograph shows the control computer, gas sampling system, and gas analyzer.

II.B. Analysis Code

Once concentration history data have been collected, they must be analyzed if any tracer gas was detected outside the barrier. In other barrier verification techniques, post test analysis was typically performed where field results were matched to results from diffusion models through an iterative process. This is a time consuming artful process, as the leak geometry, dimensions, and location are variable, the medium properties are often not well characterized, and the source concentration is variable. To overcome the difficulties of standard diffusion models, SEAtrace™ uses a global optimization technique to effectively search multi-dimensional "space" to find the best fit solution based on all of the input parameters.

II.B.1 Assumptions of the SEAtrace™ Forward Model

This SEAtrace™ code is a key feature of the SEAtrace™ system. The code methodology has been developed and a prototype code has been written and tested with analytically generated input. The prototype code developed is of general applicability and avoids many unnecessary assumptions. However, to reduce the scope of the prototype development effort, the details of the functional design were based on an idealized leak geometry of spherical diffusion. The model is further restricted by assuming a constant source concentration is maintained inside the barrier, the barrier is a plane, and that the medium outside the barrier is homogenous (e.g., that

the diffusivity of the tracer gas through the soil pores is constant). While this diffusion model is simplistic, to a first order it is realistic. If the area of the barrier wall is much greater than the area of the leak, at some distance from the leak the gas will approach spherical diffusion regardless of the true geometry of the leak. Additionally, the barrier wall will act as a flat, no-flow boundary and the medium that the tracer gas is diffusing into can be assumed to be semi-infinite. Thus, the partial differential equation describing this transient process is:

$$\frac{\partial c}{\partial t} = \frac{D}{r^2}\frac{\partial}{\partial r}\left(r^2 \frac{\partial c}{\partial r}\right)$$

c = concentration
t = time
D = diffusivity
r = radial position

Diffusivity of the tracer in the soil gas, which includes the effect of porosity and soil tortuosity, is the controlling parameter. If the barrier is well constructed (e.g., there are only a limited number of breaches in the barrier walls), the mass of tracer gas that can be injected into the internal pore volume of the barrier will be very large when compared to the mass of tracer gas that can diffuse through the leak area(s). Thus, the barrier will serve as an infinitely large reservoir of tracer gas at a fixed concentration (once the injected tracer gas has been completely injected and equilibrated). Boundary conditions can be set as:

$$c(r_o, t) = c_c \text{ at } t \geq 0 \text{ and } c(r, t) = 0 \text{ at } t \geq 0$$

Solving the differential equation results in a straightforward expression of:

$$c\left(r_o, t\right) = \frac{r_o}{r} c_o \operatorname{erfc}\left(\sqrt{\frac{\left(r - r_o\right)^2}{4D\left(t - t_o\right)}}\right) r > r_o, t > {}_{to}$$

where

$r^2 = (x-x_o)^2 + (y-y_o)^2 + (z-z_o)^2$,
$y_o = a + b\, x_o$ (the barrier surface is a plane described by $y = ax + b$),
(x_o, y_o, z_o) is the location of the leak,
(x, y, z) is the location of the sampling point,
t_o is the time that the leak began, and
r_o is the constant radius of the leak after time t_o

It is important to understand how the assumptions used in the model may effect the predicted results. In predicting the location of the leak, only the assumption of spherical isopleths must be true. Gravity and heterogeniety of the medium are the two main factors which will influence the shape of the isopleths. Initial estimates have predicted that for the maximum expected concentrations measured in the surrounding medium (5000 ppm), gravity effects will not be significant. The effect of a heterogeneous medium is harder to predict. Layers of materials with different properties near a breach are expected to have a greater impact than rock

lenses of material having different properties than the surrounding medium. However, these effects cannot be adequately predicted without field tests and/or modeling.

Prediction of the leak size is very non-trival. For the forward model to accurately calculate this parameter in addition to maintaining spherical isopleths, the source concentration must be constant and flow through the breach must not be more restrictive than flow into the surrounding medium. The barrier thickness, leak geometry, or leak-flow properties could easily cause the flow of the tracer gas to be flux, rather than diffusion, limited.

A multiphase, multi-component transport code, T2VOC, was used to address the most significant difference between the forward model used in the prototype code and reality: the effect of flux rather than diffusion-limited flow of the tracer gas into the medium. Flux limited diffusion was created by modeling a barrier of finite thickness. T2VOC is capable of modeling three-phase (gas, aqueous, NAPL), three-component (water, air, VOC), nonisothermal flow and transport through porous media (Falta, R., Pruess, K., Finsterle, S., Battistelli, 1995). Prior to modeling the flux limited problem, work was performed with the code to determine appropriate gridding of the problem (Appendix B).

The problem was modeled using a two-dimensional cylindrical mesh. Figure 4, a schematic of the model, shows the pertinent grid dimensions. The barrier volume, the leak, and the surrounding medium were modeled as a homogeneous medium with a porosity of 30% and an effective diffusivity of the tracer through the soil gas of 3.509e-5 m^2/s. The barrier was modeled using a very low porosity (.05%) giving an effective diffusivity of the tracer gas through barrier approaching 0 m^2/s. Cells surrounding the barrier volume were decoupled from the barrier, boundary cells around the medium were defined to be at a constant concentration of 0 kg/m^3. Nodalization near the leak diameter allowed for multiple leak sizes and barrier thickness to be assessed. A constant source concentration of .304 kg/m^3 (100,000 ppm at standard temperature and pressure) was used in all calculations.

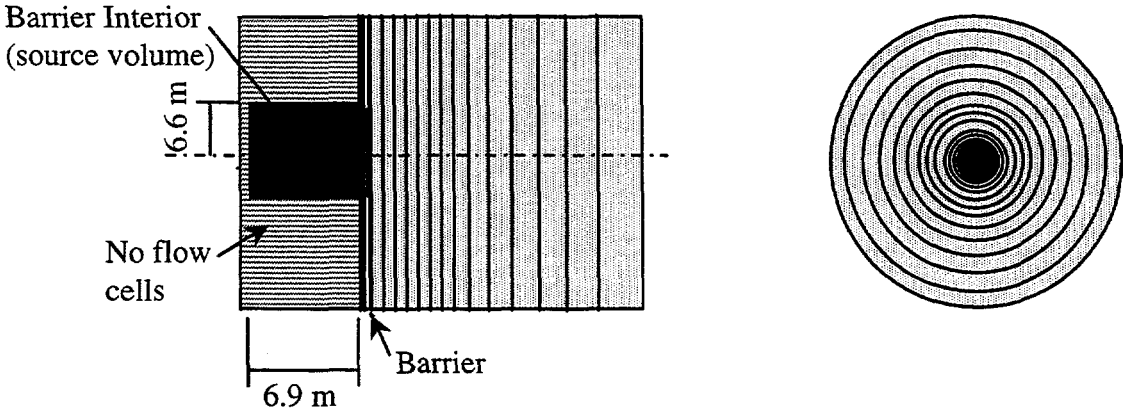

Figure 4. Schematic of the two-dimensional cylindrical model used in the T2VOC numerical calculations where diffusion through the barrier was flux limited.

Concentrations of the tracer gas in the region outside the barrier calculated with T2VOC were significantly (orders of magnitude) lower than those predicted with the one-dimensional spherical model presently used with SEAtrace™, (Figure 5). Clearly, a more accurate analytical model was needed to predict tracer concentrations outside the barrier for a given leak. The problem was split into two parts: a) the leak through the barrier, and b) the medium outside the barrier. A separate solution was developed for each part of the problem.

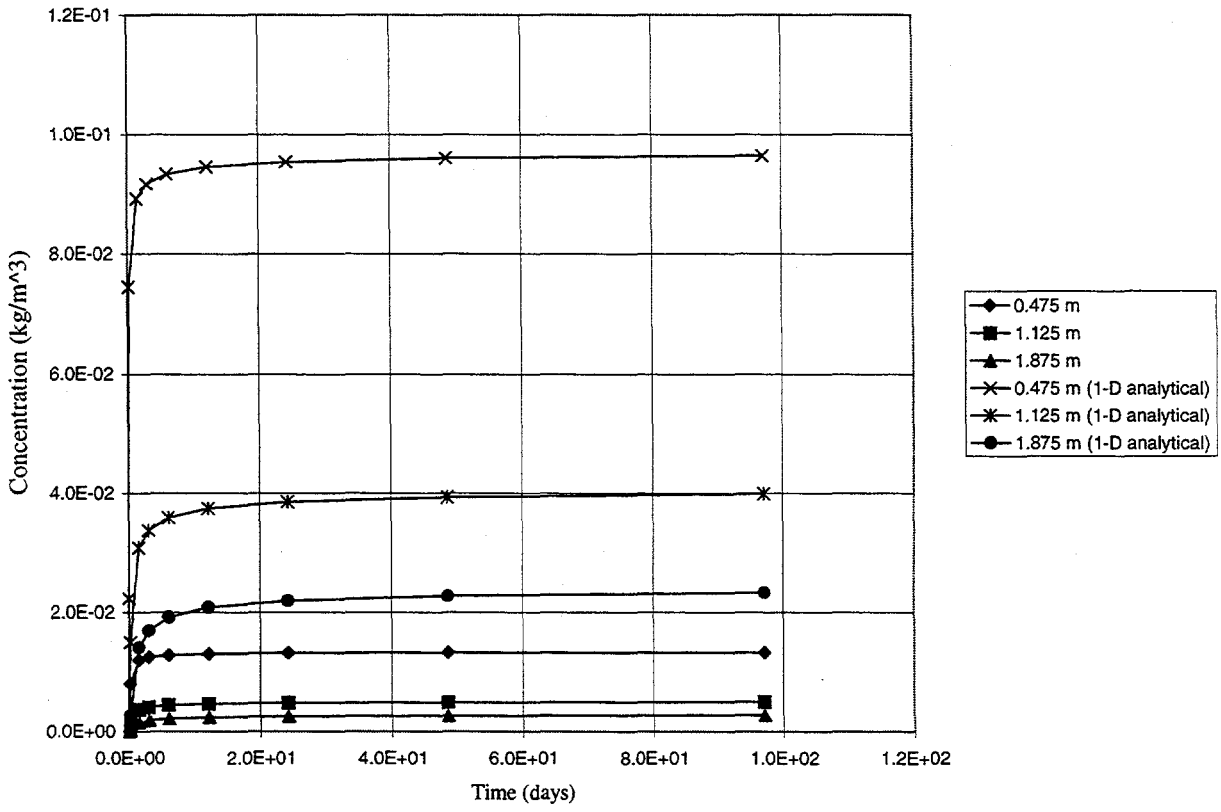

Figure 5. Comparison of the one-dimensional forward model developed for the prototype inversion code with results from T2VOC numerical calculations.

The Leak Through the Barrier. Diffusion of the tracer through the hole in the barrier was modeled using a two dimensional cylindrical model. The T2VOC runs suggested that the hole through the barrier acts as a conduit, allowing diffusion of gas from the source concentration within the barrier, C_o, to a much lower concentration in the soil immediately outside the barrier, C_{exit}. T2VOC results showed the tracer gas concentration along the axis of the mesh (e.g. across the width of the barrier) rapidly, within hours, approached a steady state condition. At steady state, the tracer gas concentration varied linearly along the length of the leak. The diffusive mass flux through the leak also reached its steady state value within hours from the start of the leak. Further, the concentration gradient across the diameter of any section of the leak was very small after steady state conditions were achieved (e.g. flow was predominantly one-dimensional).

A one-dimensional analytical model describing this geometry can be described by:

$$\frac{1}{R}\frac{\partial^2 (RC)}{\partial R^2} = \frac{1}{D}\frac{\partial C}{\partial t}$$

Using the boundary and initial conditions of:

$C = C_o$	@ $z = 0$ and $t > 0$
$C = C_{exit}$	@ $z = L_h$ and $t > 0$
$C = 0$	@ $t = 0$ and $0 \le z \le L_h$

the equation can be solved to provide the following equations for concentration profile and mass flux:

Concentration Profile

$$C(x,t) = C_o + (C_{exit} - Co)\frac{z}{L_h} - \frac{2}{L_h}\sum_{m=1}^{\infty} e^{-D\beta_m^2 t}\,\frac{\sin(\beta_m z)}{\beta_m}$$

Mass Flux

$$q''(x,t) = \frac{D(C_o - C_{exit})}{L_h}\left[1 + 2\sum_{m=1}^{\infty} e^{-D\beta_m^2 t}\cos(\beta_m z)\right]$$

where:

$C(x,t)$ = the concentration within the leak at a given distance from the leak entrance and time;
C_o = source concentration
C_{exit} = concentration at the exit of the leak
L_h = thickness of the barrier
$q''(x,t)$ = flux through the leak
D = diffusivity within the leak

Results from T2VOC showed steady state conditions were reached very quickly within the leak. If only steady state conditions are considered, the above equations reduce to:

$$C(x) = C_o + (C_{exit} - Co)\frac{z}{L_h}$$

$$q''(x) = \frac{D(C_o - C_{exit})}{L_h}$$

These analytical equations were able to match results from T2VOC within ± 10% if C_{exit} is assumed to be equal to ½ C_o for barriers thicker than 0.15 m (6 inches). The validity of this assumption should be confirmed for other combinations of leak diameter/barrier thickness with future parametric runs.

Medium outside the barrier: If the medium is homogeneous, the region outside the barrier can be described as 1-D spherical diffusion of the flux moving through the leak into a semi-infinite medium of effective diffusivity D_m. Such a process can be described by:

$$\frac{1}{R}\frac{R^2(RC)}{\partial R^2} = \frac{1}{D}\frac{\partial C}{\partial t}$$

subjected to boundary conditions:

$C = 0,$	$@\ t = 0$ and $0 \le R \le \infty$
$-D\,(\partial C/\partial R) = q''$	$@\ R = R_h$ and $t > 0$
$C = 0$	$@\ R = \infty$ and $t > 0$

Employing the Laplace transformation technique and several transformations, the solution to this set of equations is:

$$C(R,t) = \frac{q'' R_h^2}{DR}\left[\operatorname{erfc}\left(\frac{R}{\sqrt{4DT}}\right) - e^{-Hz + H^2 Dt} \bullet \operatorname{erfc}\left(H\sqrt{Dt} + \frac{R}{\sqrt{4Dt}}\right)\right]$$

Very close to the leak exit, the equation predicts that the tracer gas concentrations reach a steady state value very quickly (msec). Thus in anything but highly transient phenomena, the equation can be reduced to:

$$C(R,t) = \frac{q'' R_h^2}{DR}\left[\operatorname{erfc}\left(\frac{R}{\sqrt{4DT}}\right)\right]$$

where:

C(R,t) = the concentration within the leak at a given radial distance from the leak exit and time;
q" = steady state flux through the leak
Rh = radius of the leak
R = radial distance from the leak
D = diffusivity in the medium outside the leak
T = time

To assess the accuracy of the derived analytical equations, results were compared to the original T2VOC runs. It was found that the equations compared reasonably well with T2VOC predictions. Typical results are shown in Figure 6. The analytical model consistently over-predicted the tracer concentrations in the medium outside the barrier at early times. This was expected, as assumptions made with the analytical model ignored early transient phenomena.

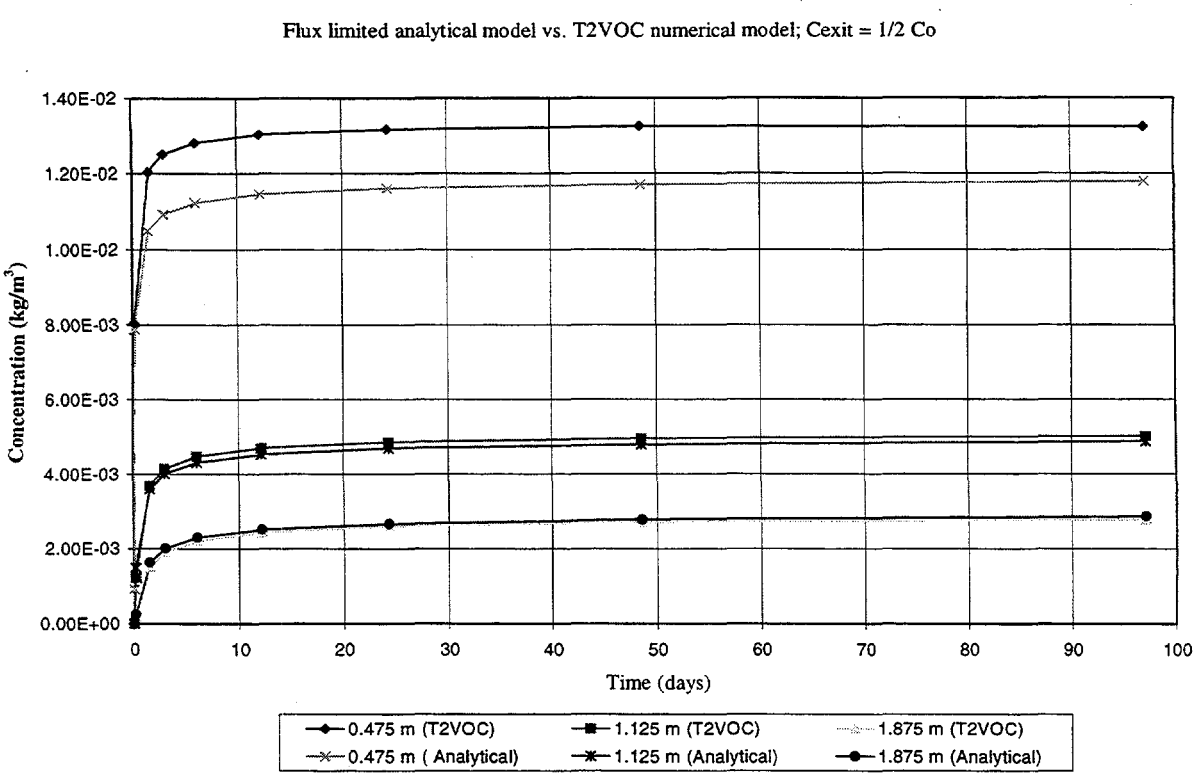

Figure 6. Typical comparison of T2VOC numerical calculations with the derived flux limited analytical model.

II.B.2 Methodology of the SEAtrace™ Code

Global Optimization is used to reverse calculate flow and transport processes to understand unknown properties and transport conditions. This can be accomplished with numerical or analytical techniques, depending upon the complexity of the process and the detail required in the final result. For this application a numerical method was chosen which would allow near real time assessment of recorded gas concentration data. Consequently, the solution method chosen is readily programmed for use on a portable personal computer, which can also control data acquisition, archiving data, and reporting/transmitting the results.

The estimation of the size and location of a leak from measured concentration histories is an inverse problem of multiphase flow in porous media. From measured tracer concentrations C_{ik} taken at locations, $\underline{x}_i = (x_i, y_i, z_i)$ and times t_{ik} one seeks estimates for a set of parameters $\underline{p}$ that characterize the leak.

The inverse problem requires a leakage model:

$$c(\underline{p}; \underline{x}, t)$$

that solves the forward problem; that is, it maps each point $\underline{p}$ from a multiparameter space into a set of predicted concentration histories. For example, an idealized leakage model (the one-dimensional forward model) for a vertical barrier surface described by $y = a+bx$ is:

$$c(\underline{p};x,t) = \frac{r_o}{r} c_o \operatorname{erfc}\left(\sqrt{\frac{(r-r_o)^2}{4D(t-t_o)}}\right), \; r > r_o, \; t > t_o$$

where:

$r^2 = (x\text{-}xo)^2 + (y\text{-}yo)^2 + (z\text{-}zo)^2$,
$y_o = a + bx_o$,
(x_o, y_o, z_o) = leak location
t_o = time leak begins
r_o = constant radius of leak after time to
c_o = uniform tracer concentration within the hemisphere of radius ro after time t_o
D = uniform diffusivity of the medium
erfc(o) = complement of the error function

In the prototype code at least the first four parameters are unknown. In a realistic application, the model may be more complex, perhaps a finite element model, and there may be many unknown parameters.

The inverse problem can be cast in the form of a nonlinear global optimization problem. The objective function, E, to be minimized may be taken as the sum of the squares of the differences between predicted and measured tracer concentrations:

$$E(\underline{p}) = \sum_{i,k}\left[c(\underline{p};\underline{x}_i,t_{ik}) - C_{ik}\right]^2$$

The problem is made difficult by the fact that there may be more than one set of parameter values for which E achieves the minimum. No algorithm can solve a general, smooth global optimization problem in finite time. This fact has lead to the use of stochastic methods, some of which are called Simulated Annealing (SA). An SA method has been used to solve an inverse porous flow problem to obtain relative permeability and capillary pressure as a function of water saturation (Ounes, Ahmed, 1992). A similar approach is used for barrier integrity assessment.

The simplest stochastic method for global optimization is to repeatedly select points in the parameter space at random, using a uniform probability distribution. The objective function is evaluated at each point; the minimum value and the point with the minimum value are remembered, all other information is discarded. Even with a large sample of points, the Pure Random Search method may not find the global minimum, but it probably will come close. As the sample increases, the probability of success converges to one.

SA methods are similar to Pure Random Search. Points are selected at random and the best point is remembered. The difference is that an SA method does not use a uniform distribution to select points in the parameter space. Instead, the probability distribution depends

in a complex way on the objective function of previous points. In an SA method the probability distribution for the next point is centered around a particular point in parameter space, which is called the base point. The base point need not be the best point found in the number of selections performed. One way in which various SA methods differ from each other is in the exact form of the probability distribution.

The rule for determining the base point is responsible for the name "Simulated Annealing." If the objective function is smaller at the next point than it was at the base point, then the base point is moved to the new point. If the objective function is larger, it may or may not be moved, depending on the probability function. If the objective function is much larger at the next point, the probability of moving the base point is less, because that probability is given by:

$$e^{-\Delta E/T}$$

This is analogous to the physical annealing process, where ΔE is the difference in energy states and T is proportional to the temperature. When T is relatively large, there is a good possibility that the base point will climb out of a local minimum to look for other minima. If T is small, the base point is more likely to avoid "uphill" steps. In an SA method, the temperature is reduced as the process proceeds, just as in physical annealing.

To select the next set of parameter values to be tested, each parameter is selected independently, using a probability distribution proportional to

$$e^{-w\left|p_j-q_j\right|/\left(M_j-m_j\right)}$$

where: p_j = the new point
q_j = the base point
$[m_j, M_j]$ = the interval of allowed values of p_j
w = a shape constant

This is a relatively simple probability distribution that satisfies the requirements that the probability density be positive over all possible parameter values and that the density be a maximum at the base point.

In a previous SA algorithm for an inverse porous flow problem, the "temperature" was periodically reduced by a factor between 0.7 and 0.95. Other studies suggest that the temperature should be

$$T \propto E(\underline{p}_b) - E_o$$

where: $\underline{p}_b$ = more recent base point
E_o = estimate of the minimum value for E

In order to assure that T converges to zero even when E_o is underestimated, the present algorithm uses

$$T = V\frac{E(\underline{p}_b) - E_o}{\ln(n+1)}$$

where: n = the number of points for which E is evaluated
V = constant.

The value for E_o is based on the fractional measurement errors, e_i, at the various monitors; that is,

$$E_o = \sum_i e_i^2 \left(\sum_k C_{ik}^2 \right).$$

For the calculations reported here, V was set to 100. With this choice, the probability of accepting a point that would "double" the error is about 98.6 % for n=1 and about 86 % for n=2000.

An SA algorithm needs a stopping rule, which tends to be problem-dependent. The present algorithm stops a search when $E(\underline{p}) \leq E_o$ or after a fixed number of evaluations N.

In order to estimate the uncertainty in the result, several sequences are run, each starting from the same initial $\underline{p}$ but using a different sequence of random numbers. Because of this repetition, it is reasonable to use a relatively small value of N for each search. This iterative methodology was incorporated into a C++ code developed to run on a standard personal computer. A brief description of the code design is included in Appendix C.

II.B.3 Prototype Code Validation and Testing of the SEAtrace™ Code Using Analytical Input

Initial testing of the inversion code was performed by generating concentration histories for monitoring points in a typical barrier monitoring/verification configuration. The sample configuration was a vertical barrier 100 ft deep and 200 ft wide (Figure 7). Four multipoint monitoring wells were located in a plane 20 ft from the barrier surface. The 40 ft spacing of the points within each well was equal to the spacing of the wells from one another. This spacing allowed for all points on the surface of the barrier except those near the top and side edges to be within 30 ft of a monitoring point. The location of the leak was arbitrarily chosen. The distance from the leak center to each monitoring point was calculated, and a one-dimensional radial analytic solution for molecular diffusion was used to generate concentration histories at each of the monitoring points.

The total number of times (30) calculated for each point was chosen assuming a soil gas sample would be collected once a day with data downloaded from the MultiScan™ system once every 30 days. In calculating the concentrations, it was assumed that the barrier did not begin to leak until the beginning of the 8th day after the last collection time. Two different leak radii, 10 cm and 1 m, were used in the calculations. Once concentrations were calculated from the

analytical solution, random errors were incorporated in the values. It was assumed that under field conditions the gas analyzer could measure the tracer gas to within ±5 percent accuracy for values under 500 ppm, and within ±10 percent for values over 500 ppm. These inaccuracies are greater than what should actually be measured, and therefore are very conservative. A 1 ppm lower detection limit was assumed for the field conditions, even though the gas analyzer can measure SF_6 to 5 ppb in laboratory analysis. The source concentration of the tracer used in calculations was 70,000 ppm, the upper calibrated detection limit of the gas with the proposed gas analyzer. The effective diffusion constant of the tracer in the soil gas was assumed to be 1.0 (10^{-5}) m^2/s (value measured in the vadose zone at the Chemical Waste Landfill at Sandia National Laboratory). The information used to calculate concentration histories for the two baseline cases is summarized in Table 1.

Table 1. Description of information used to calculate analytical diffusion concentrations at monitoring points for the baseline cases.

	Case 1	Case 2
Leak location (X,Y,Z) meters	32.92, 0, -14.02	32.92, 0, -14.02
Monitor location (X,Y,Z) meters		
#1	48.78, 6.10, -9.14	48.78, 6.10, -9.14
#2	24.38, 6.10, -21.34	24.38, 6.10, -21.34
#3	24.38, 6.10, -9.14	24.38, 6.10, -9.14
#4	36.58, 6.10, -21.34	36.58, 6.10, -21.34
#5	36.58, 6.10, -9.14	36.58, 6.10, -9.14
Accuracy of monitor locations (m)	±0%	±0%
Accuracy range of measured concentrations (≤ 500 ppm)	±5%	±5%
	Case 1	**Case 2**
Accuracy range of measured concentrations (> 500 ppm)	±10%	±10%
Leak radius (m)	.1	1
Effective diffusive constant of tracer through medium (m^2/hr)	.036	.036
Source concentration (ppm)	70,000	70,000
Accuracy of measured source concentration value (%)	±10	±10
Number of independent calculations performed for each run	5	5
Maximum number of attempts per independent calculation to achieve error parameter	5000	5000

The code allows for a range of values to be input for all of the pertinent variables. Ranges for the x and z location of the leak on the barrier were chosen based on the monitor information (the barrier was vertical and coordinates chosen such that $y = 0$). The monitors closest to the leak will detect the tracer earliest and will measure the highest concentrations with time. Thus a cursory overview of the collected data will allow the user to determine a very general location of the leak. Figure 7 shows the coordinate system used to generate the input file and lists the monitoring points which were close enough to the leak to detect the tracer gas.

For the baseline case, the area of the barrier searched to find the leak was $24.38 < x < 48.77$ and $-21.34 < z < -9.14$ meters. The range of the tracer source concentration was ±10 percent of the "known" source concentration of 70,000 ppm for the baseline case (this value would be measured in the field). Comparison runs were performed where the range was increased to ±30 percent (50,000 < source concentration < 90,000 ppm). The effective diffusivity of the medium was a constant of 1.0×10^{-5} m^2/s in the baseline case, with comparison runs changing the range to 5.0×10^{-6} to1.5 x 10-5 m^2/s. Additionally, changes to the base runs were made to determine the effect of other potential errors from field conditions. The input location of the monitoring points were altered in one run so that they were one to 2.25 meters off from their true location. Finally, a stratified medium was crudely modeled in calculating the tracer concentration histories. In this medium, the diffusivity between the leak and three of the monitoring points (2, 3, and 4) was 5 times lower than the diffusivity between the leak and the remaining monitoring points 6 and 7 (Figure 7).

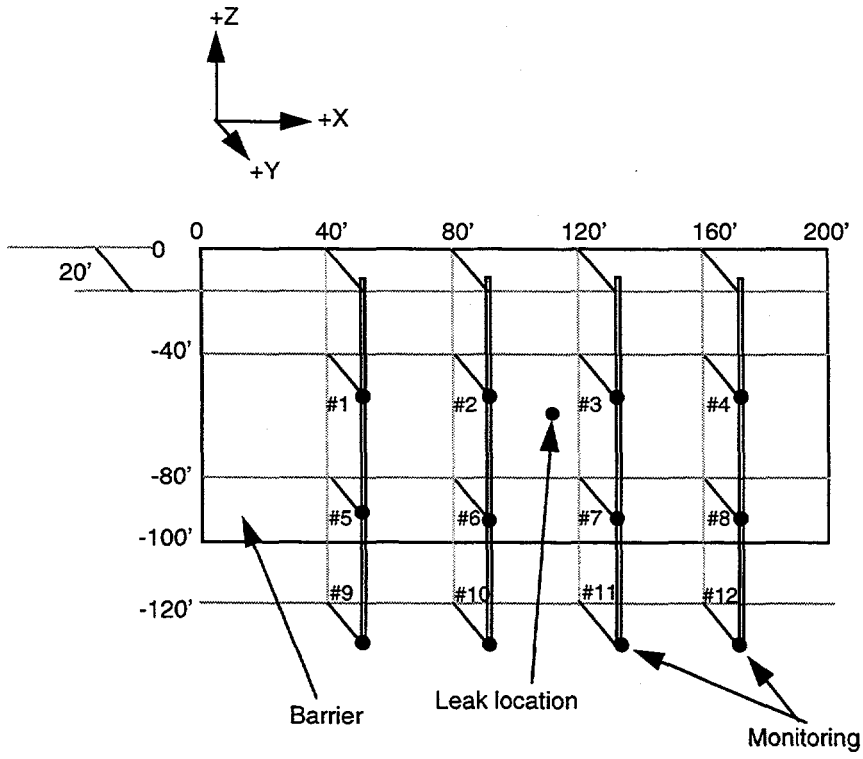

Monitor points 2, 3, 4, 6, and 7 were close enough to the leak to detect the tracer within the first 30 days after the leak began (using baseline case 1 information).

Figure 7. Typical SEAtrace™ barrier verification/monitoring configuration.

Table 2 shows several examples of the input parameters for the analytic calculations and the code results. The code was consistently able to accurately determine the location of the leak even as the number of unknown parameters increased. For most of the cases, the calculated X, Z locations were within 0.5 m of the actual values. Because diffusion is very sensitive to radial distance from the leak source, uncertainties in the sample port locations with respect to the barrier will have a significant impact on the results of any diffusion based system. The simulation with the greatest uncertainty in port location, where the ports were within 1.0 to 2.25 m of their true positions, resulted in the largest error (3 m) in the calculated location of the leak. Consequently, the ultimate uncertainty in the SEAtrace™ leak location determination is closely related to the uncertainty in both the barrier and sample port locations. Calculation of the leak radius also showed good agreement with the actual values, within 20 percent in all runs. In most cases, the best fit was very close to the real value, and in all cases, the calculated range of values did encompass the true value. The code was also able to determine the time the leak began with uncertainties of less than ±2 days. As expected, as more unknowns were introduced into the code (larger ranges) or as the accumulation of errors increased in calculating the analytic histories, the accuracy of the code diminished. However, even under the worst case simulated conditions, results were still good. Under true field conditions where additional data and monitor points would be included in the calculations with time, the results should be more accurate.

Table 2. Sampling of input parameters for the analytic calculations plus the codes results.				
	Baseline case with small leak radius	**Small leak radius case with ranges for concentration and diffusivity**	**Baseline case with large leak radius**	**Large leak readius case with ranges for concentration and diffusivity**
Leak location (X,Y,Z) in meters - ACTUAL	(32.92,0, -14.02)	(32.92,0, -14.02)	(32.92,0, -14.02)	(32.92,0, -14.02)
Leak location (X,Y,Z) in meters - CALCULATED	(32.89, ± 35, 0, -14.22 .± 93)	(33.09 ± 27, 0, -13.65 ± .35)	(33.10 ± .60, 0, -14.33 ± .51)	(31.97 ± .50, 0, -17.12 ± .59)
Leak radius (m) - ACTUAL	0.1	0.1	1.0	1.0
Leak radius (m) - CALCULATED	0.12 ± 0.03	0.10 ± 0.04	1.17 ± 0.24	1.04 ± 0.34
Effective diffusive constant of tracer through medium (m^2/hr) - ACTUAL	0.04	0.04	0.04	0.04
Accuracy of diffusion constant in code input (%)	±0	±50%	±0	±50
Effective diffusive constant of tracer through medium (m^2/m) - CALCULATED	0.04 ± 0	0.05 ± 0.01	0.04 ± 0	0.04 ± 0
Source concentration (ppm) - ACTUAL	70,000	70,000	70,000	70,000
Accuracy of measured source concentration value in code input (%)	±10	±30	±10	±30
Source concentration (ppm) - CALCULATED	69,527 ± 3438	52,890 ± 21,320	65,483 ± 6,031	68,195 ± 4,610
Time leak began (days) - ACTUAL	8	8	8	8
Time leak began (days) - CALCULATED	8.07 ± .65	9.80 ± 1.28	9.65 ± 1.13	8.42 ± 0.96
Accuracy of monitor locations (m)	±0 m	±0 m	±0 m	± 2.25
Accuracy of range of measured concentrations (≤ 500 ppm)	±5%	±5%	±5%	±5%
Accuracy of range of measured concentrations (> 500 ppm)	±10%	±10%	±10%	±10%
Number of independent calculations performed for each run	5	5	5	5
Maximum number of attempts per independent calculation to achieve error parameter	5000	20,000	5000	20,000

Intentionally Left Blank

III. FIELD TEST OF THE SEAtrace™ METHODOLOGY

A simple field experiment was designed to test the SEAtrace™ system. A non-contaminated site near Sandia National Laboratories Chemical Waste Landfill was chosen to conduct the test. The site was chosen as it had been well characterized in previous studies of vapor movement in the vadose zone and monitoring ports were already installed. In particular, the diffusivity of the tracer gas through the medium had been measured.

The field test was primarily intended to be proof-of-concept. It was designed to test the main assumption used with the SEAtrace™ system (spherical diffusion of the tracer gas), the individual components of the system, and to test the performance of the model set-up/logic, and the hardware under field conditions. Secondary purposes of the test were to determine how quickly the system would be able to detect a leak of a given diameter, to determine the accuracy of the system, and to collect real data to be used in future parametric studies of the inversion code.

III.A. Set-Up

Field test design requirements were that the leak location, geometry and diameter be known, that there be no non-engineered leaks in the barrier, and that the source concentration be maintained at a constant value. As such, either creating or using an existing subsurface barrier was impractical. Instead, a simple although non-ideal experiment was chosen. Figures 8 shows a plan view of the test set-up. Figure 9 shows a cross sectional view along the E-W array of monitoring ports. The "barrier" was a thick piece of non-permeable plastic sheeting layed on top of the ground surface. To protect the sheeting from damage and degradation, it was covered with rock free soil and sand. This cover material also assured good contact between the barrier and the ground surface. A hole in the center of the sheeting acted as the leak. A baseplate covering the hole was used to adjust the leak diameter as desired. The tracer gas source volume (e.g. the "barrier interior") was a large (100 ft^3) impermeable laminate bag. The thin film bag allowed the volume to adjust to accommodate for changes in temperature and pressure over the duration of the test. This minimized advective forces on the tracer gas mixture.

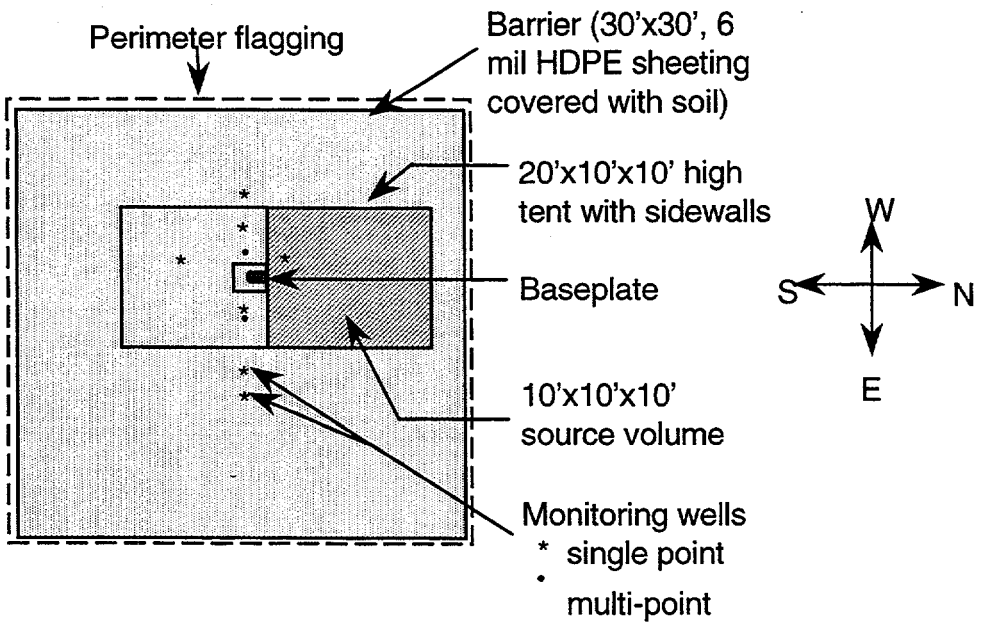

Figure 8. Plan view of the proof-of-concept field test set-up.

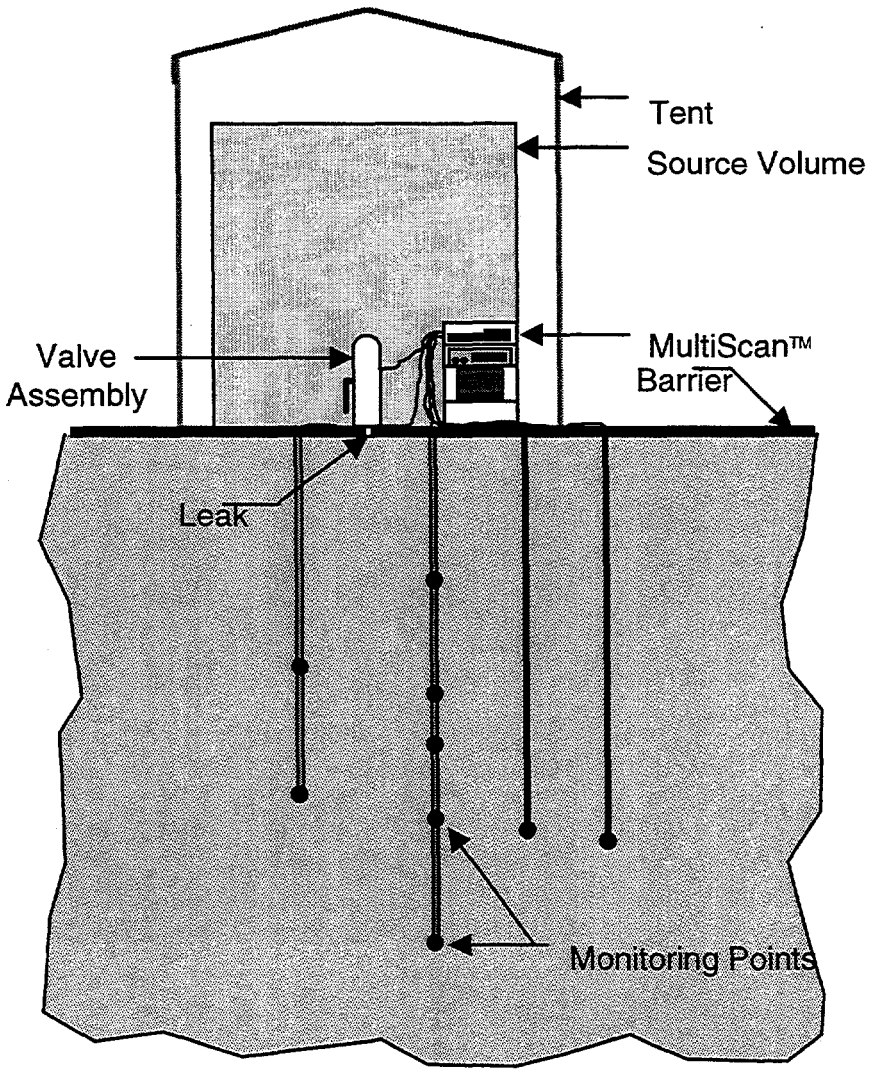

Figure 9. Cross-sectional view of the proof-of-concept field test.

The source volume was connected to the barrier by an 8-inch diameter butterfly valve that was attached to the baseplate. The valve was large enough so that it would not limit the diffusion rate of the tracer gas into the medium. The valve allowed for a well-controlled starting time for the leak. The leak diameter was defined by the baseplate which could easily be interchanged between tests. The level range was ~0.5 inch to almost 8 inches in diameter (equivalent to a maximum r_o of 10 cm). The baseplate was held in place and sealed against the barrier with heavy weights. Ports on the baseplate valve allowed for (1) injecting the tracer gas into the source volume during the test (as necessary to maintain a constant source concentration), (2) measuring the source concentration; and (3) measuring any pressure differential between the source volume and the atmosphere. The source volume, valve assembly and most of the surface tubing from the monitoring points were enclosed in a large tent with sidewalls. Initially, the source volume was supported by the tent. After results from the first test showed motion of the tent introduced significant advective movement of the tracer gas into the medium, the source volume was decoupled from the tent and enclosed in a wooden structure. These precautions

helped protect the tracer gas source from wind and direct solar gain, minimizing advective forces on the tracer gas source mixture in subsequent tests.

The site chosen for the experiment had an extensive array of existing single and multipoint Geoprobe monitoring wells. The surface penetrations of the wells formed a cross, with seven wells along the E-W leg of the cross and two wells along the N-S leg. Two of the wells along the E-W leg were multi-point sample wells, 2 inches in diameter and 15 to 18 feet deep. The wells were lined with SEAMIST™ membranes and filled with a bentonite/water slurry. There were nine sampling ports in each of these wells. Ports were located at depths between 3 and 16 feet below ground surface. The remaining seven Geoprobe wells in the experimental array were completed as standard gas sampling wells. The punched holes were 1 inch in diameter and had a 6-inch long screened sample region at the bottom of the well. Each of these wells was between 9 and 11 feet below ground surface. The holes were completed with bentonite. During well installation the inclination of the drill rod from vertical in both the N-S and E-W directions was estimated and noted, however no attempt was made to measure these values. This omission made calculating the exact location of the points relative to one another less accurate than desired for the experiment. Appendix D gives a detailed history of the well array emplacement.

Monitoring ports used for the field test were chosen based on their radial distance from the defined leak. These values are listed in Table 3, with the ports used in this test in bold face type. Most ports chosen were located in multi-port well #3. This minimized the inaccuracy of the port locations relative to one another since the distance between the ports was certain, and also provided several near surface (near the "leak") ports. Ports from the other wells were then chosen to be at or near the same radial distances from the leak to determine if the isopleths were indeed spherical or to fill in gaps. All of the ports chosen were between 1 and 5 meters from the engineered leak. This range encompasses the anticipated distances a leak would be from monitoring ports in reality. However, because these ports were all near surface, measured concentrations would be influenced by atmospheric changes. In addition, all monitoring ports were in the same plane as the leak. This was an over site in planning the test, which made it more difficult for the inversion code to determine the x location of the leak. Because the sampling ports had not been actively maintained over the two plus years since they were emplaced, there was some concern about port integrity. Tubing from the single point wells had been unprotected at the grounds surface and its exposure to ultraviolet light made the tubing very brittle, and most of the tubes were broken near the ground surface. Several were filled with 10 to 12 inches of soil where they had broken. Damaged tubing was replaced. Flow tests performed on each port showed all but one port (#7) was open to flow.

Table 3. Tagged depths and estimated radial distance from the barrier "leak" for the proof-of-concept field test. Bold faced type indicates ports used during the test series.				
	Tagged depth			Approximate distance from leak
Port i.d. #	(in)	(ft)	(m)	(m)
3-1	**33**	**2.8**	**0.8**	**1**
3-2	55	4.6	1.4	1.5
3-3	**80**	**6.7**	**2.0**	**2.1**
3-4	**97**	**8.1**	**2.5**	**2.5**
3-5	108	9.0	2.7	2.8
3-6	**120**	**10.0**	**3.0**	**3.1**
3-7	137	11.4	3.5	3.5
3-8	**161**	**13.4**	**4.1**	**4.1**
3-9	185	15.4	4.7	4.7
5-1	49	4.1	1.2	1.3
5-2	**72**	**6.0**	**1.8**	**1.9**
5-3	96	8.0	2.4	2.5
5-4	**113**	**9.4**	**2.9**	**2.9**
5-5	126	10.5	3.2	3.2
5-6	137	11.4	3.5	3.5
5-7	156	13.0	4.0	4
5-8	179	14.9	4.5	4.5
5-9	202	16.8	5.1	5.1
1	**130**	**10.8**	**3.3**	**3.9**
2	**125**	**10.4**	**3.2**	**3.4**
4	106	8.8	2.7	2.7
6	102	8.5	2.6	2.7
7	133	11.1	3.4	3.6
8	131	10.9	3.3	
9	133	11.1	3.4	

III.B. Test Results

A total of five tests were performed. Different combinations of leak diameter and source concentrations were chosen for the test sequences. Three different leak sizes were used throughout the test sequence. Two tests were completed with both the smallest (.01 m radius) diameter and the largest (0.1 m radius) diameter leaks. A single test was completed with an

intermediate .05 m radius diameter. A high source concentration (50,000 – 60,000 ppm) was used for all but one of the tests to shorten the required test duration. This minimized the risk of large atmospheric pressure and temperature changes occurring during the test, as well as reduced the cost of the test series by reducing the total test time.

Measurements for each test included atmospheric pressure and temperature; the internal pressure of the source volume; the temperature inside the scanning system (near the photoacoustic gas analyzer); and concentrations of TCE, carbon dioxide, sulfur hexafluoride and water vapor for each of the measurement ports. One port was reserved for an atmospheric sample (results from this sample would indicate any increase in the residual tracer concentration due to inadequate purging of the tedlar sample bag or manifold system). One port was located inside the tent (results from this sample would indicate any increase of the tracer gas in the tent due to a leak in the source volume). Two measurement ports were include in the source volume. One was placed inside and at the bottom of the bag. The other was in the valve, approximately 18" from the leak. Measurements were taken every 3 hours. Nine subsurface ports were recorded. The remaining ports on the scanning system (14 in all) were used to assure the internal chamber of the B&K was adequately purged between samples.

Results from the field tests were very encouraging, fulfilling all of the success criteria. The scanning system autonomously collected data under adverse conditions for long periods of time. The inversion code was able to process the collected data and provide accurate estimates of the leak location and radius. The collected data showed that the diffusion of the tracer into the medium was spherical, justifying one of the major assumptions used in developing the forward model used with the inversion code.

The first two tests yielded pertinent data, even though they were not completed as planned. Background data was collected for a week. Analysis of the background data showed several significant facts:

- There was a low level (10-20 ppm) background concentration of TCE at the site.
- The measured concentration inside the source volume was stable, indicating there were no leaks in the source volume.
- The configuration of the B&K analyzer posed some unique problems:
  (1) The unit automatically calculates a purge time to clear residue from the previous sample from its' internal chamber and sample tube. This time varies directly with the length of the sample tubing that is input into the unit. Collected data showed that the internal chamber was not being adequately purged after samples of high concentration of the tracer gas were analyzed (e.g. after the source concentration was measured). Increasing the set tube length to a value large enough to alleviate this problem would have created other problems without significant changes to the scanning systems software. Most importantly, it would have significantly increased the volume of soil gas removed for each sample. Given the scale of the experiment, it was felt this would adversely impact the results. Instead, atmospheric "purge" samples were included between each subsurface sample ports (numerous atmospheric samples were added between the measurement of the source volume and the

subsurface ports). The only adverse impact on the experiment to this solution was an increase in the overall time required to complete a scan of the ports. While this proved to be an adequate solution for the experiment, it is unacceptable for future applications of the system and will need to be further addressed.

(2) The B&K configuration was that it was unable to adequately cross compensate between the TCE and the low and high range SF_6 filters when high concentrations of SF_6 were being measured. Because of this inability, the high range (0 to 80,000 ppm) and low range (0 to 5,00) SF_6 filters could not be used at the same time. Turning different filters on / off via the control computer proved to be very difficult and was not pursued. The unit was returned to the laboratory and cross compensation values were adjusted so that just the TCE and the high range SF_6 filters were used.

The valve between the source volume and the defined leak was opened for the first test (Julian day 88). Data was recorded continuously over duration of the test (four days). The first test was performed without a rigid protective shell around the source volume. Wind gusts caused the tent and the bag to move considerable, forcing the tracer gas to be pumped out of the source volume and into the medium. This was compounded by an ineffective seal between the impermeable membrane and the ground surface. The poor seal quality at this interface allowed the tracer gas to move laterally between the two surfaces, effectively creating a much larger and non constant "leak" radius than desired. Because of the large leak area and the advective motion of the tracer, much higher concentrations of the tracer were recorded at the monitoring ports than expected. While the problems created several unknowns with the test, collected data still proved to be very useful. The measured isopleths appeared to be spherical, as seen in both direct comparisons of ports at similar radii from the leak and in contour plots of the data (Figures 10 and 11, respectively). Figures 12 and 13 show other pertinent data collected during the test sequence. Inversion of the data provided acceptable results for the location of the leak (within 0.5 m or the true location) and an estimate of what the effective leak radius was. Table 4 gives a comparison between the SEAtrace™ systems' results and the actual experimental set-up for each test sequence.

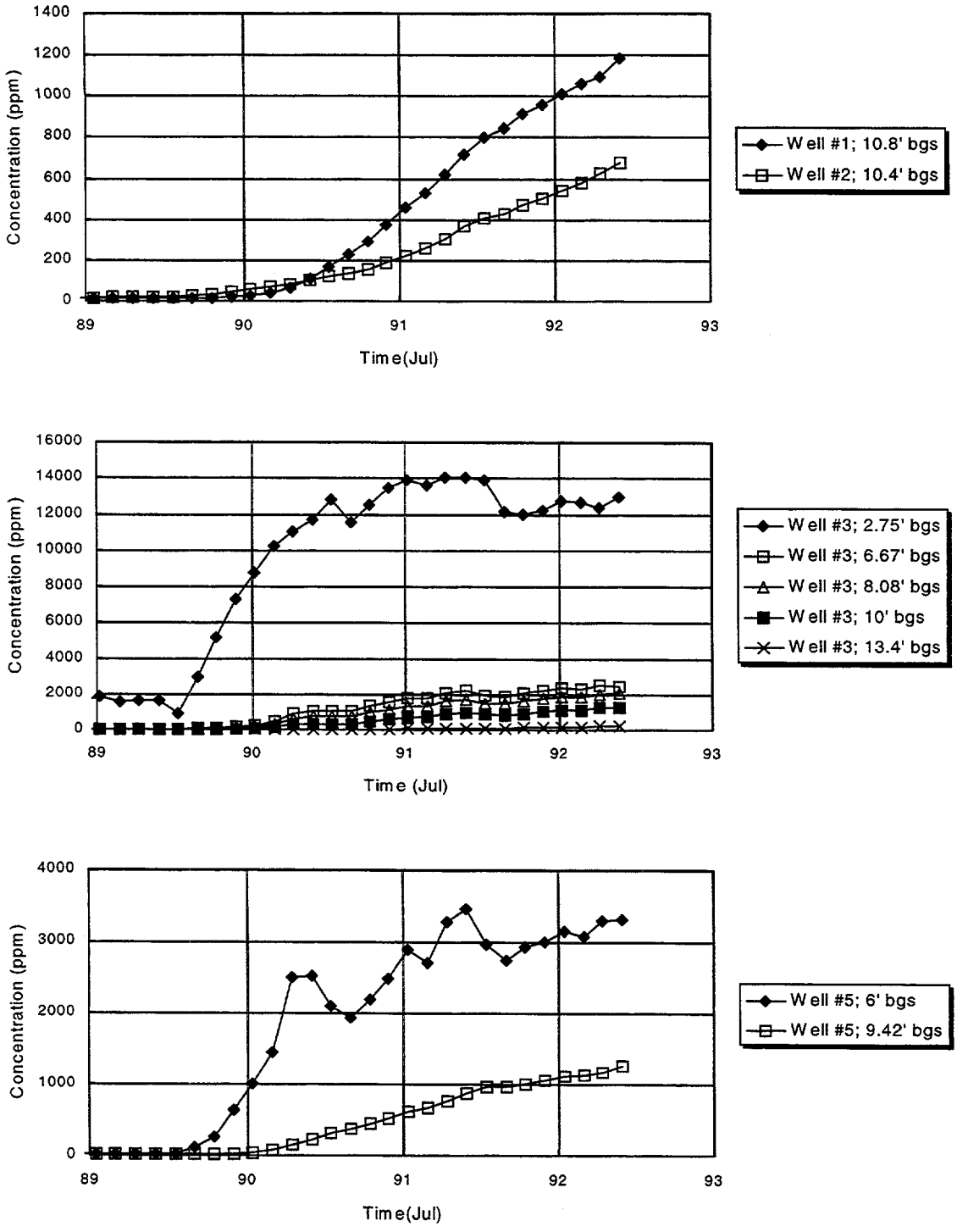

Figure 10. Measured concentration histories of the subsurface monitoring ports for the proof-of concept field test #1.

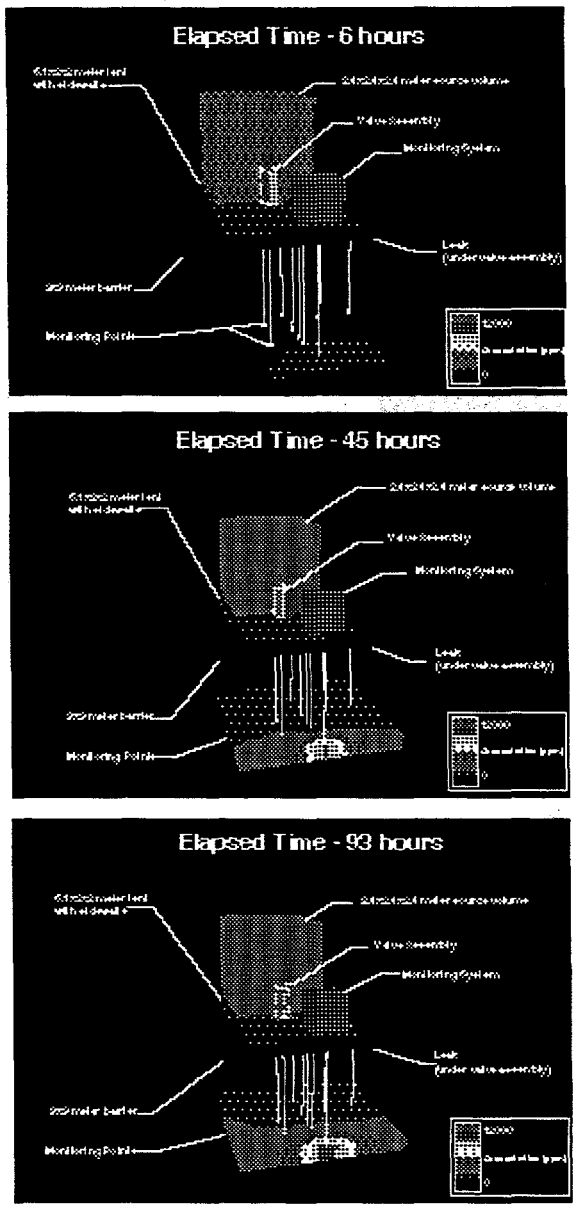

Figure 11. Contour plot of concentration data collected during the first field test.

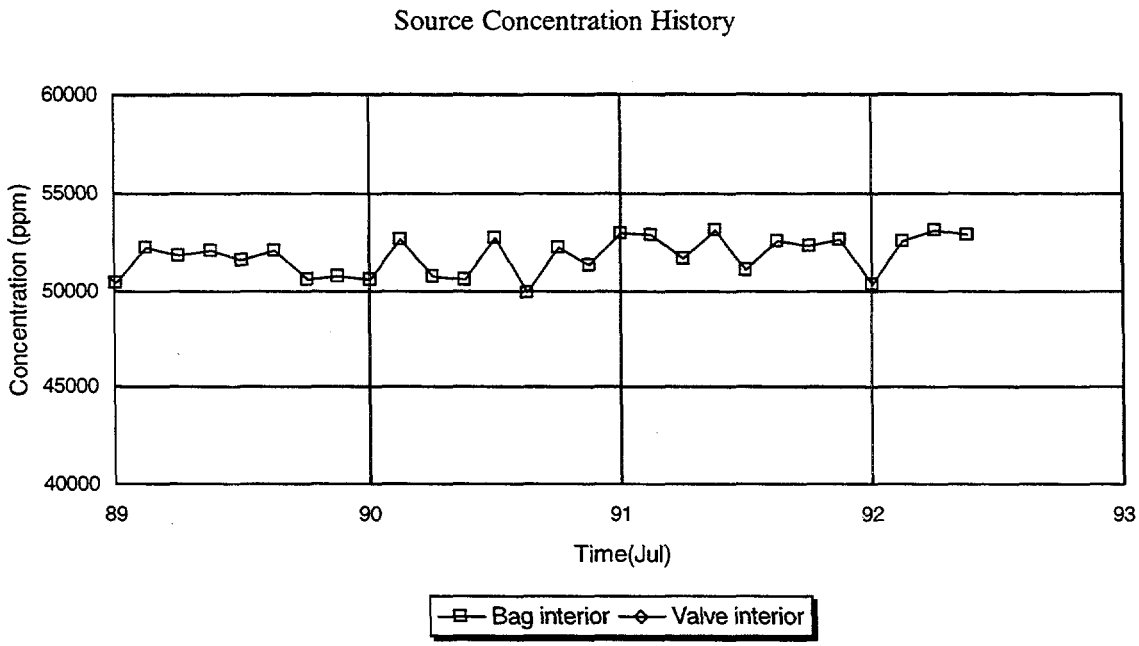

Figure 12. Measured concentration histories of the source volume ports for the proof-of concept field test #1. The valve interior port was unhooked after initial data showed inadequate purging of the B&K between samples.

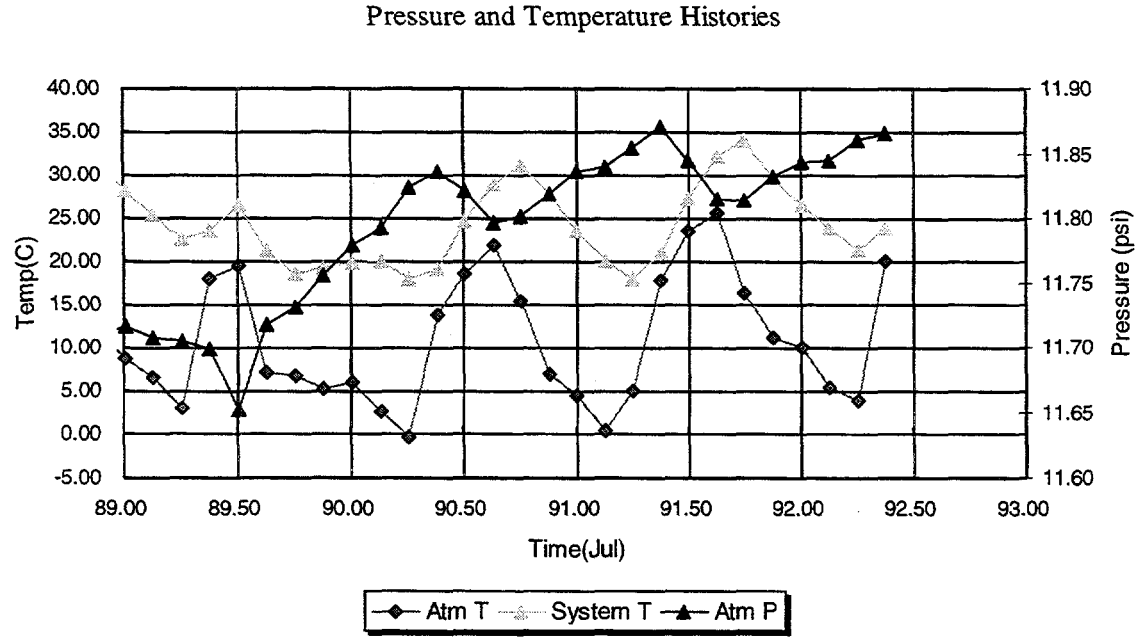

Figure 13. Measured pressure and temperature for the proof-of concept field test #1.

Table 4. Summary of field results. All data collected was inverted; Input concentration was held constant at average measured value for the test duration.					
	Test #1	Test #2	Test #3	Test #4	Test #5
x(m); calculated	3.5 +/- 0.4	3.5 +/- 0.4	3.7 +/- 0.6	2.9 +/- 0.2	2.5 +/- 0.4
x(m); actual	3.0	3.0	3.0	3.0	3.0
z(m); calculated	3.1 +/- 0.4	3.0 +/- 0.3	3.0 +/- 1.0	2.9 +/- 0.7	2.5 +/- 2.6
z(m); actual	3.0	3.0	3.0	3.0	3.0
r(m); calculated	0.34 +/- 0.08	3.E-02 +/ 3.E-03	0.16 +/- 0.09	0.19 +/- 0.02	0.27 +/- 0.06
r(m); actual	unknown	unknown	0.05	0.10	0.10

Prior to conducting subsequent tests, the source volume was decoupled from the tent and placed inside a rigid protective enclosure, and a bentonite layer was added between the membrane ground surface to assure a good seal. These changes in the test set-up minimized advective motion of the tracer gas for the remaining tests.

Before the second test could begin, the tracer gas that had diffused into the medium during the first test had to be removed. The natural decay of the tracer proved to be slow. A vacuum manifold that could be connected to the monitoring ports was devised and used to help extract the SF_6. Two and one-half months elapsed between the end of the first test and the beginning of the second test. The monitoring system was kept on during this entire time, although it was sampling atmospheric air during the extraction. Measured background concentrations of the tracer gas prior to the second test, ranged from 50 to 60 ppm.

Data collection for the second test was started on Julian day 150. The test duration was fourteen days, however, data collection was not continuous due to equipment failure. A belt in the B&K Analyzer failed as a result of high daytime temperatures at the site (maximum of 40° C was recorded). No data was collected from day four to day eight. In addition, heavy rains immediately prior to this test resulted in moisture infiltration near the defined leak. The localized saturated region restricted diffusion of the tracer gas into the medium, effectively reducing the leak size. The test integrity was further compounded by a leak in the source volume, resulting in a decrease in source concentration throughout the test duration. Figures 14 through 16 show plots of the collected data. Concentrations measured at the majority of the monitoring ports throughout the test period were not significantly above background levels. The accuracy of the data was further compromised by the B&K operating outside of its' desired temperature range. Even with the difficulties encountered during the test, inversion of the data provided surprisingly good results in locating the leak (within 0.5 meters – see Table 4).

Prior to beginning the third test sequence, the source volume was repaired, a cooling fan was installed in the scanning system, and the soil gas was vented using an extraction manifold. Two weeks elapsed between the end of the second test and the beginning of the third test.

Test sequence number three was initiated Julian day 177. After only 36 hours of data collection, an electrical storm damaged the photoacoustic analyzer, causing data collection to be terminated. Only four ports recorded increased concentrations of the tracer during this time frame. Figures 17 and 18 show the measured concentration histories. Figure 19 shows measured pressure and temperature histories. Table 4 gives the results of the inversion of this data. The leak was located within 0.7m of the actual position. The estimated leak radius was 0.11 m larger than the true radius.

The fourth test was conducted after repair of the B&K Analyzer. The valve was opened on Julian day 256 and data was collected for 7 days. Data is shown in Figures 20, 21 and 22. Analysis of the data provided excellent results. The leak was found within 0.14 m of the actual location, and the leak radius was estimated to be within 0.09 m of the true value.

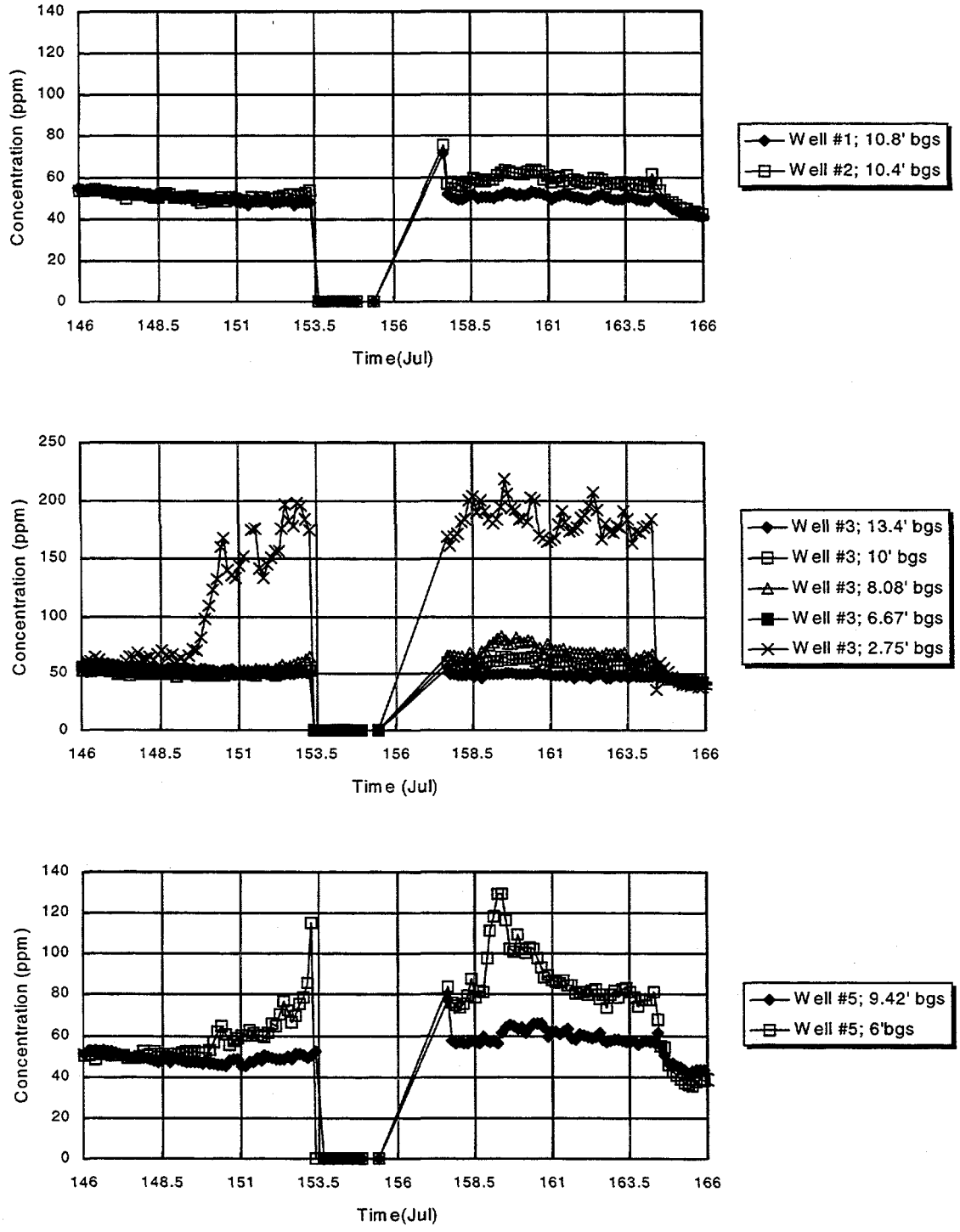

Figure 14. Measured concentration histories of the subsurface monitoring ports for the proof-of concept field test #2.

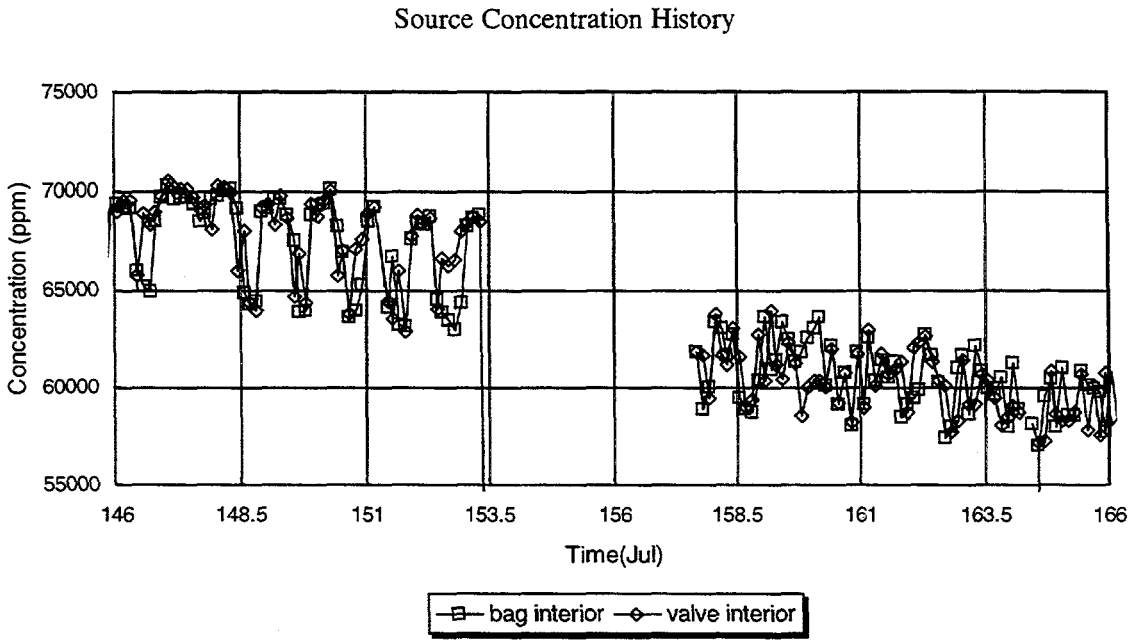

Figure 15. Measured concentration histories of the source volume ports for the proof-of concept field test #2.

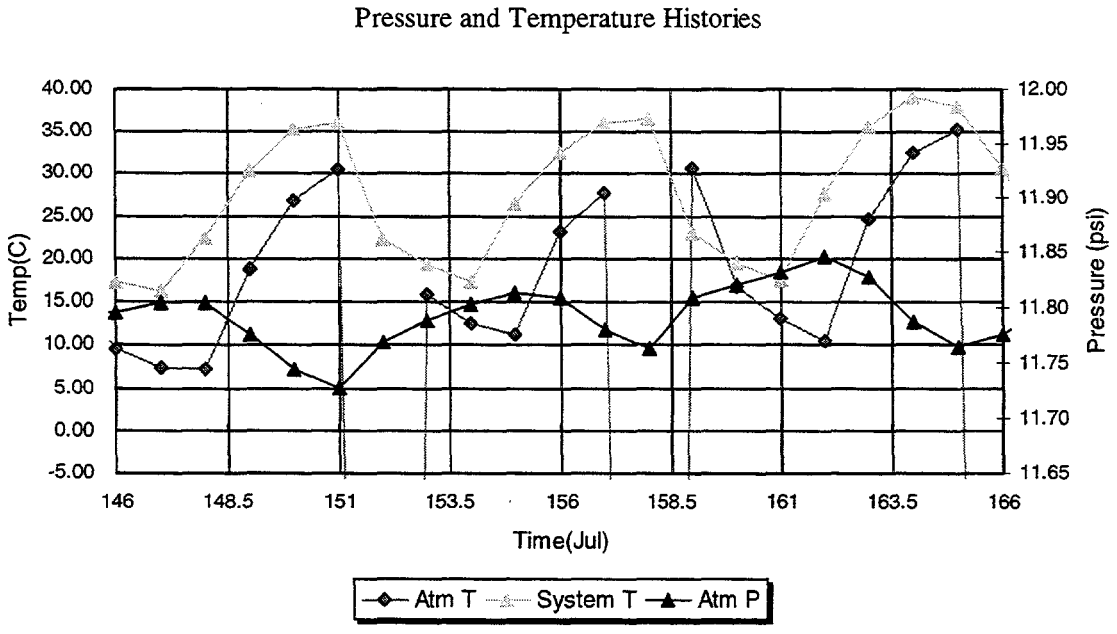

Figure 16. Measured pressure and temperature for the proof-of concept field test #2.

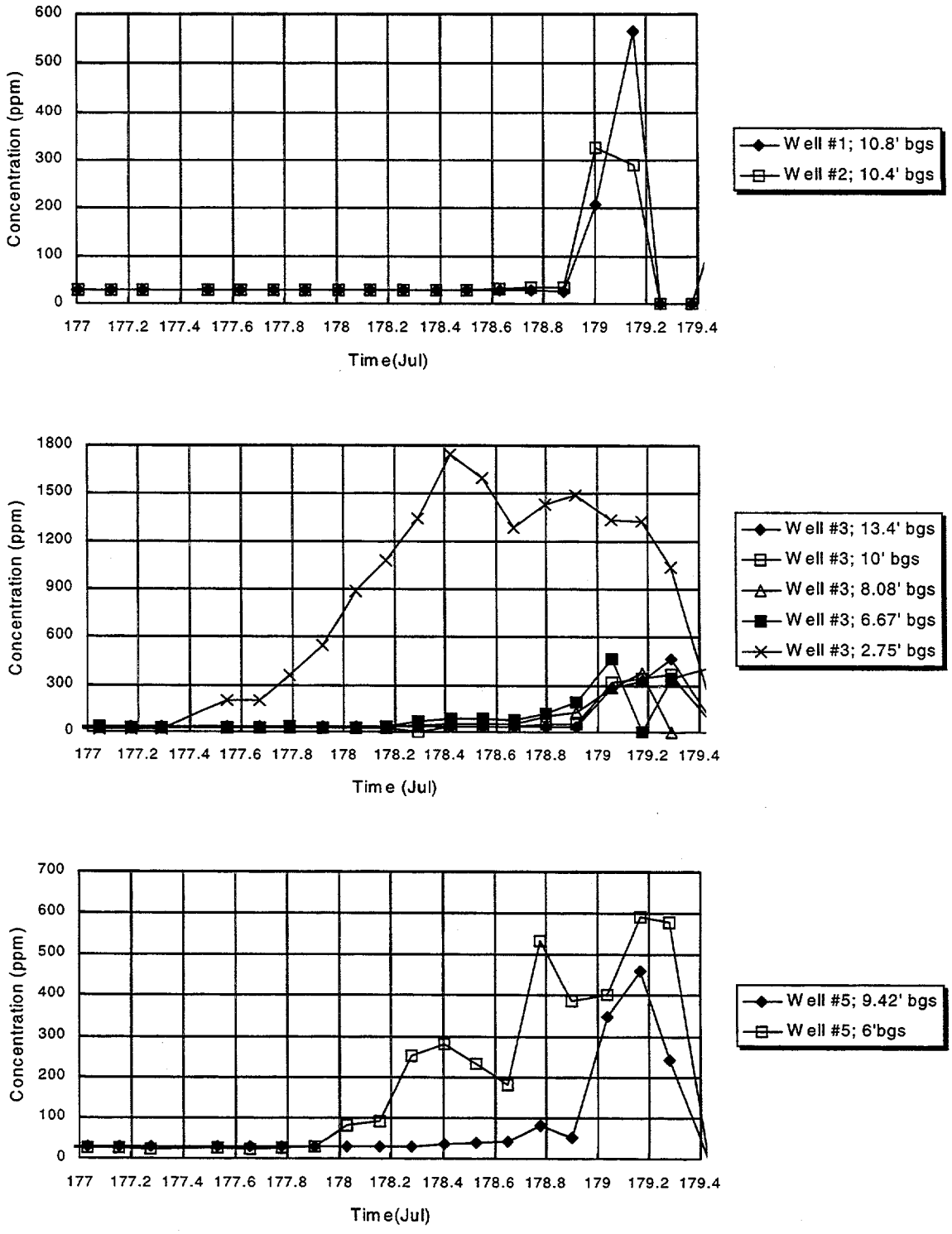

Figure 17. Measured concentration histories of the subsurface monitoring ports for the proof-of concept field test #3.

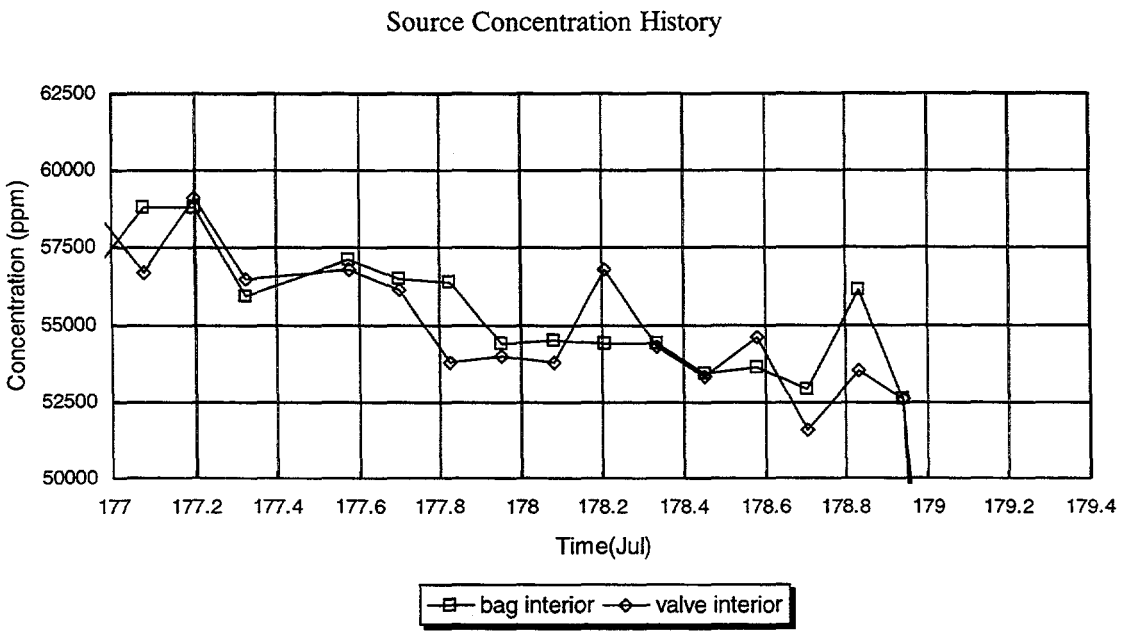

Figure 18. Measured concentration histories of the source volume ports for the proof-of concept field test #3.

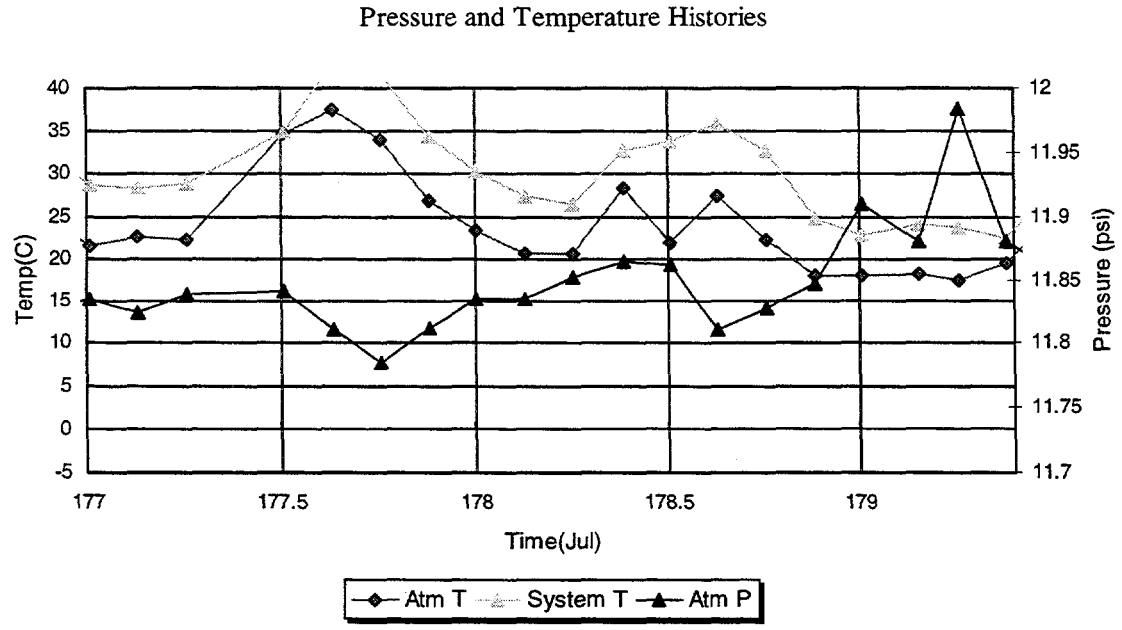

Figure 19. Measured pressure and temperature for the proof-of concept field test #3.

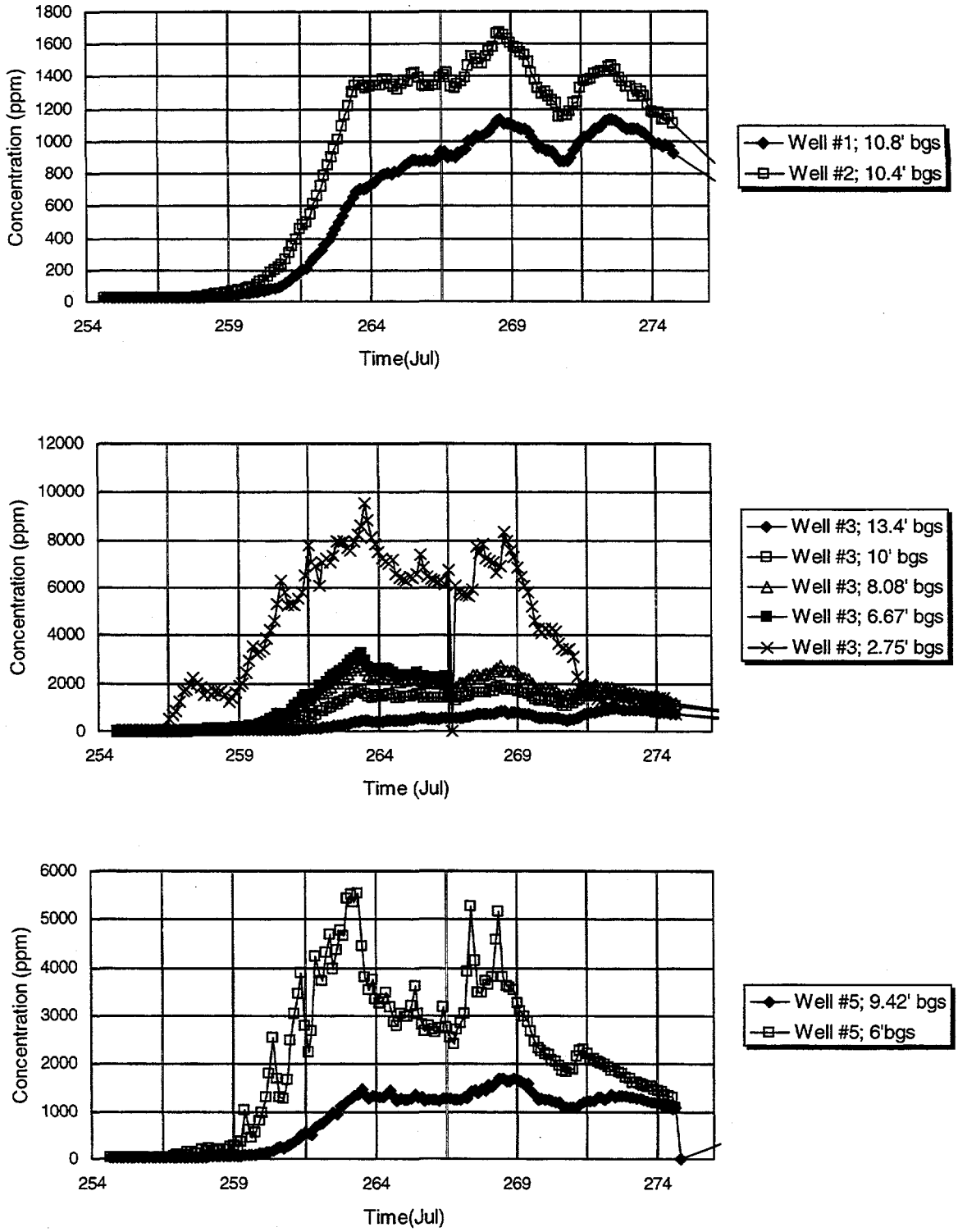

Figure 20. Measured concentration histories of the subsurface monitoring ports for the proof-of concept field test #4.

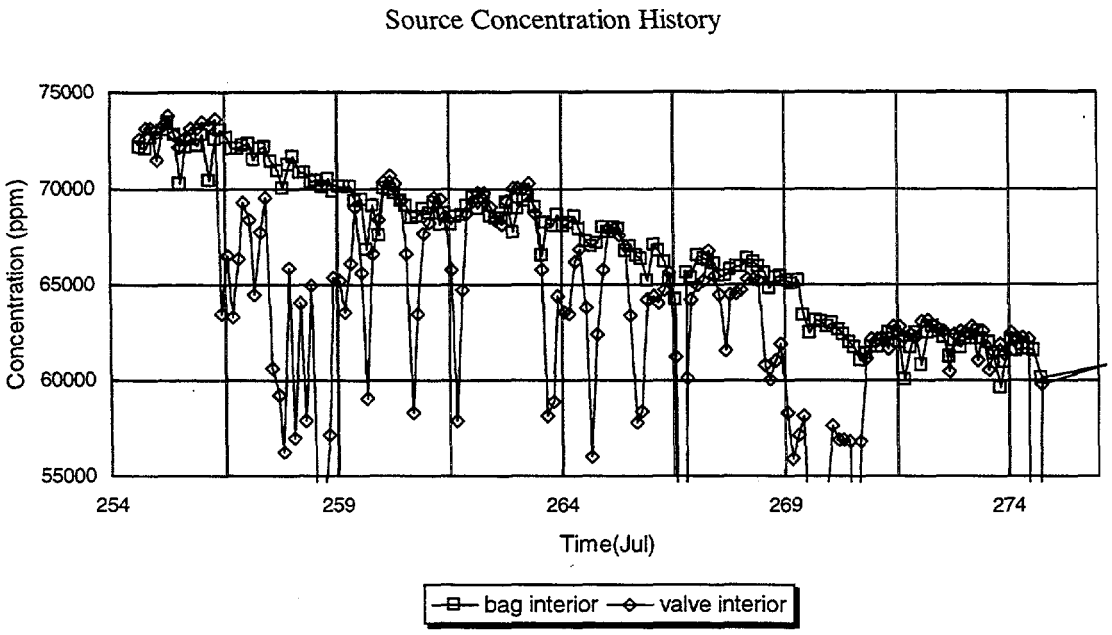

Figure 21. Measured concentration histories of the source volume ports for the proof-of concept field test #4. The valve interior port was partially plugged, resulting in an inadequate sample volume collection and erroneous readings throughout much of the test.

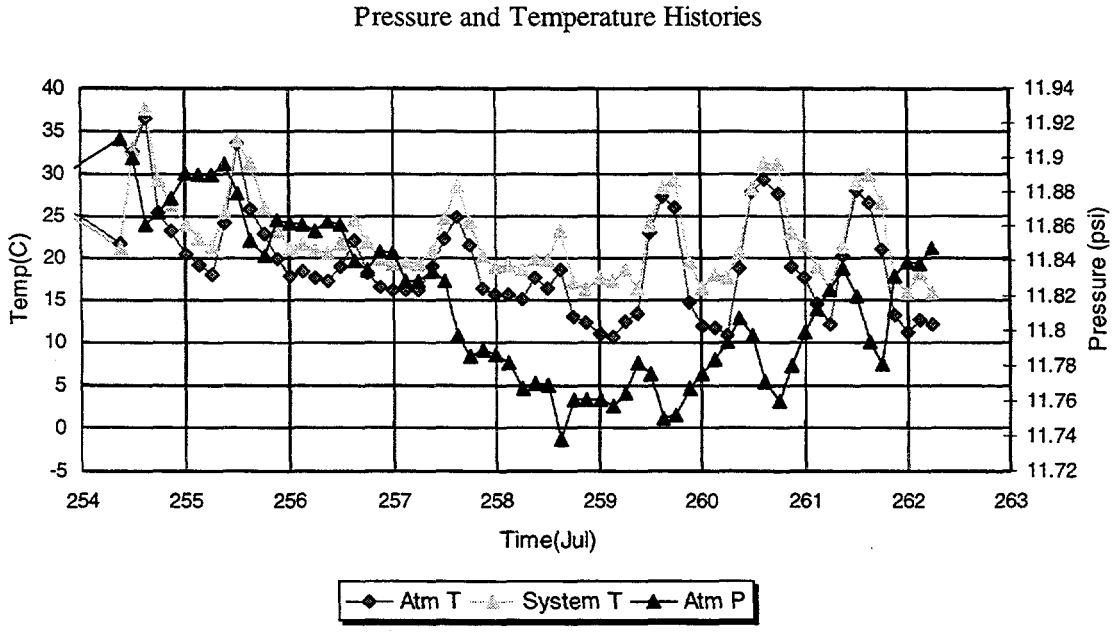

Figure 22. Measured pressure and temperature for the proof-of concept field test #4.

There was a two month time lag between test 4 and 5. However, data was continually collected at the site by the SEAtrace system. The fifth test sequence was initiated Julian day 32. Within days of the start of the test the source volume began to leak, causing a steady and significant decrease in the source concentration. Over a six-day period, the source concentration dropped almost 30%. Measured concentration, pressure and temperature histories are presented in Figures 23 through 25. Analysis of the data resulted in an estimated leak radius almost three times larger (0.17m) than actual size. This over-prediction is thought to be a direct result of the non-constant source concentration. Prediction of the leak location was reasonable although not as accurate as prior test. The calculated value was within 0.75 meters of the true location (Table 4).

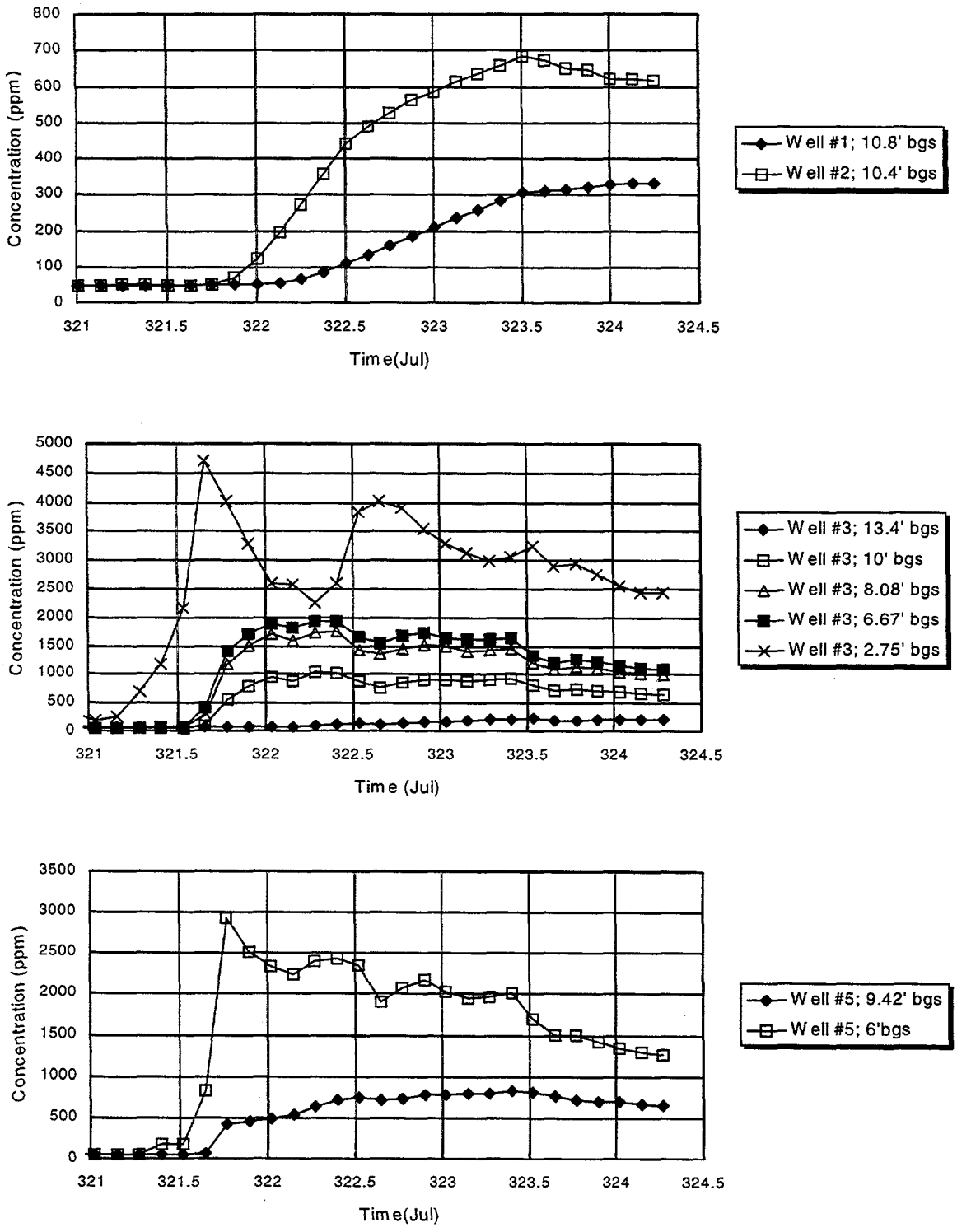

Figure 23. Measured concentration histories of the subsurface monitoring ports for the proof-of concept field test #5.

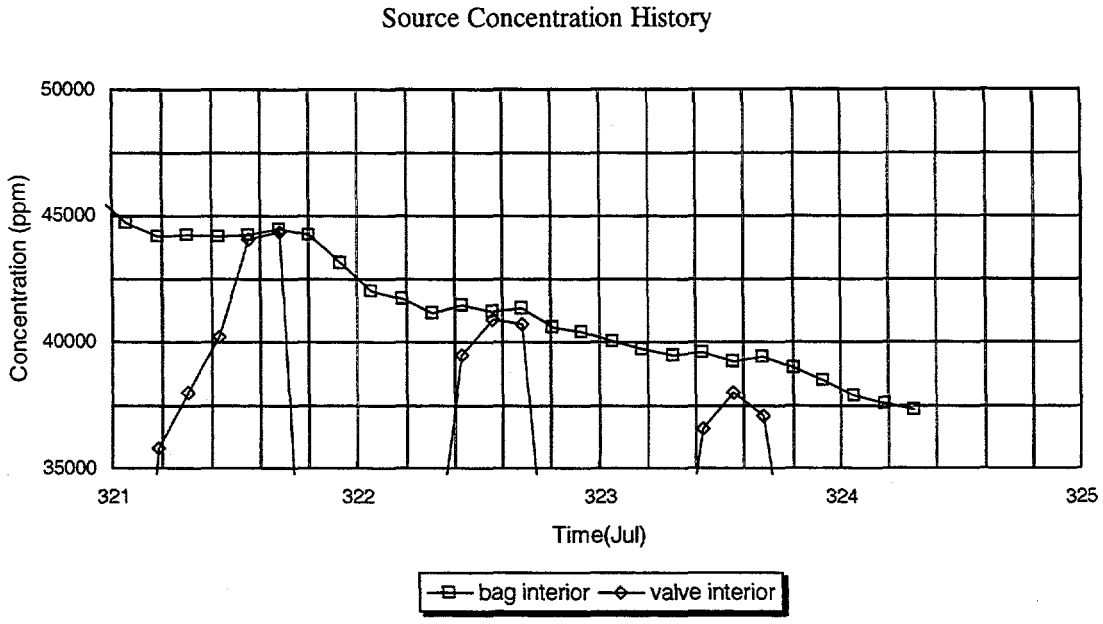

Figure 24. Measured concentration histories of the source volume ports for the proof-of concept field test #5. The valve interior port was partially plugged, resulting in an inadequate sample volume collection and erroneous readings throughout much of the test.

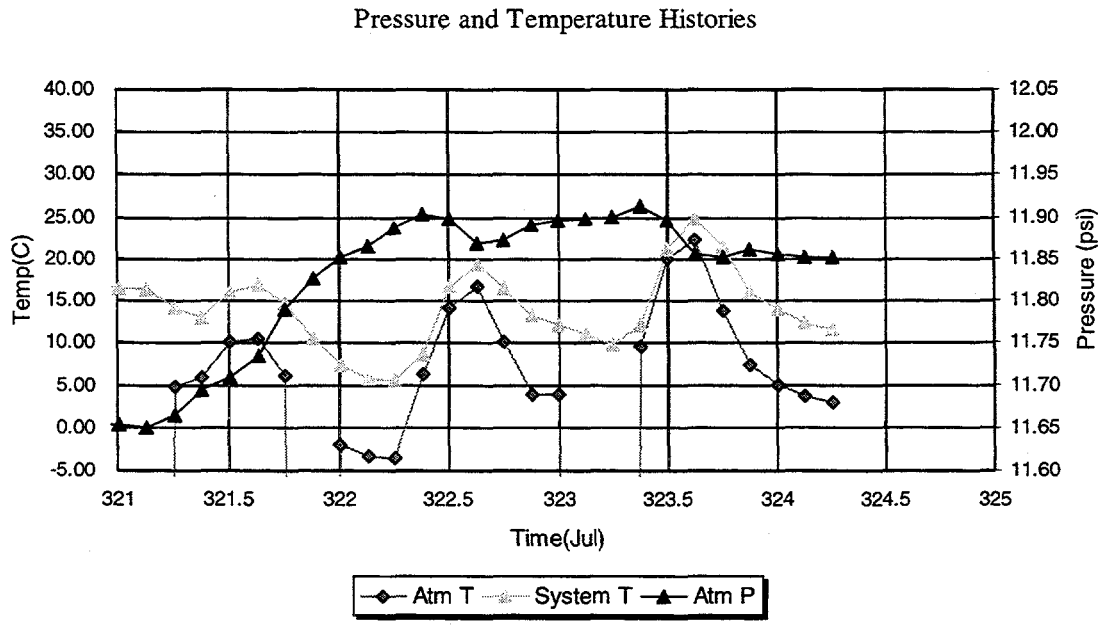

Figure 25. Measured pressure and temperature for the proof-of concept field test #5.

Intentionally Left Blank

IV. ADDITIONAL WORK REQUIRED

While the results of these field tests were very encouraging, creating a fully autonomous field unit capable of monitoring enough ports to cover a real barrier still requires a considerable amount of work. In particular, there are several significant changes which need to be made. These include:

- The amount of maintenance must be reduced. Replacing the B&K analyzer with a more rugged, simpler device would eliminate many of the problems seen in the field. If such a device is unavailable, the communications between the control program and the photoacousitc analyzer would need to be greatly improved. The ability to change the filters used with the system coupled with the ability to change the set tubing length for a given sample would both increase the accuracy of the measured concentrations in the medium and decrease the amount of time required to complete a full sample sequence.
- More rigorous diagnostics are required. Leak detection for the entire system is needed, such as is a flowmeter. Error messages must be expanded and the control program must be able to automatically adjust to certain errors insure data integrity.
- The scanning system needs to be enclosed in a temperature and dust controlled environment. This would minimize both inaccuracies in the measured results and reduce required maintenance on the system. The scanning system also needs to be expanded to handle at least 64 ports.
- The MultiScan^{TM} code needs to be more easily adaptable to field changes (port locations) and must account for "bad" data / no data in the output. A time stamp needs to be recorded for each port.
- The inversion code needs to be re-written to be more general. It needs to be able to accommodate different forward models, calculate the leak position in three dimensions, and must be more user friendly.
- The flux-limited forward model must further tested and incorporated into the inversion code.
- An intermediate processing package needs to be developed for the control program so that data will be processed in the field immediately after collection. This package should be able to automatically look at the data collected with the scanning system, adjust the data as necessary, create the input files required for the inversion code, and call the inversion code to perform data analysis.
- Additional modeling work needs to be performed to analyze how different assumptions used in the forward model will effect the systems results.

A full scale demonstration of the system needs to be performed upon completion of these improvements. This demonstration should be performed under well controlled conditions with leaks of known locations, sizes and geometries.

Intentionally Left Blank

V. SUMMARY

The SEAtrace™ system offers an integrated, turnkey monitoring and assessment solution for subsurface barrier installations. There are presently no technologies in regular use which provide a quantitative, real-time indication of the location and size breaches in barriers, either immediately after installation or during the course of their lifetime. The SEAtrace™ system is applicable to impermeable barrier installations above the water table. The system requires that multiple vapor sampling points be installed around the perimeter of the barrier, and one or several tracer injection points be emplaced inside the contained volume. Vapor point installation can be accomplished in virtually any geologic media, using a variety of techniques. Any barrier type, including grout wall, cryogenic, viscous, and sheet barriers, is a viable application for the SEAtrace™ monitoring system.

The global optimization methodology, coupled with real time autonomous soil gas sampling and analysis, provides a capable and sophisticated barrier assessment system. Comparison of the methodology's results with uniform diffusion modeling predictions indicates good locating (within 0.5 m in most cases) and sizing (within 20 percent) capabilities. Locating accuracy is closely coupled to the uncertainties in sample port and barrier location.

The proof-of-concept field tests performed evaluated the SEAtrace™ system's effectiveness in non-ideal conditions. Even with all of the difficulties with the tests, SEAtrace™ was able to consistently predict the location of the leak to within 0.75 m , and the leak radius to within 0.15 m. Additionally, the measured concentration histories at points equi-distant from the leak were very similar, confirming that the diffusion was roughly spherical and the field monitoring system continuously collected data for long periods of time (several months), under very harsh conditions. The MultiScan™ system was in the field over a total of 11 months. It collected data over the majority of this time. Weather conditions were severe. Temperatures were unseasonably high (>40 C). Monsoon moisture was intense, with severe thunderstorms, winds and cloud bursts. Power to the site was lost on several occasions. October saw unseasonably cold weather accompanied with snow. Wells drilled near the site (< 80' away) caused ground vibration. Still, the system functioned extremely well. There was only one occasion which required the system to be removed from the field for repair although regular maintenance was required.

Intentionally Left Blank

REFERENCES

Betsill, J. D. and Gruebel, R. D. "VAMOS, The Verification and Monitoring Options Study, Current Research Options for In-Situ Monitoring and Verification of Contaminant Remediation and Containment within the Vadose Zone." TTP#AL2-2-11-07. May 1995.

Jeiser, H. "Subsurface Barrier Verification Technologies." BNL-61127. Brookhaven National Laboratory, June 1994.

Ounes, Ahmed. "Application of Simulated Annealing to Reservoir Characterization and Petrosphysics Inverse Problems." Ph.D. Thesis. New Mexico Institute of Mining and Technology, 1992.

Falta, R., Pruess, K., Finsterle, S., Battistelli, A.; Earth Sciences Division, Lawrence Berkeley Laboratory, University of California, Berkeley, LBL36400; 1995

Intentionally Left Blank

APPENDIX A: THE MultiScan™ DATA ACQUISITION SYSTEM

The MultiScan™ system is an antonomous field monitoring system that performs automatic real time measurement of soil gas composition and pressures. Up to 32 sampling ports in either single or multi-point wells can be monitored. The system is very rugged and can function unattended for extended periods of time (months). MultiScan's™ hardware and software is modular in design allowing maximum flexibility. Additional monitoring ports may be added in banks of 16. Additional soil property measurements (such as matric potential or temperature) can be added at all or some of the ports. Additional chemical sensors (e.g., oxygen sensors) can be incorporated in the system or different equipment can be used to perform the chemical analysis.

The real-time, long-term unattended operation of MultiScan™ is achieved by utilizing a Bruel and Kjær (B&K) model 1302 photoacoustic gas analyzer controlled via a lap-top computer. All data collected, including the systems self-diagnostic information, is stored in the computer. Data acquisition is performed by American Advantech's Adam™ modules. Solenoid valves in the manifold system sequentially isolate up to 32 sample ports. The manifold is controlled by two SEA-designed multiplexer cards. The isolated sample port is connected to either the B&K analyzer or a high-precision Honeywell pressure transducer via two three-way solenoid valves. Soil gas samples are drawn into an intermediate tedlar sample bag by a Brailsford diaphragm pump. The B&K uses its own pump to drawn the sample from the tedlar bag into its' test chamber. The tedlar bag, the manifold and its associated tubing, and the tubing from the MultiScan™ system to the subsurface port are purged by sequencing the Brailsford pumps. A schematic of the MultiScan™ system is depicted in Figure A-1. Mechanical and electrical connections are shown.

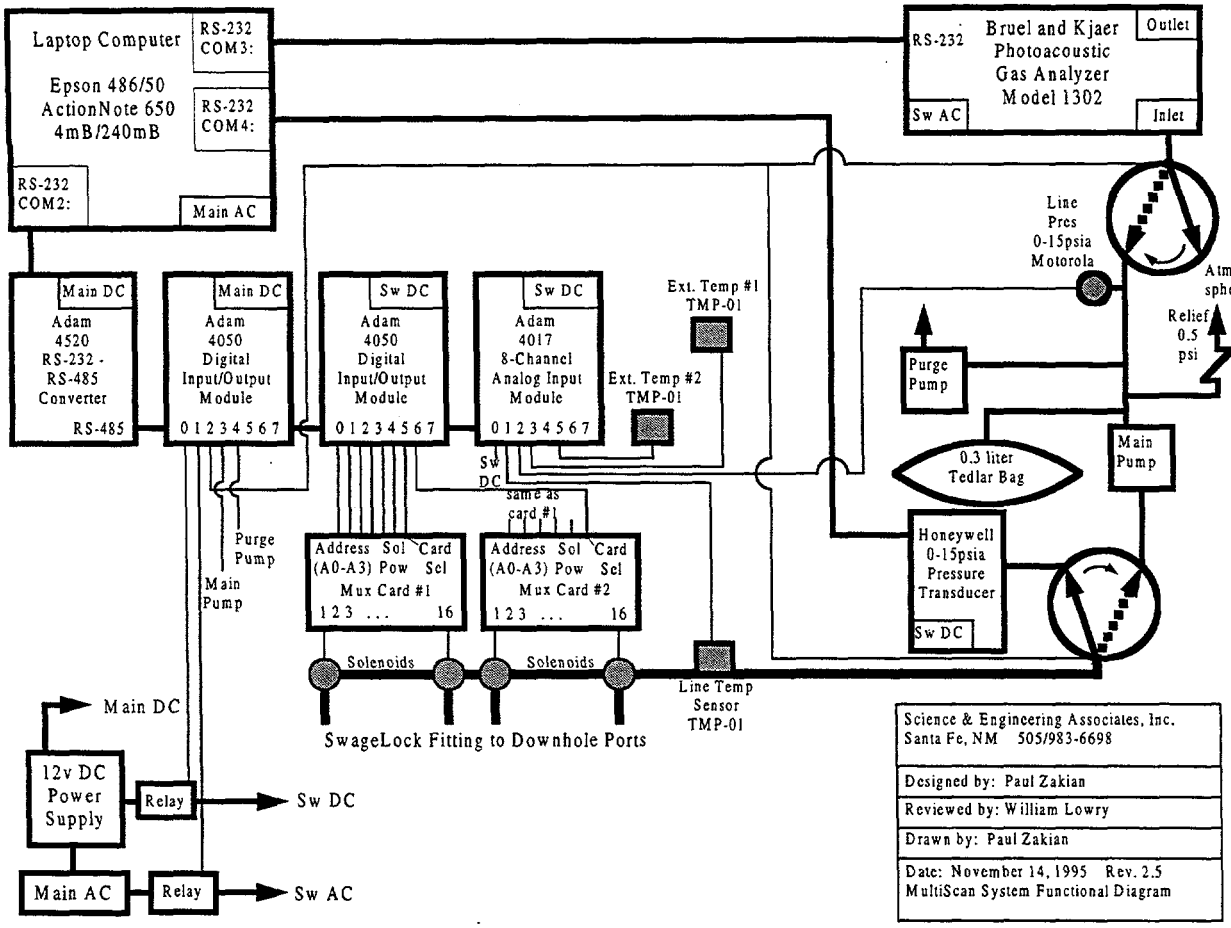

Figure A-1. Schematic of the MultiScan™ system.

For this barrier verification and monitoring, the Bruel and Kjær (B&K) gas analyzer identifies and measures the concentrations of three gases: trichoroethylene (TCE), carbon dioxide (CO_2), and sulfur hexafluoride (SF_6). The unit operates on photoacoustic principles where an intense infrared light is shined on the gas collected in a sample chamber and very sensitive microphones "listen" to the response of the gas to the light. The analyzer can read concentrations up to five orders of magnitude from the lower detection limit of the gas, to within 10 percent accuracy. The SF_6 filter has been specifically calibrated to measure concentrations between 1 and 80,000 ppm. The B&K unit has an operating temperature range of 5 to 40°C with a temperature influence of ±10 percent of the detection threshold per °C. Performance reliability of the analyzer is ensured by a series of self tests. If a problem is detected, the appropriate error message is recorded by MultiScan's™ control computer.

MultiScan™ performs numerous diagnostic tests to assure continuous sample quality. To assure gas samples are not diluted by leaks in the systems plumbing, the manifold and tedlar bag are always kept at a slight overpressure. A vacuum test is performed on the manifold before each gas analysis sequence is initiated to determine if there are any leaks in the plumbing. To assure adequate purging between measurements, an atmospheric sample is analyzed at the beginning of each sequence. The pressure and temperature in the manifold are monitored to assure these

parameters are within the hardwares' specified operating ranges. Monitoring the pressure of the intermediate sample bag while collecting a sample can be indicative of the integrity of the sample bag, pump, and pressure sensor. Finally, any errors recorded by the B&K analyzer are collected and stored.

The control software of the MultiScan™ system was written in QuickBasic. It is very robust, and will try to recover from most errors (it will not recover from power failure). Any programming crashes are signaled by an entry in an error file named ERROR.DAT. Errors due to the program are recorded using the QuickBasic error codes. Errors due to the B&K analyzer are recorded using the analyzers error codes. Errors due to the systems' hardware are specific to the portion of the code where they were encountered.

Flow diagrams of the MultiScan™ code, including all significant subroutines and functions, are included in figures A-2 through A-25. The main program flow diagram is given first, followed by subroutines and functions (in alphabetical order). A brief description of each routine is included. In addition to the routines listed, there are several switch subroutines. These routines are used only to turn a device on or off.

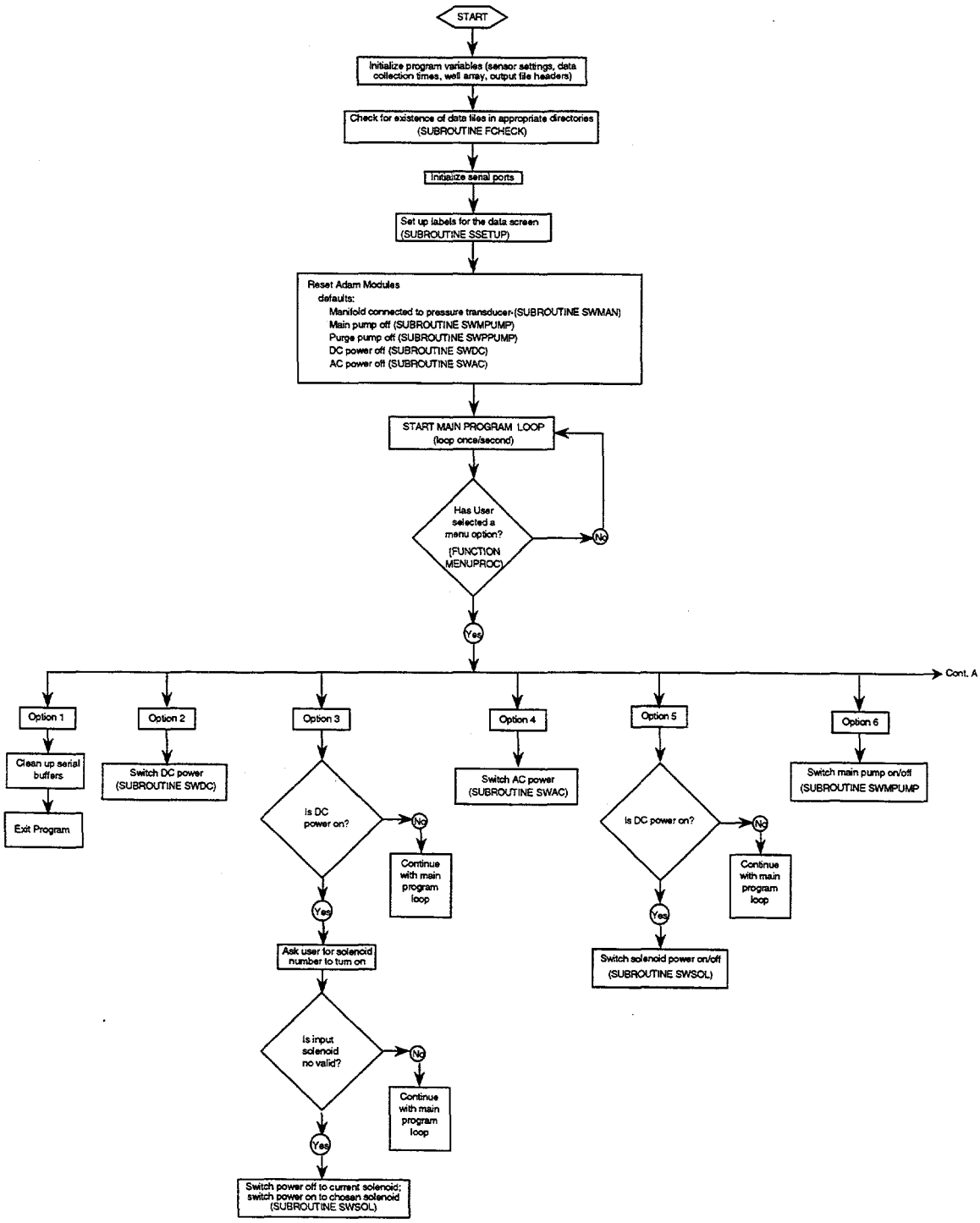

Figure A-2: Flow chart of the main program used in the MultiScan™ system.

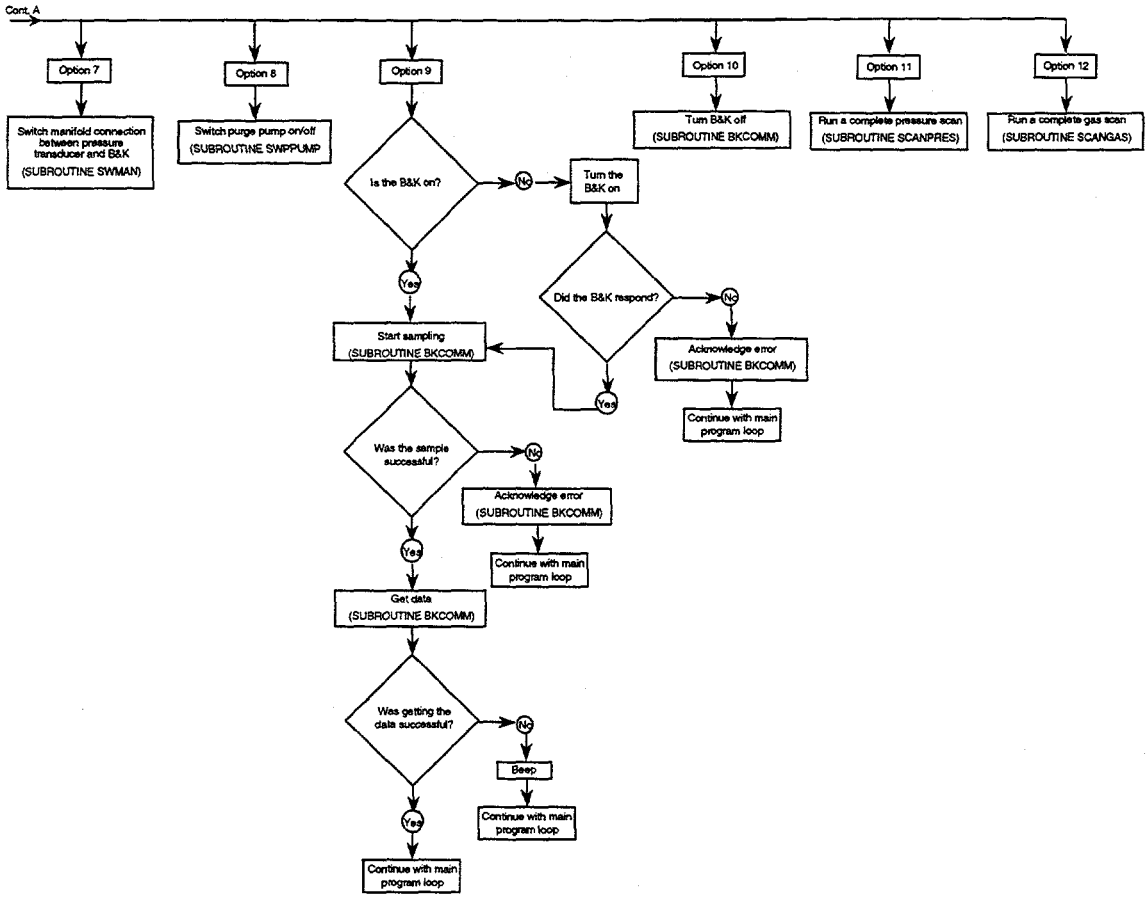

Figure A-3: Flow chart of the main program used in the MultiScan™ system (continued).

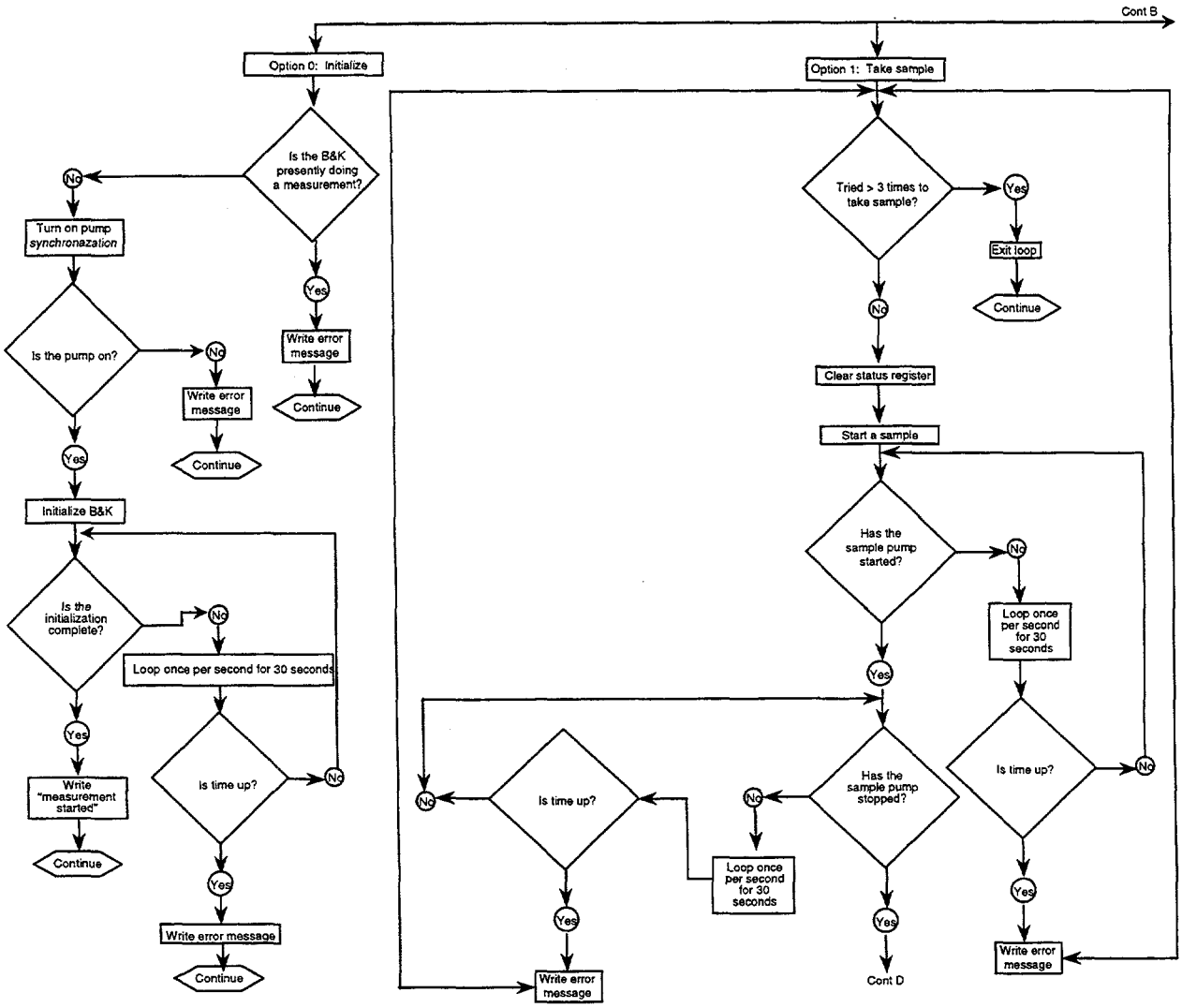

Figure A-4: Flow chart of the subroutine Bkcomm (handles communication with the B&K analyzer).

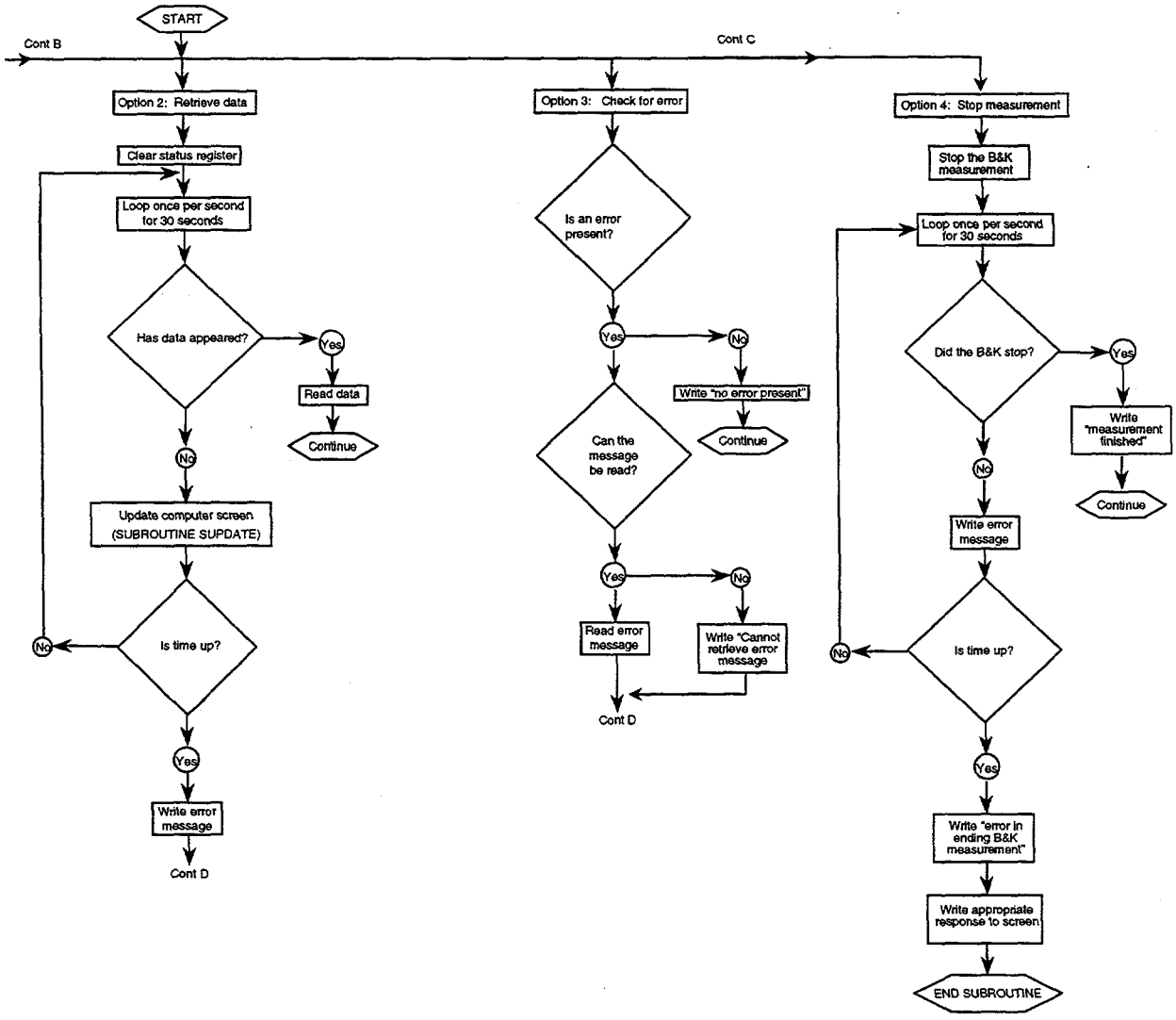

Figure A-5: Flow chart of the subroutine Bkcomm (continued).

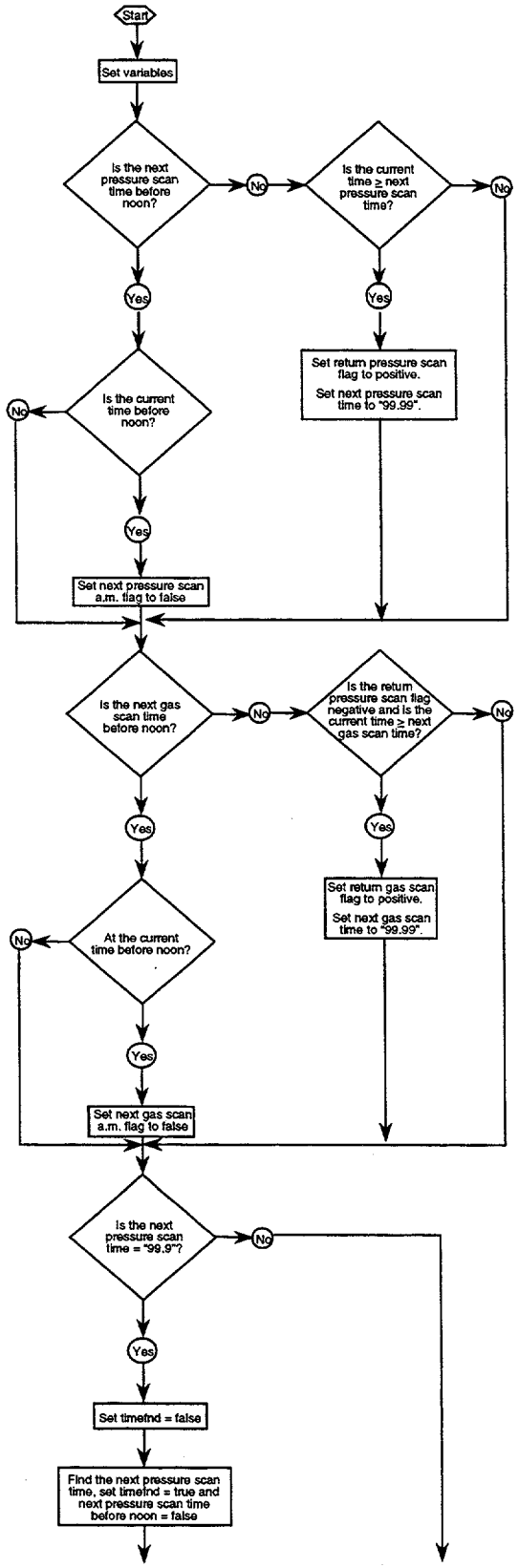

Figure A-6: Flow chart of the function Cktime (Checks to see if it's time for a pressure or gas scan).

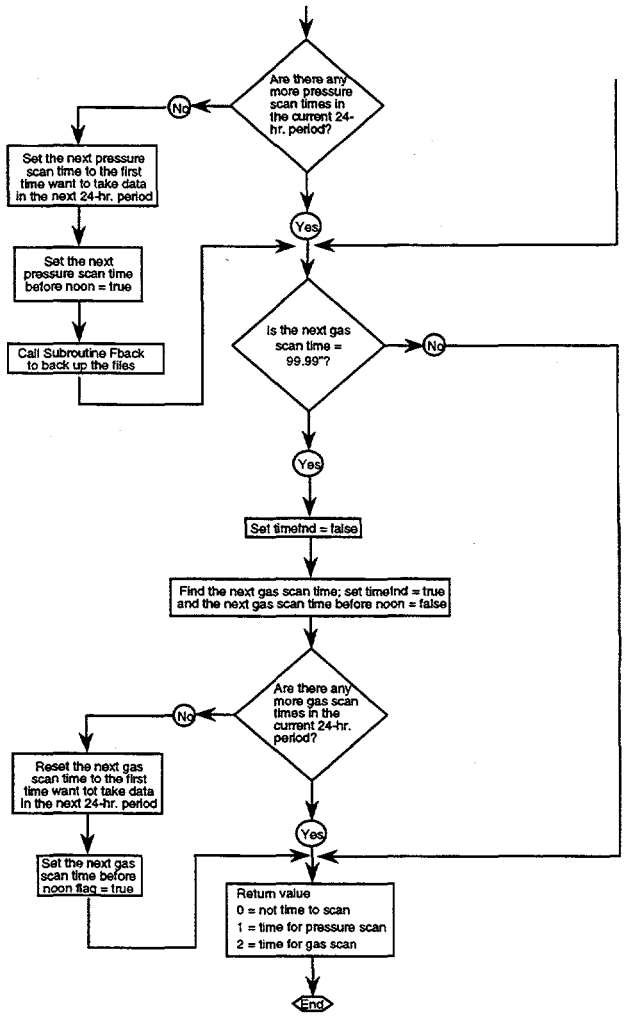

Figure A-7: Flow chart of the subroutine Cktime (continued).

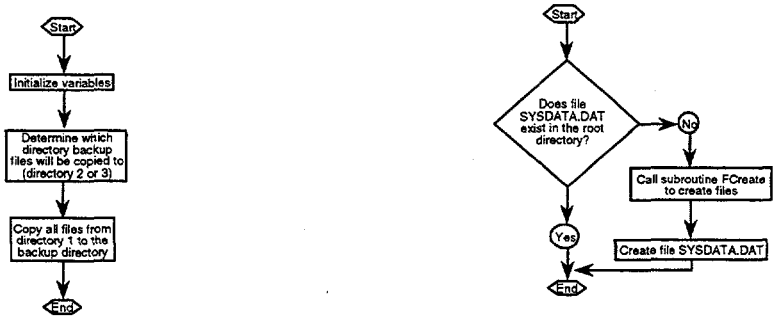

(a) (b)

Figure A-8: Flow chart of the subroutines (a) Fback – backs up all data files once per day; and (b) Fcheck – Checks for the SYSDATA.DAT file in the root directory. If the file doesn't exist it will create new data files with appropriate headers.

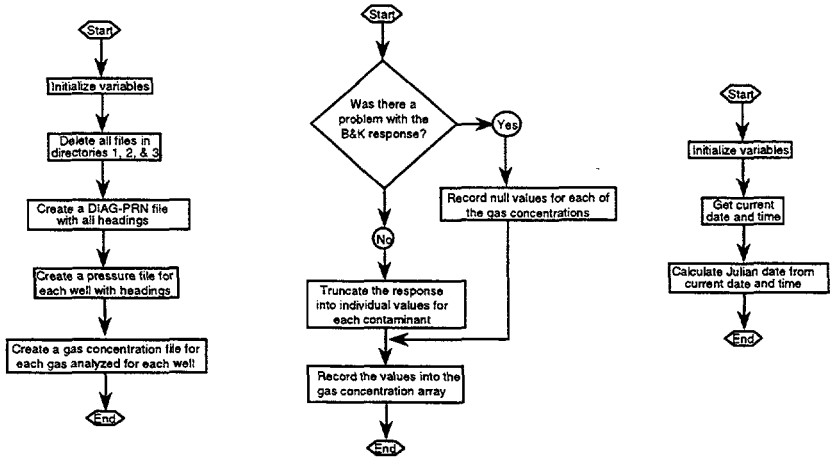

(a) (b) (c)

Figure A-9: Flow chart of the subroutines (a) Fcreate – Deletes old datafiles then creates new files according to well data structure specified in the program, and (b) GasConc – Converts text responses from the B&K into numerical concentrations; and the function (c) JulTime – Calculates a fractional Julian date/time from the current date/time.

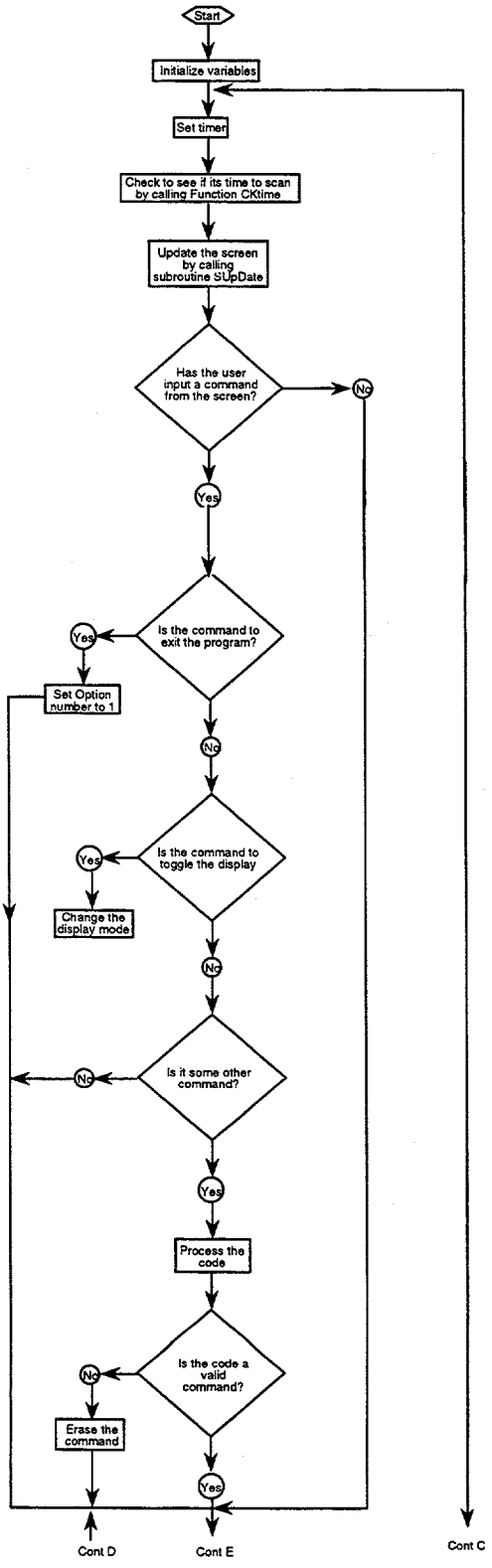

Figure A-10: Flow chart of the function MenuProc (processes user menue selections).

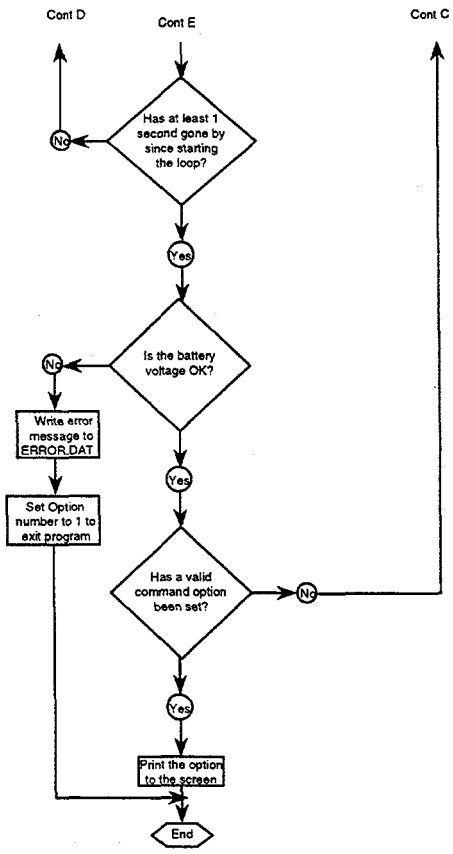

Figure A-11: Flow chart of the subroutine MenuProc (continued).

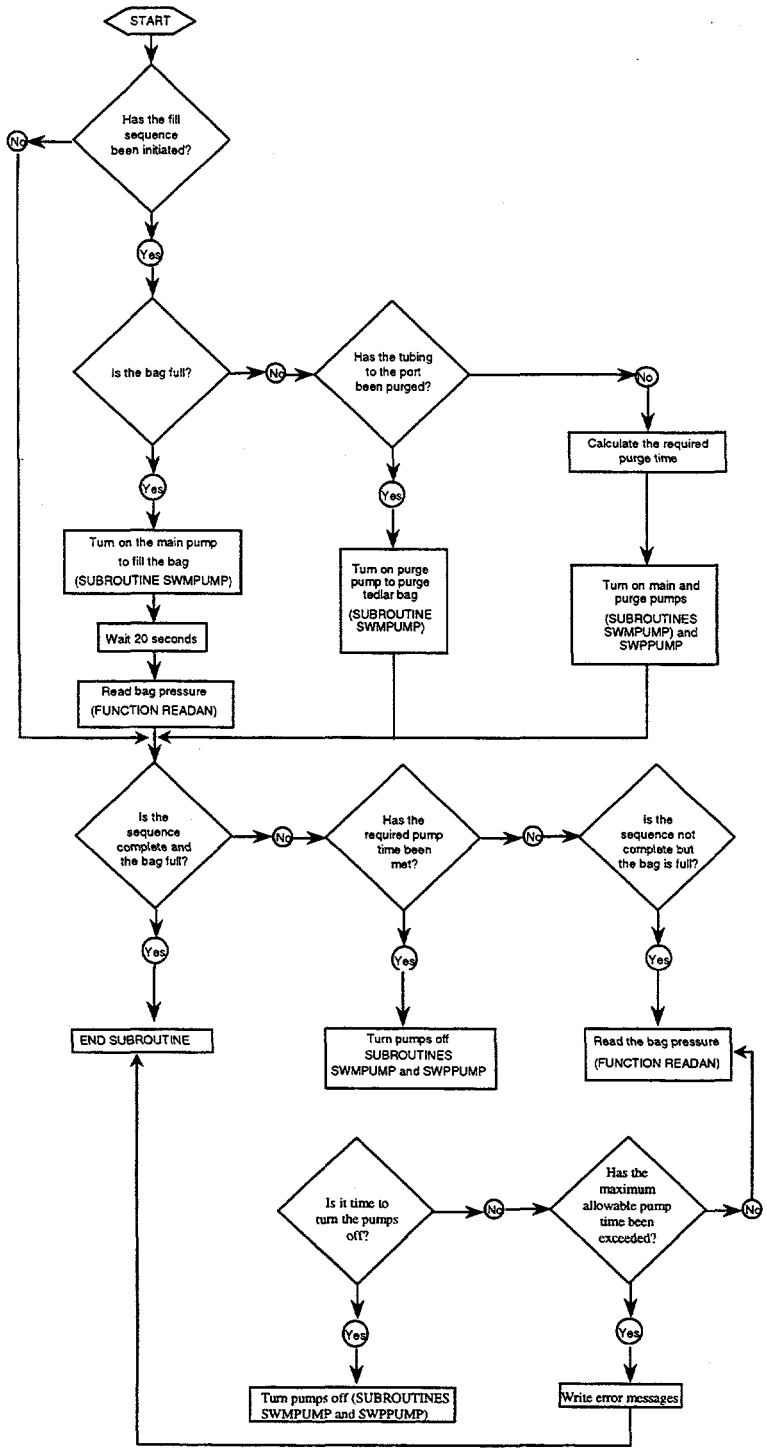

Figure A-12: Flow chart of the subroutine Newbag (Controls the pumping logic to bring samples into / out of the tedlar sample bag).

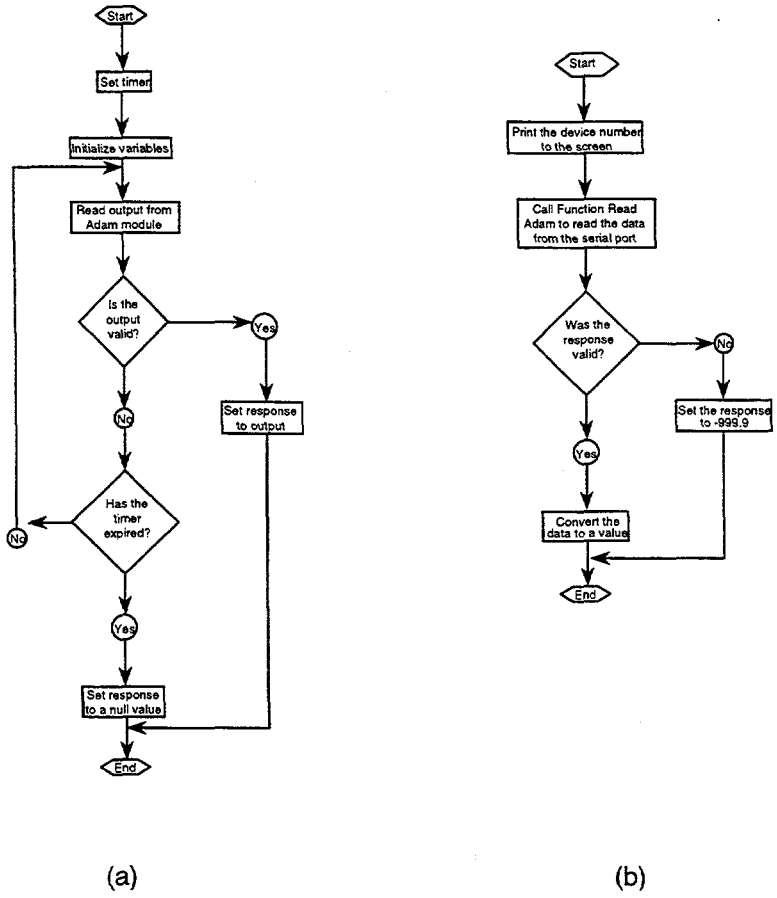

Figure A-13: Flow chart of the functions (a) ReadAdam – reads the Adam modules raw data from the serial port; and (b) ReadAN – reads the Adam analog input module.

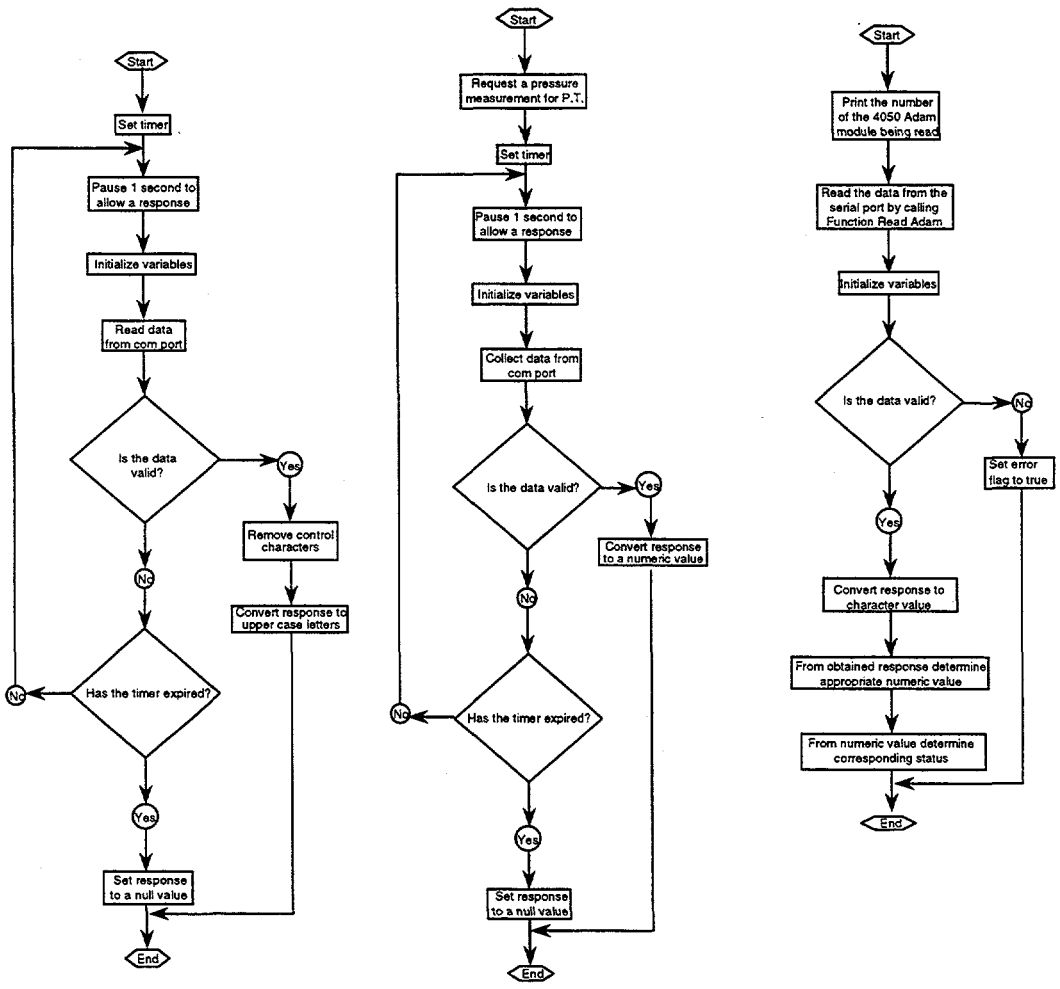

(a) (b) (c)

Figure A-14: Flow chart of the functions (a) ReadBK – reads raw B&K data from the serial port, and (b) ReadHW – reads the Honeywell pressure transducer, and the subroutine (c) ReadStat – gets digital I/O status from the Adam 4050 modules.

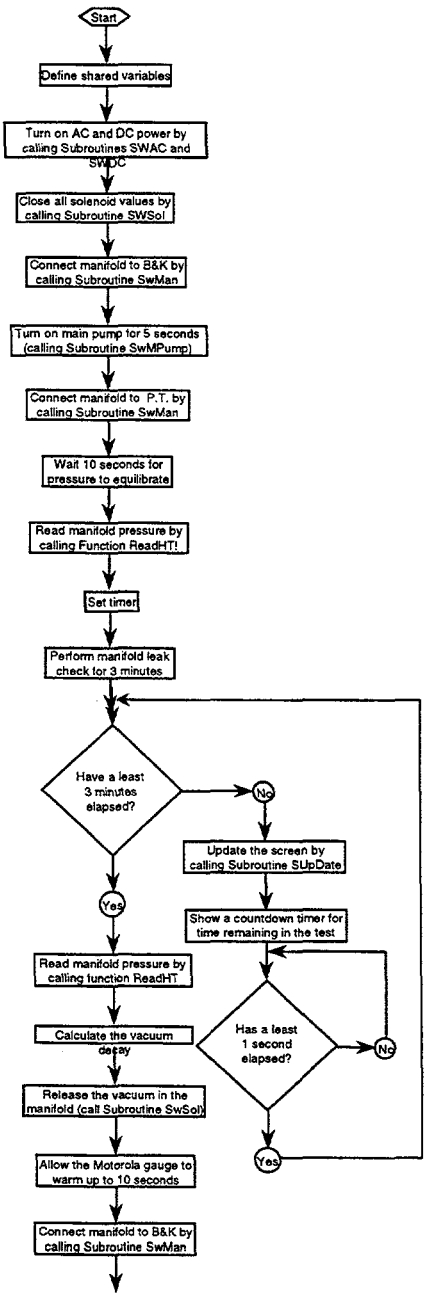

Figure A-15: Flow chart of the subroutine ScanGas (Measures concentration of gas for each port in the well definition array and writes the results to datafiles.

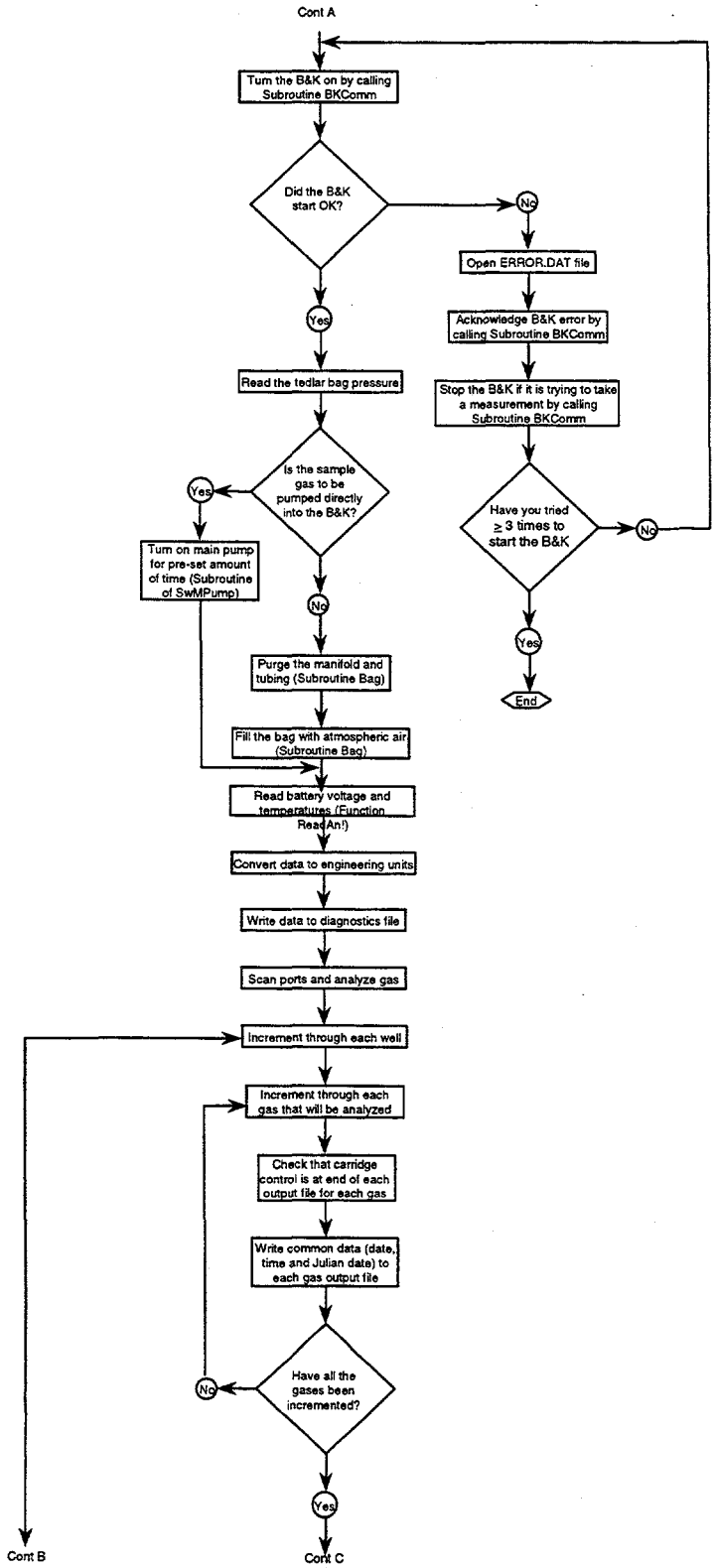

Figure A-16: Flow chart of the subroutine ScanGas (cont).

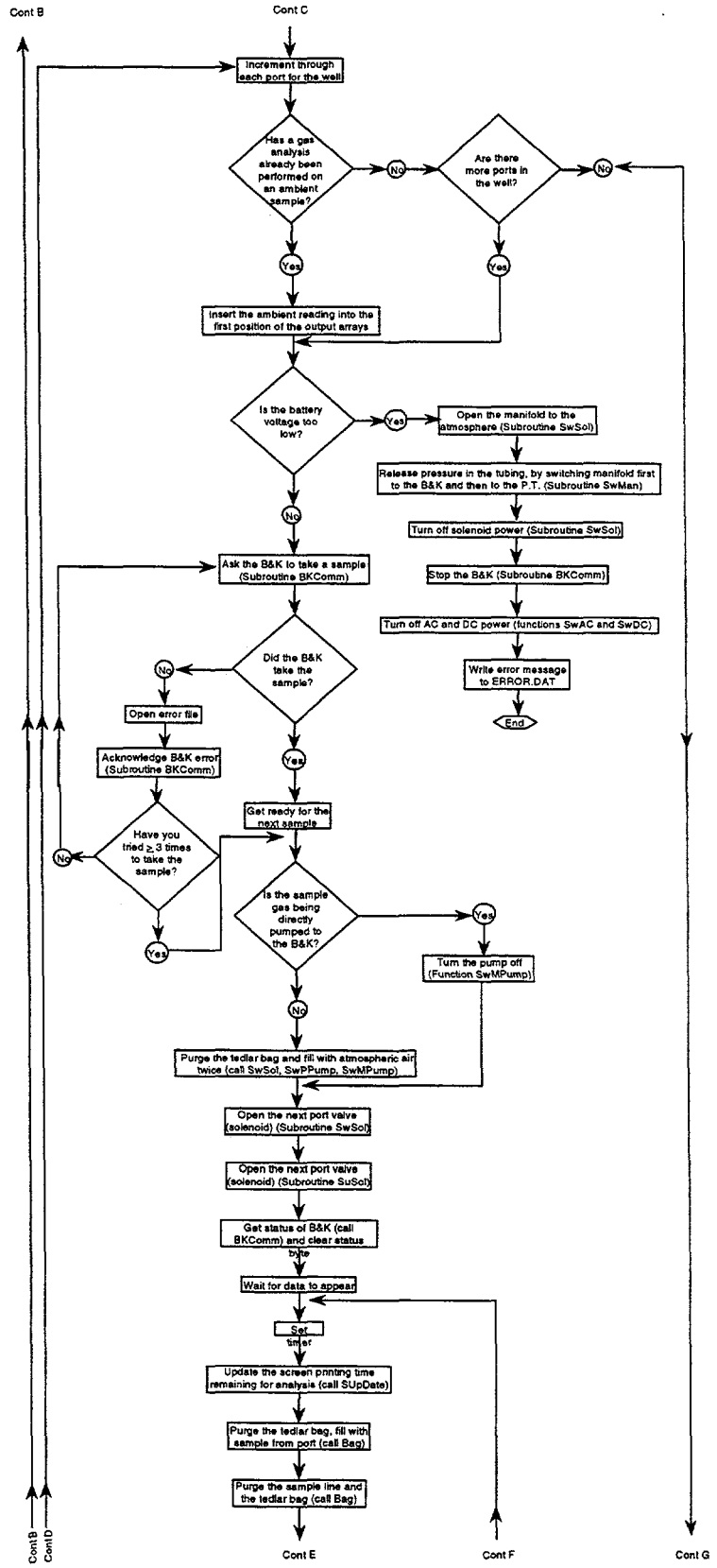

Figure A-17: Flow chart of the subroutine ScanGas (cont).

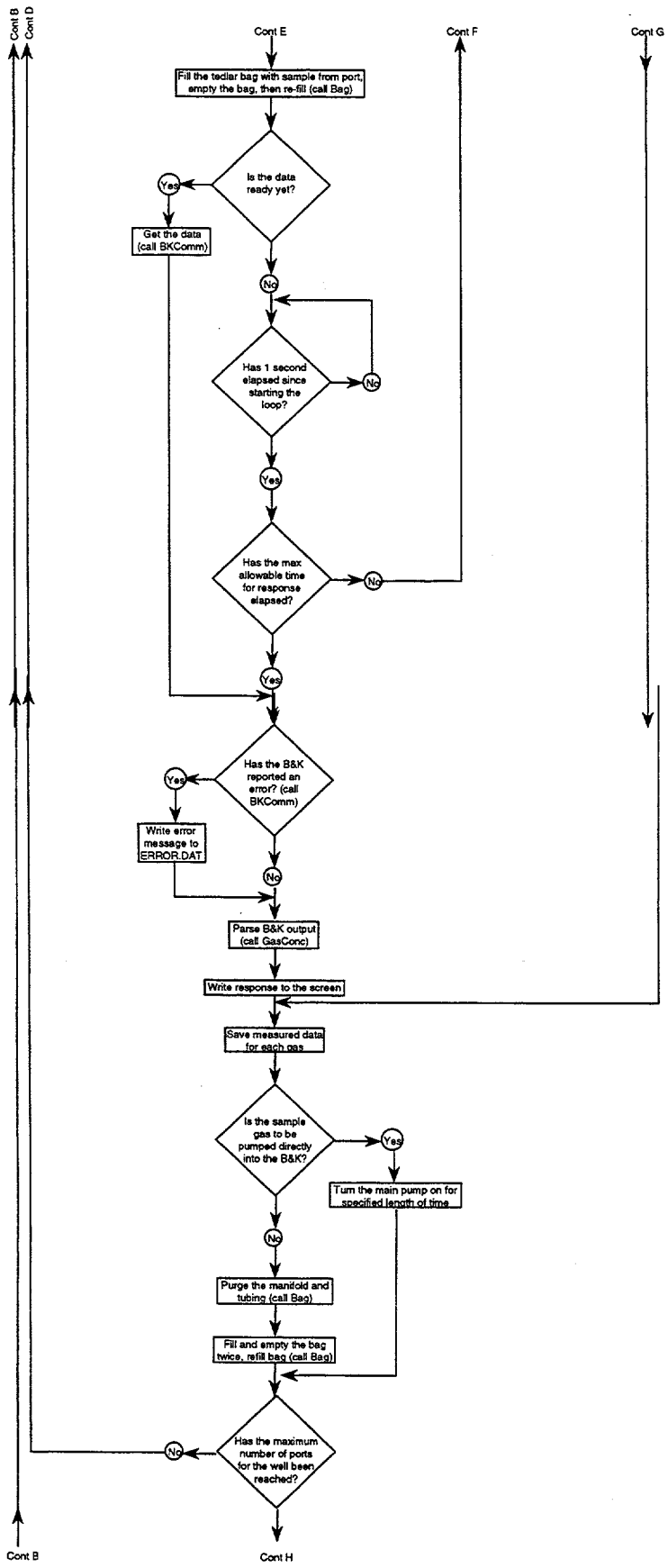

Figure A-18: Flow chart of the subroutine ScanGas (cont).

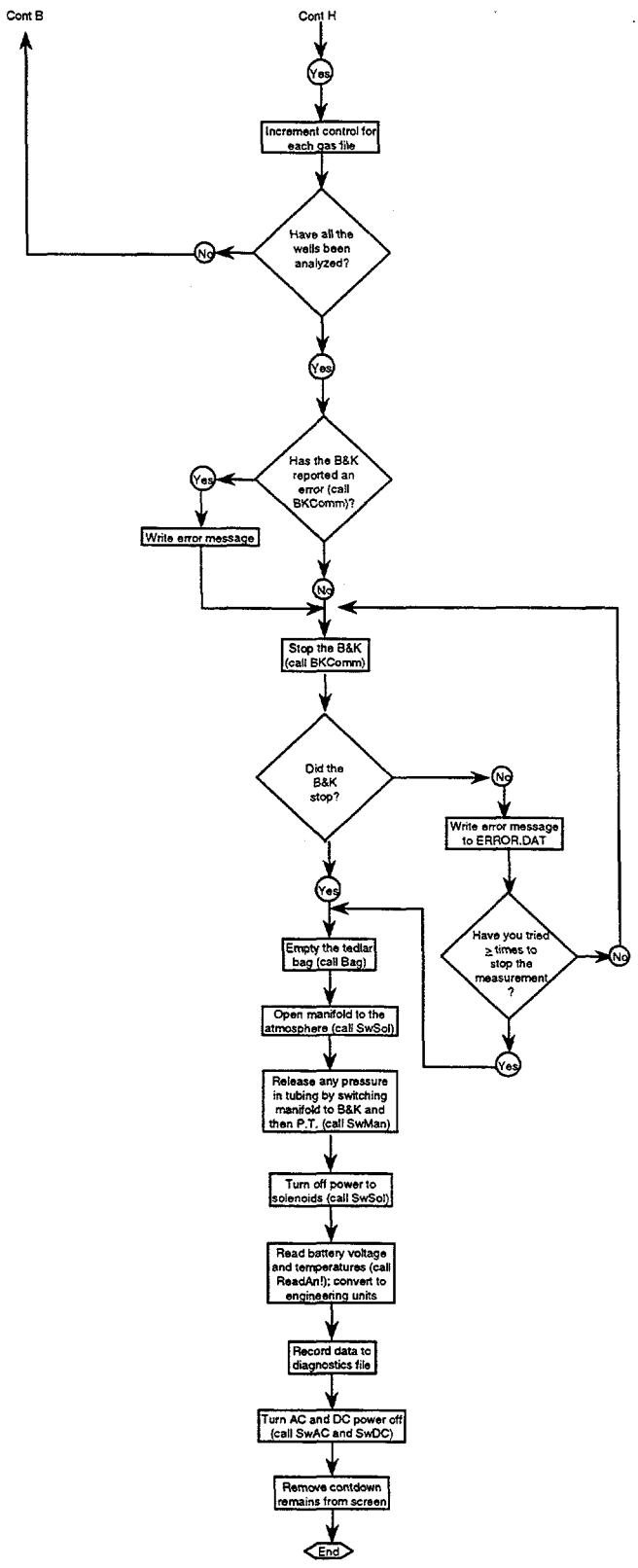

Figure A-19: Flow chart of the subroutine ScanGas (cont).

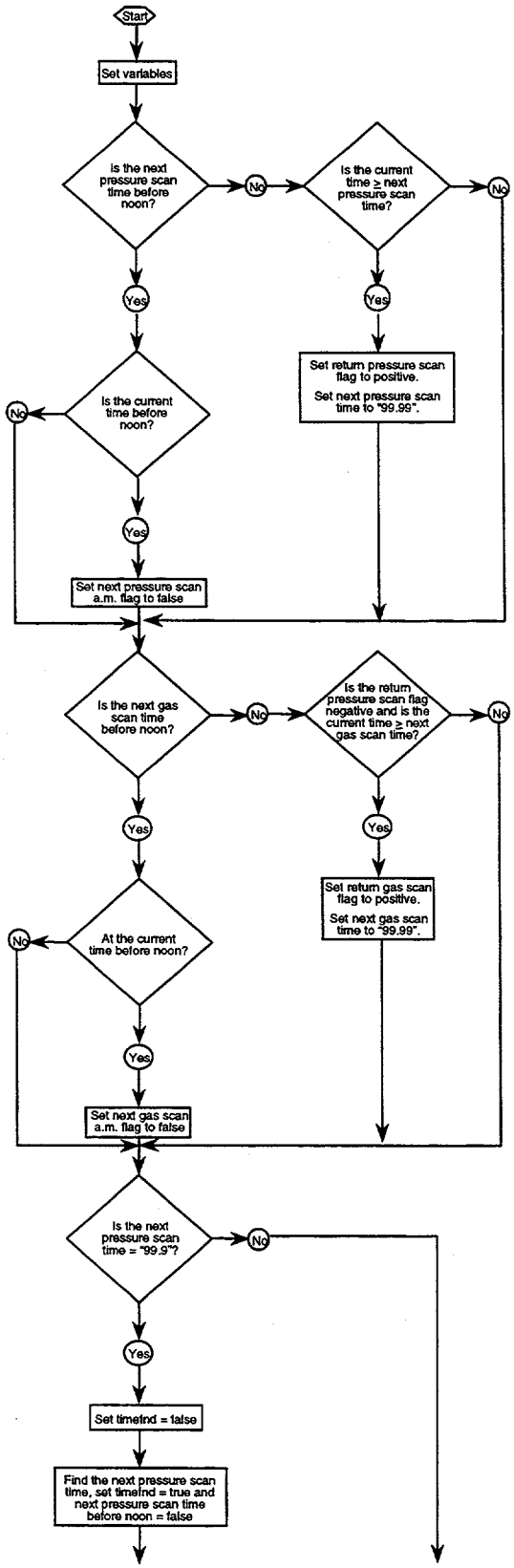

Figure A-20: Flow chart of the subroutine ScanPres (completes a pressure scan for each of the ports in the well definition array and writes the results to datafiles).

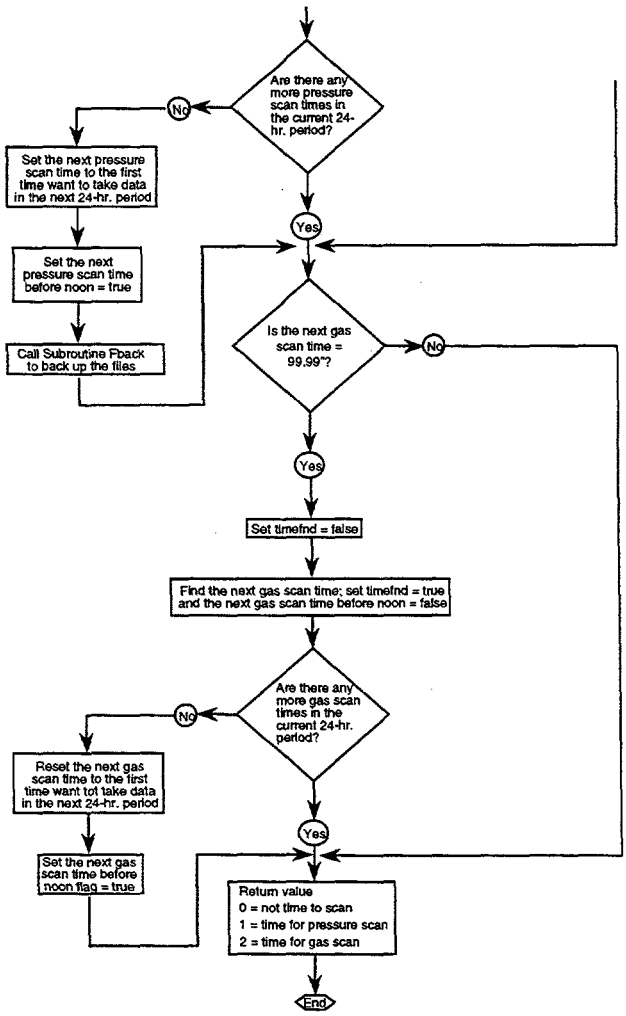

Figure A-21: Flow chart of the subroutine ScanPres (cont).

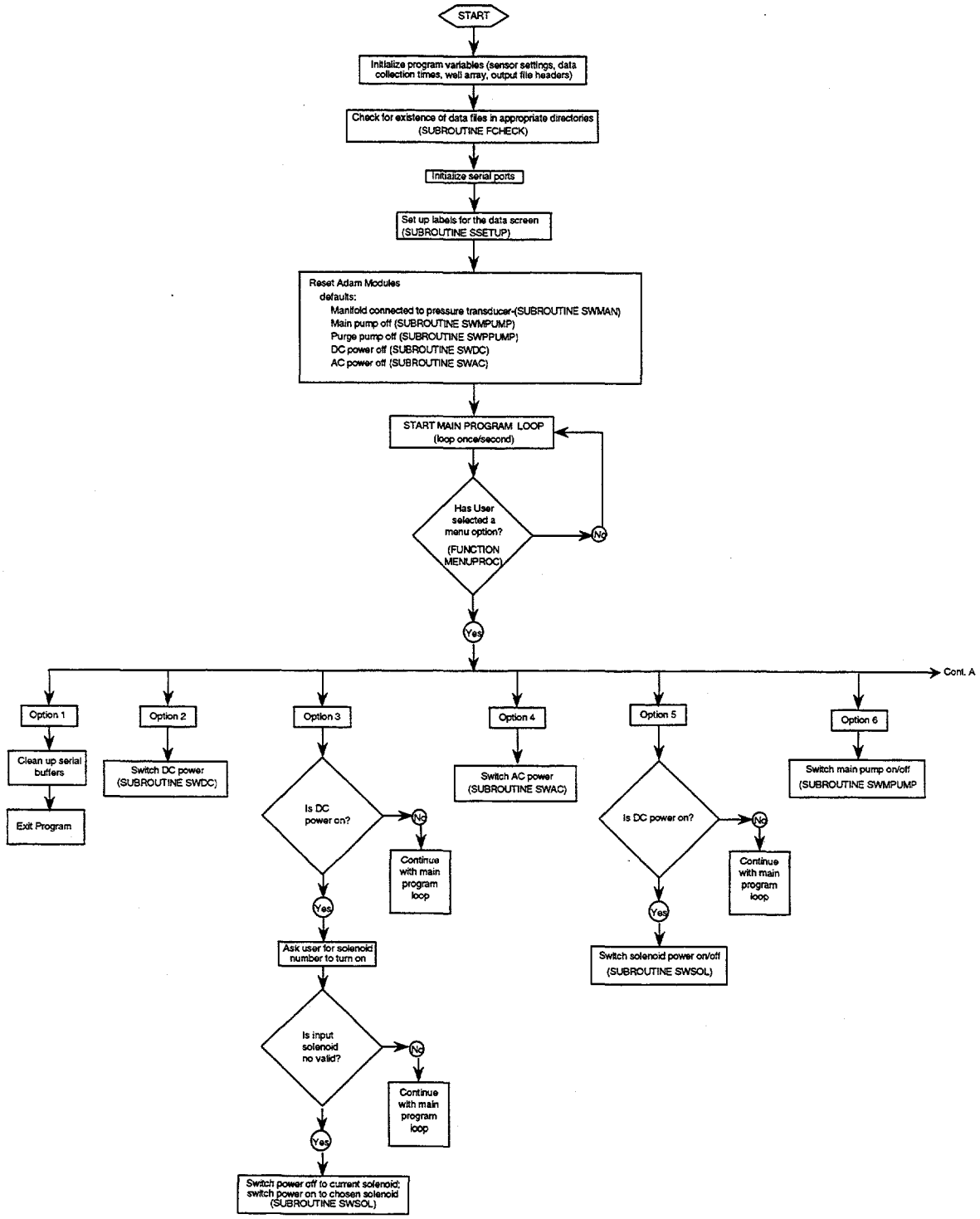

Figure A-22: Flow chart of the subroutine SupDate (updates the computer screen with current system parameters).

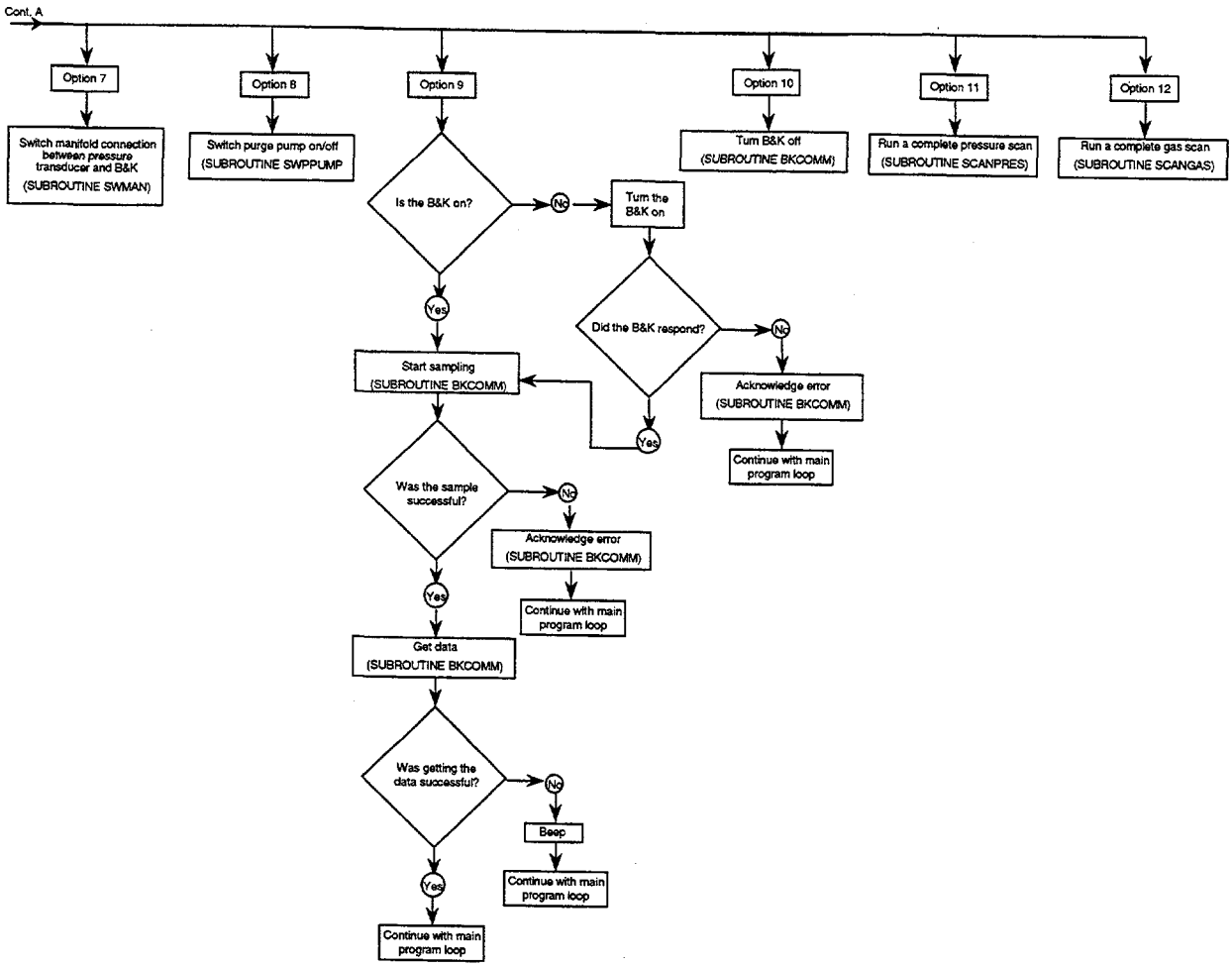

Figure A-23: Flow chart of the subroutine SupDate (cont).

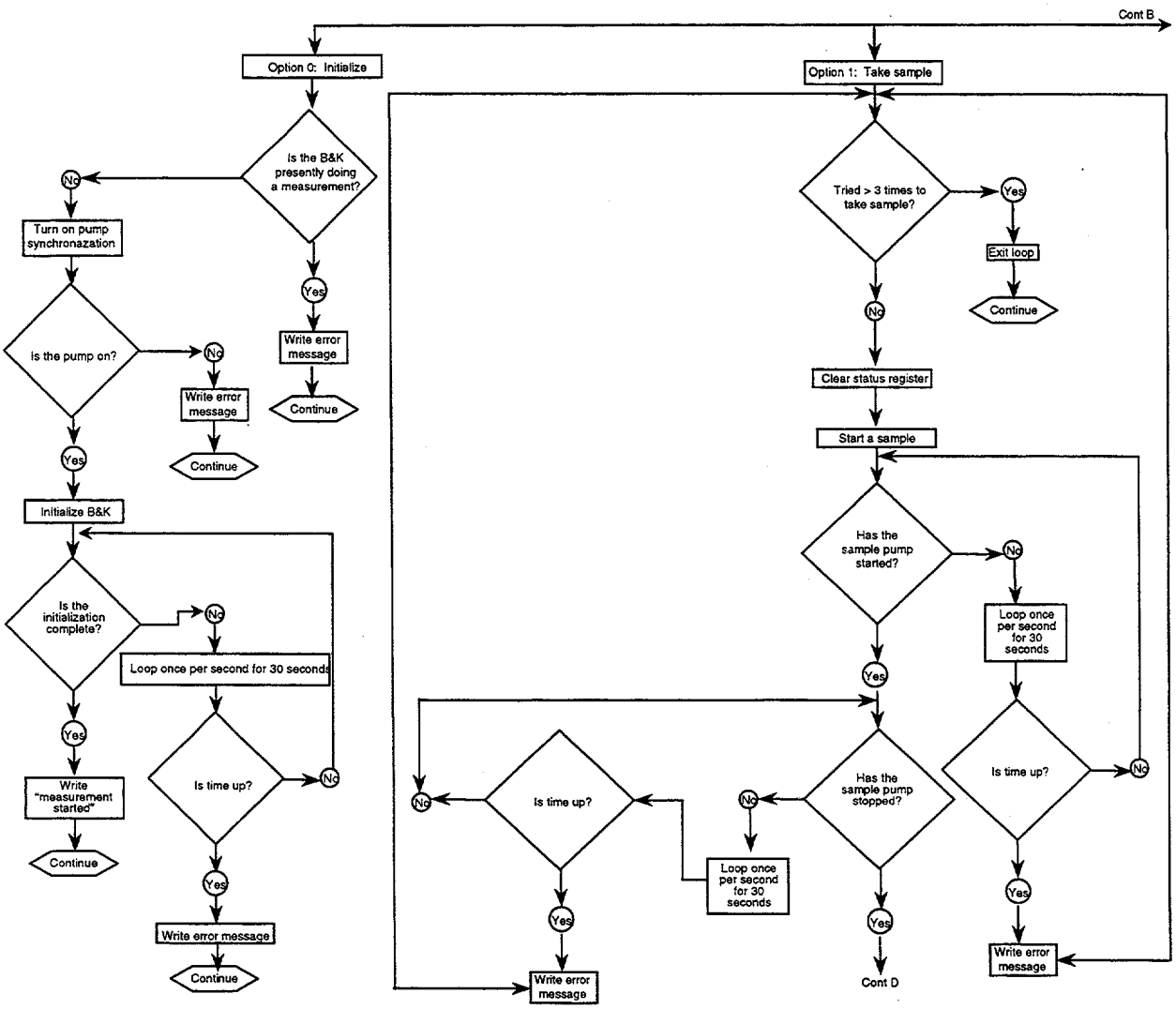

Figure A-24: Flow chart of the subroutine SupDate (cont).

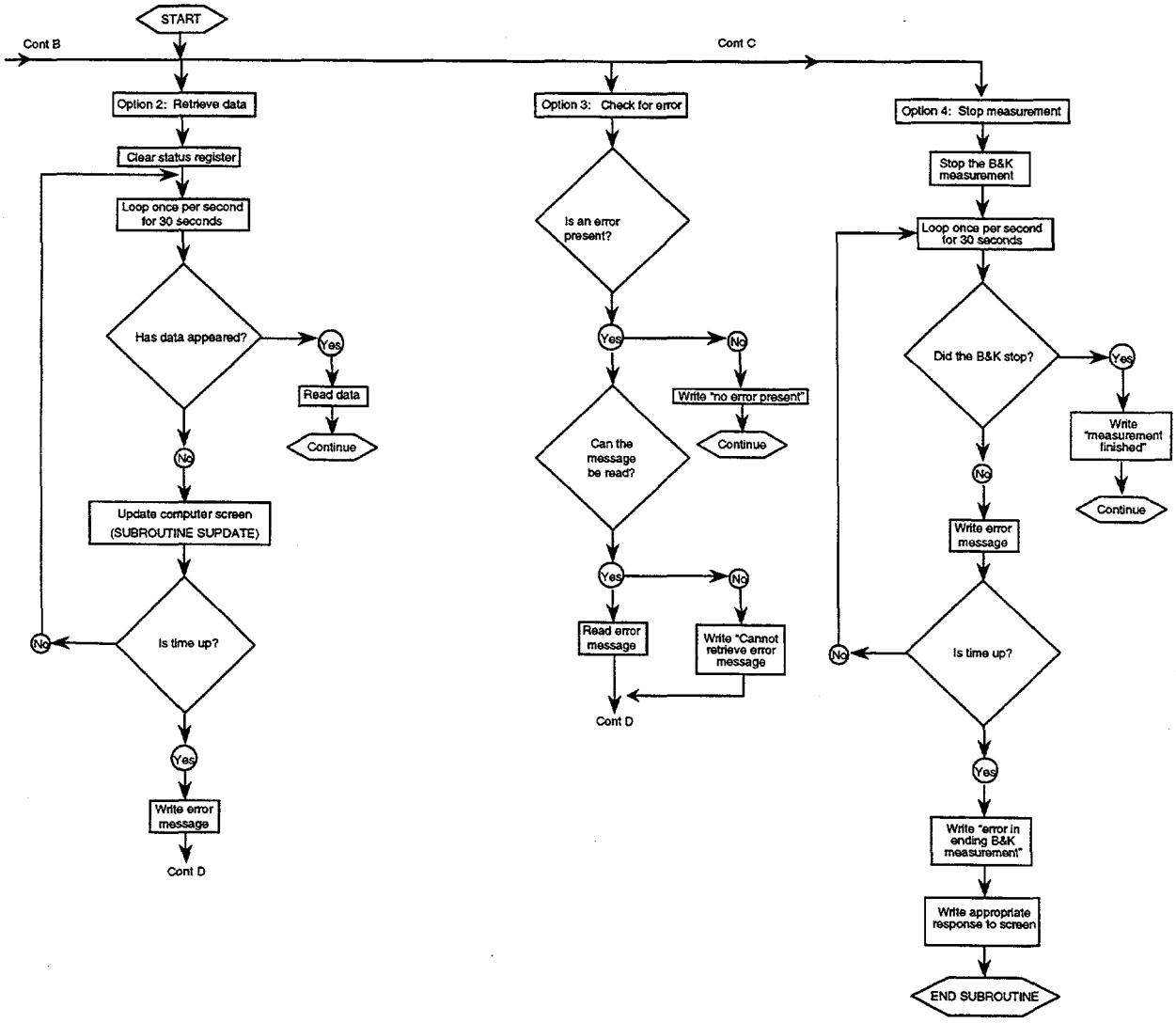

Figure A-25: Flow chart of the subroutine SupDate (cont).

APPENDIX B: VERIFICATION AND VALIDATION OF T2VOC CALCULATIONS

1.0 PURPOSE

The purpose of these calculations was to validate the results of T2VOC simulations for diffusion of tracer gas through soil. In the SEAtrace simulations, soil layers as thick as 2 m were used to reduce the number of calculational elements and thus the calculational time. This raised concerns on the accuracy of the code predictions and their sensitivity to the gridding choice. The present set of calculations were performed to address these concerns.

2.0 METHODOLOGY

Two test problems for which exact analytical solutions were available were used to validate T2VOC calculations. The first test problem employed a 1-D calculational domain subjected to boundary conditions of the first kind on both sides and the second test problem employed R-Z calculational domain, also with the first-kind boundary conditions. In both cases, first exact analytical solutions were derived by solving the diffusion equation. Then, T2VOC simulations using very refined grid arrangements were used to solve the same test problems. Comparison of solutions obtained from these two different approaches was used to establish the validity of T2VOC. In addition, several T2VOC runs were made using varying grid arrangements to draw insights regarding the maximum grid length that provides reasonable agreement with the analytical solution. The final section of this report documents these 'critical dimensions'.

3.0 TEST PROBLEM #1: 1-D DIFFUSION THROUGH UNSATURATED SOIL

3.1 PROBLEM DESCRIPTION

Consider a 1-D soil of length L through which gas is allowed to diffuse from a known higher concentration, C_o (kg/m^3), on the left hand side to a lower concentration, 0 (kg/m^3), on the right hand side. Assume that the soil consists of homogeneous medium with a known diffusivity of D and an initial gas concentration of 0 (kg/m^3). The objective of the problem is to obtain the concentration profiles in the soil as a function of time as the gas diffuses from the left to the right.

3.2 ANALYTICAL SOLUTION

A closed form analytical solution for such a case can be obtained by solving 1-D diffusion equation of the form:

$$\frac{\partial^2 C}{\partial x^2} = \frac{1}{D}\frac{\partial C}{\partial t} \quad \text{in } 0<x<L \text{ and } t>0$$

Subjected to the following boundary conditions:

$C=C_o$ at $x=0$ and $t>0$
$C=0$ at $x=L$ and $t>0$
$C=0$ $0 \leq x \leq L$ and $t=0$

This problem is non-homogeneous by the virtue of the fact that the left hand side boundary condition is non-homogeneous. However, the solution can be obtained to be:

$$C(x,t) = C_o\left[1 - x/L - \frac{2}{L}\sum_{m=1}^{\infty} e^{-D\beta_m^2 t}\,\frac{\sin\beta_m x}{\beta_m}\right]$$

where,

C_o is concentration on the lhs boundary (kg/m^3),
D is effective diffusion coefficient of gas through the medium (m^2/s),
L is length of the soil medium (m),
• $_m$ is eigen value (m• /L),

Figure B-1 plots the solution of this equation as a function of distance for several selected time intervals for an assumed domain length of 20 m, effective soil diffusivity of 1.0E-5 m^2/s, and C_o of 0.3017 kg/m^3. As shown in this figure, the solution reached steady state within 144.5 days.

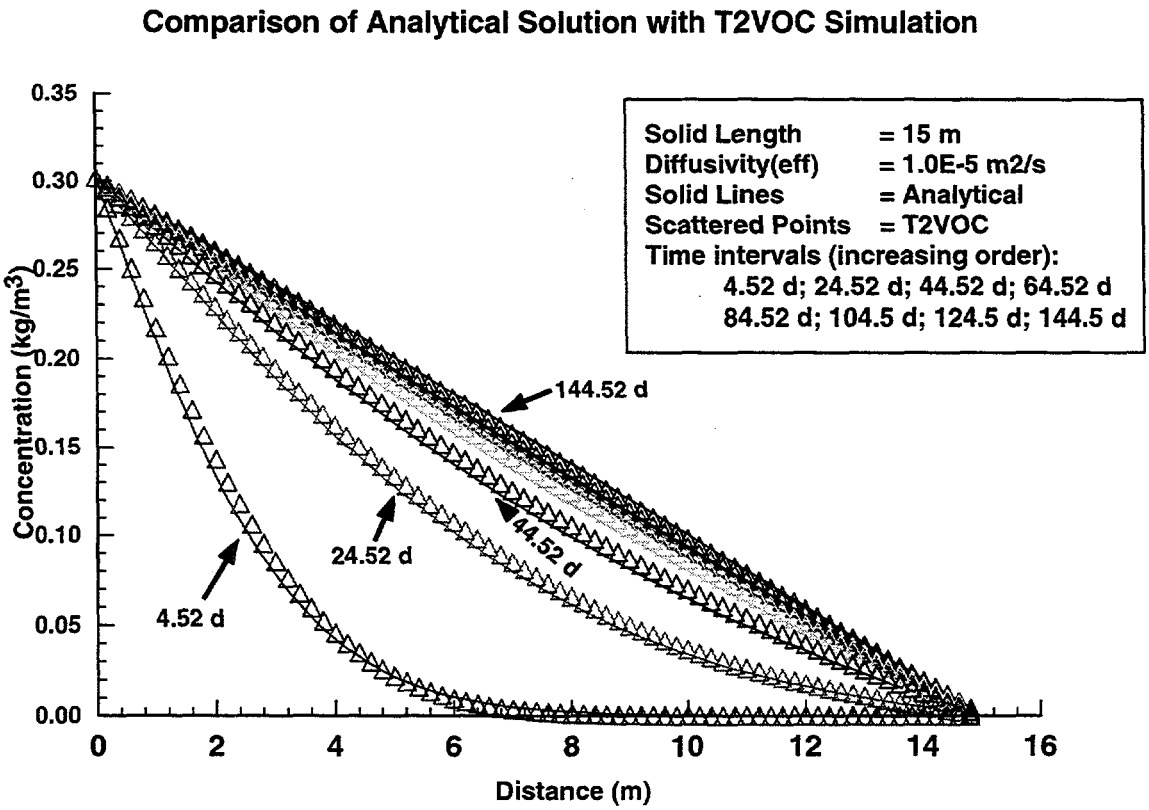

Figure B-1. Comparison of T2VOC simulation using Finer Mesh with Analytical Solution.

3.3 T2VOC SIMULATION

The same test problem was simulated using T2VOC, but employing three different grid geometries. Table B-1 presents the T2VOC input file used for this run. Note that due to a feature offered by T2VOC, all three geometry cases described below were incorporated into a single run input file provided in Table 1. These and additional features of T2VOC can be found in the User's Manual (Falta, Pruess, Finsterle, and Battistelli 1995).

Table B-1. Description of information used to calculate analytical diffusion concentrations at monitoring points for the baseline cases.

	Case 1	Case 2
Leak location (X,Y,Z) meters	32.92, 0, -14.02	32.92, 0, -14.02
Monitor location (X,Y,Z) meters		
#1	48.78, 6.10, -9.14	48.78, 6.10, -9.14
#2	24.38, 6.10, -21.34	24.38, 6.10, -21.34
#3	24.38, 6.10, -9.14	24.38, 6.10, -9.14
#4	36.58, 6.10, -21.34	36.58, 6.10, -21.34
#5	36.58, 6.10, -9.14	36.58, 6.10, -9.14
Accuracy of monitor locations (m)	±0%	±0%
Accuracy range of measured concentrations (≤ 500 ppm)	±5%	±5%
Accuracy range of measured concentrations (> 500 ppm)	±10%	±10%
Leak radius (m)	.1	1
Effective diffusive constant of tracer through medium (m^2/hr)	.036	.036
Source concentration (ppm)	70,000	70,000
Accuracy of measured source concentration value (%)	±10	±10
Number of independent calculations performed for each run	5	5
Maximum number of attempts per independent calculation to achieve error parameter	5000	5000

3.3.1 Finer Mesh:

In the first T2VOC simulation, a fine mesh was used by sub-dividing the 20 m soil layer into 125 nodes. The first 50 layers were 0.1 m long while the remaining 75 layers were 0.2 m long. Two inactive elements BN-01 and BN-02, of volume 0.0 m^3, were used to simulate boundary conditions of first kind on both sides. The chemical constants needed to calculate SF_6 properties were included in the data block CHEMP. These properties (especially molecular weight), assumed a mole fraction of 0.05 and together with the selected porosity of 0.3 resulted

in a gas concentration in BN-01 of 0.3017 kg/m^3. The effective soil diffusivity was set equal to 1.0E-5 m^2/s, by artificially setting tortuosity to 1.0 (see last entry in data block ROCKS; line #2). The initial conditions as set in INCON and assumed soil porosity of 0.3 resulted in BN-01 concentration of 0.3017 kg/m^3, and the rest of the soil concentration of 0.0 kg/m^3. Thereafter the concentration in cells BN-01 and BN-02 was held constant (by rendering both elements 'inactive'), while the concentration in the rest of the domain was allowed to vary with time. The code simulation was terminated after steady state was reached, at 144.5 days after start of simulation. The results of this simulation are compared with the analytical solution in Figure B-1. As evident from this figure, the T2VOC calculations closely agree with the analytical solutions; the difference being less than 0.5% -- which is obviously an excellent agreement. This test confirms that T2VOC can simulate the test problem very accurately provided the soil geometry can be simulated using a finer mesh. The following two simulations were used to examine if such good agreement could be maintained while the grid length of each element was increased.

Table B-2. Input data file for 1-D Diffusion of SF_6 vapor in unsaturated sample (edited to fit a page).

```
TITLE    Test #1 -- Comparison with SEA 1-D Diffusion Model Results for SNL/Sandy
ROCKS----1----*----2----*----3----*----4----*----5----*----6----*----7----*----8'
DIRT1000012.6500E+033.0000E-011.0000E-141.0000E-141.0000E-143.1000E+001.0000E+03
0.0000E+000.0000E+000.0000E+001.0000E+00
CHEMP----1----*----2----*----3----*----4----*----5----*----6----*----7----*----8'
3.1869E+023.7710E+012.6500E-010.0000E+00       1.6
2.2022E+02-3.560E-020.0000E+000.0000E+000.0000E+00
1.4605E+02   -33.890      .5631 -4.522E-4  1.426E-7
1.1060E+03     293.01.0000E-05    283.15      1.00
    -4.573  1.196E+3   1.37E-3 -1.378E-6     308.0
  7.996E-50.0000E+000.0000E+000.0000E+00
1.5000E-025.0000E-050.0000E+00
MULTI----1----*----2----*----3----*----4----*----5----*----6----*----7----*----8'
    3    3    3    6
PARAM----1----*----2----*----3----*----4----*----5----*----6----*----7----*----8'
0002035000000020100000000000004000000002.1300E-050.0000E+00
0.0000E+003.1558E+071.0000E+008.6400E+04AA  1xxxxx9.8060E+000.0000E+000.0000E+00
1.0000E-051.0000E+000.0000E+000.0000E+000.0000E+000.0000E+00
1.01330000000000E+055.00000000000000E-020.00000000000000E+001.00000000000000E+01
RPCAP----1----*----2----*----3----*----4----*----5----*----6----*----7----*----8'
00006     4.0000E-011.0000E-011.0000E-031.0000E+000.0000E+000.0000E+000.0000E+00
00009     0.0000E+000.0000E+000.0000E+000.0000E+000.0000E+000.0000E+000.0000E+00
ELEME----1----*----2----*----3----*----4----*----5----*----6----*----7----*----8'
AA 010004900001DIRT11.0000E-01
BB 010004900001DIRT12.0000E-01
aa 010000300001DIRT11.5000E-01
aa 050000000000DIRT10.4000E+00
bb 010001300001DIRT11.0000E+00
cc 010000400001DIRT11.0000E+00
dd 010000400001DIRT12.0000E+00
BN 010000100001DIRT10.0000E+00
BN 020000100001DIRT10.0000E+00
CONNE----1----*----2----*----3----*----4----*----5----*----6----*----7----*----8'
BN 01AA 01000000000000000000011.0000E-045.0000E-021.0000E+000.0000E+0000000
AA 01AA 02000480000100001000015.0000E-025.0000E-021.0000E+000.0000E+0000000
AA 50BB 01000000000000000000015.0000E-021.0000E-011.0000E+000.0000E+0000000
BB 01BB 02000480000100001000011.0000E-011.0000E-011.0000E+000.0000E+0000000
BB 50BN 02000000000000000000011.0000E-011.0000E-041.0000E+000.0000E+0000000
BN 01aa 01000000000000000000011.0000E-047.5000E-021.0000E+000.0000E+0000000
aa 01aa 02000020000100001000017.5000E-027.5000E-021.0000E+000.0000E+0000000
aa 04aa 05000000000000000000017.5000E-022.0000E-011.0000E+000.0000E+0000000
aa 05bb 01000000000000000000012.0000E-015.0000E-011.0000E+000.0000E+0000000
bb 01bb 02000120000100001000015.0000E-015.0000E-011.0000E+000.0000E+0000000
```

```
bb 14BN 020000000000000000000015.0000E-011.0000E-041.0000E+000.0000E+0000000
BN 01cc 010000000000000000000011.0000E-045.0000E-011.0000E+000.0000E+0000000
cc 01cc 020000300001000010000015.0000E-015.0000E-011.0000E+000.0000E+0000000
cc 05dd 010000000000000000000015.0000E-011.0000E+001.0000E+000.0000E+0000000
dd 01dd 020000300001000010000011.0000E+001.0000E+001.0000E+000.0000E+0000000
dd 05BN 020000000000000000000011.0000E+001.0000E-041.0000E+000.0000E+0000000
INCON----1----*----2----*----3----*----4----*----5----*----6----*----7----*----8'
BN 0100000000003.000000000E-01
1.01325000000000E+055.00000000000000E-024.80000000000000E-021.00000000000000E+01
```

3.3.2 Intermediate and Coarse Mesh:

The second and third T2VOC simulations were run to quantify the effect of grid resolution on the accuracy of the model predictions. In the second case, the element lengths varied between 0.15 m and 1.0 m, while in the third case the element lengths varied between 1 m and 2 m. Otherwise both these cases were identical to the T2VOC simulation whose results are presented in Figure B-1. Comparison of the model predictions using intermediate and coarse grids with the finer mesh are shown in Figure B-2. As shown in this figure, increasing the grid length from 0.1 m to 2 m resulted in no net loss of accuracy. However, there was a substantial savings in computational time. In fact, the predictions are almost identical, while the estimated computational time is one quarter of the original case. Such an agreement underscores the fact that grid lengths as high as 2 m can be used, with out sacrificing modeling accuracy.

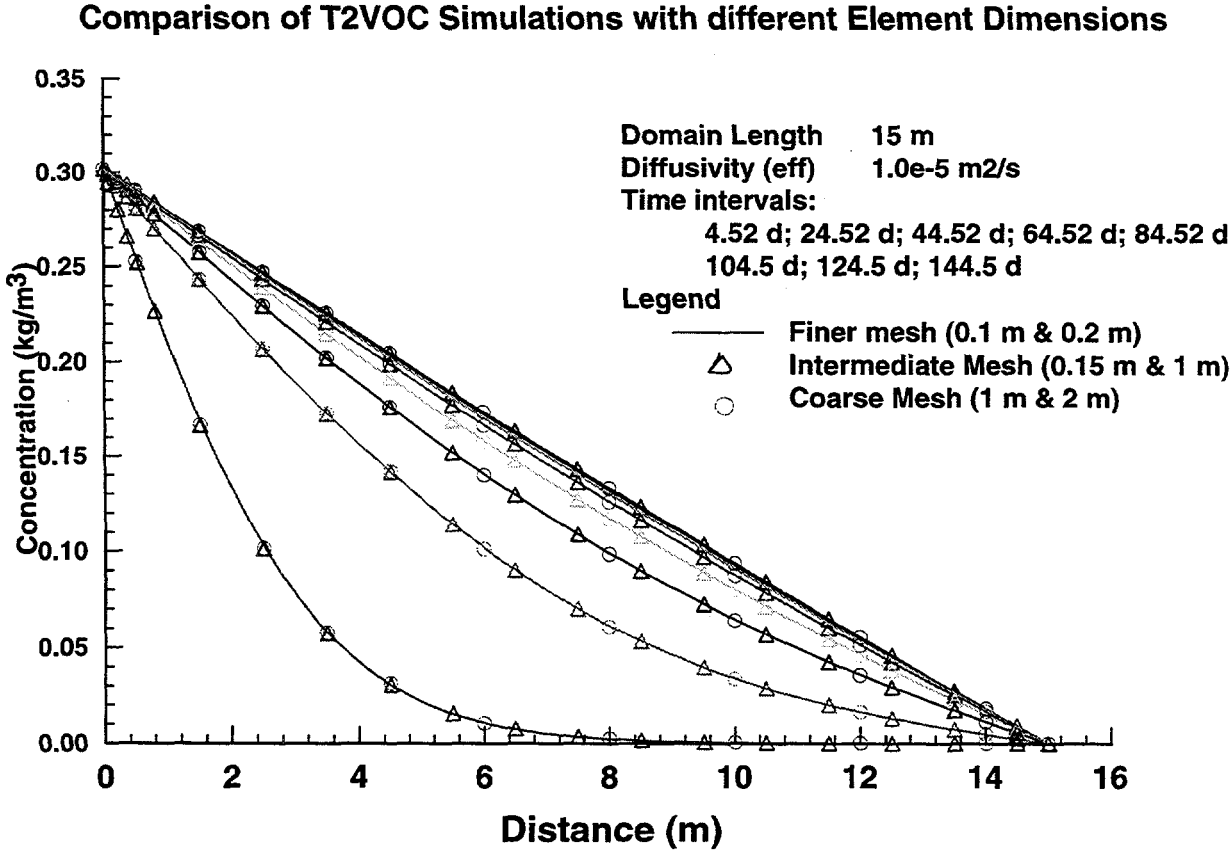

Figure B-2. Comparison of T2VOC simulations using different mesh refinements.

4.0 TEST PROBLEM #2: R-Z DIFFUSION THROUGH UNSATURATED SOIL

Consider a 2-D homogenous soil of length L and radius R_o with a soil-gas diffusivity of 10^{-5} m^2/s and an initial concentration of VOC in the soil of C_o (kg/m^3). At t=0, assume that the soil segment is exposed to a 'Zero Concentration" boundary condition at all boundaries (@z=0; @z=L; @R=R_o). The objective of this test problem is to calculate concentration profiles in the soil as a function of time.

4.1 ANALYTICAL SOLUTION

A closed from analytical solution can be obtained by solving a 2-D R-Z diffusion equation of the form:

$$\frac{\partial^2 C}{\partial R^2}+\frac{1}{R}\frac{\partial C}{\partial R}+\frac{\partial^2 C}{\partial Z^2}=\frac{1}{D}\frac{\partial C}{\partial t}$$

subjected to the boundary conditions

$C=0$; $Z=0$ and $t>0$
$C=0$, $Z=L$ and $t>0$
$C=0$; $R=R_1$ and $t>0$, and

the initial condition,

$C=C_o$, $0<Z<L$, $R<R_1$, and $t=0$

The analytical solution for this equation can be obtained as:

$$C(Z,R,t)=\frac{4C_o}{LR_1}\sum_{m=1}^{\infty}\sum_{p=1}^{\infty}e^{-D(\beta_m^2+\gamma_p^2)}\bullet\frac{J_o(\beta_m R)}{\beta_m J_1(\beta_m R_1)}\bullet\frac{(1-\cos(\gamma_p L))\sin(\gamma_p Z)}{\gamma_p}$$

where,

J_0 and J_1 are the Bessels functions,
β_m is the eigen value obtained from equation: $J_0(\beta_m R_1)=0$
γ_p is the eigen value obtained from equation: $\sin(\gamma_p L)=0$

The radial concentration profiles at the axial center obtained by solving this equation are plotted in Figure B-3 as a function of time. For the present comparison, the problem geometry was assumed to be 19 m long and 19 m in radius, with a diffusivity of 10^{-5} m^2/s and initial gas concentration of 0.3022 kg/m^3. As expected the gas concentration in the soil decreased with time approaching nearly zero concentration at about 150 days.

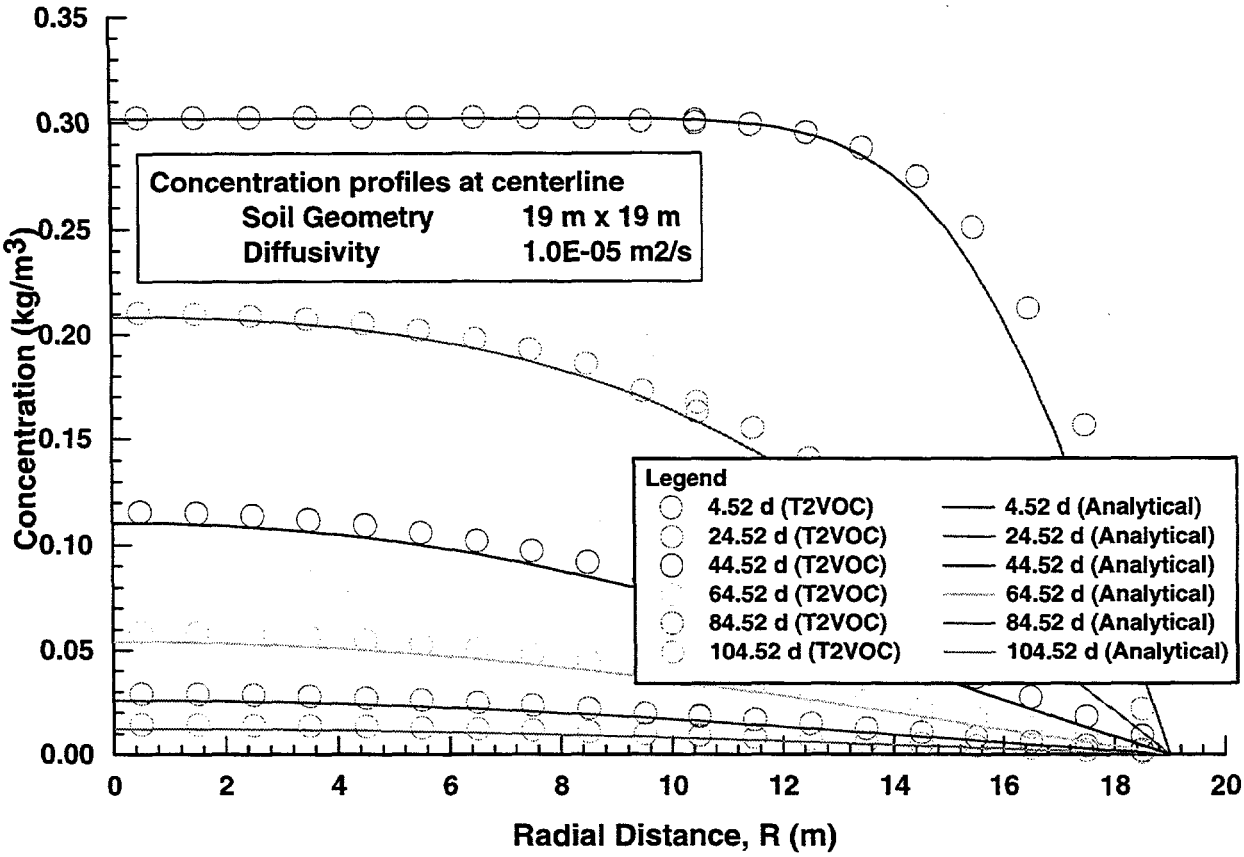

Figure B-3. Comparison of Analytical Solution with T2VOC simulation for an R-Z test problem.

4.2 T2VOC SIMULATION

The T2VOC simulation results for the test problem #2 are shown in FigureB-3 alongside the analytical solution. For this run, the T2VOC simulation employed equi-length grid elements, 1 m long and 1m radius. The same SF6 chemical properties used in the previous T2VOC test simulation were used in this problem as well. The input file used in the simulation (edited to fit the presentation format) is enclosed as Table B-2. As shown in Figure B-3, good agreement (0.5%) was noted between the T2VOC simulation and the analytical solution (deviations of the order of .1.5% near R_1 can be attributed to slight differences in simulating the boundary conditions).

5.0 INSIGHTS REGARDING GRID DIMENSIONS

One of the objectives of this verification effort is to draw insights regarding the maximum allowable grid dimensions. The test simulations suggest that grid lengths as high as 3 m and volumes as high as 150 m^3 are sufficiently refined to provide reasonable agreement with the analytical solutions. This conclusion is drawn from the following comparison (although results for all these runs are not presented in this report):

1. 1-D simulations using grid lengths as high as 3 m
2. 2-D R-Z simulations using grid radial segments of width 3 m and length 2 m.

Table B-3. Input deck used for T2VOC R-Z run.

```
TITLE    Test #2 -- Comparison with SEA R_Z Diffusion Model Results
ROCKS----1----*----2----*----3----*----4----*----5----*----6----*----7----*----8'
    1000012.6500E+033.0000E-011.0000E-141.0000E-141.0000E-143.1000E+001.0000E+03
0.0000E+000.0000E+000.0000E+001.0000E+00
    2000012.6500E+033.0000E-011.0000E-141.0000E-141.0000E-143.1000E+001.0000E+03
0.0000E+000.0000E+000.0000E+001.0000E+00

CHEMP----1----*----2----*----3----*----4----*----5----*----6----*----7----*----8'
3.1869E+023.7710E+012.6500E-010.0000E+00       1.6
2.2022E+02-3.560E-020.0000E+000.0000E+000.0000E+00
1.4605E+02   -33.890      .5631 -4.522E-4  1.426E-7
1.1060E+03     293.01.0000E-05    283.15      1.00
    -4.573  1.196E+3   1.37E-3 -1.378E-6     308.0
  7.996E-50.0000E+000.0000E+000.0000E+00
1.5000E-025.0000E-050.0000E+00
MULTI----1----*----2----*----3----*----4----*----5----*----6----*----7----*----8'
    3    3    3    6

PARAM----1----*----2----*----3----*----4----*----5----*----6----*----7----*----8'
0002035000000020100000000000004000000002.1300E-050.0000E+00
0.0000E+003.1558E+071.0000E+008.6400E+04AA  1xxxxx9.8060E+000.0000E+000.0000E+00
1.0000E-051.0000E+000.0000E+000.0000E+000.0000E+000.0000E+00
1.01330000000000E+055.00000000000000E-020.00000000000000E+001.00000000000000E+01
RPCAP----1----*----2----*----3----*----4----*----5----*----6----*----7----*----8'
00006     4.0000E-011.0000E-011.0000E-031.0000E+000.0000E+000.0000E+000.0000E+00
00009     0.0000E+000.0000E+000.0000E+000.0000E+000.0000E+000.0000E+000.0000E+00
ELEME----1----*----2----*----3----*----4----*----5----*----6----*----7----*----8'
A2  1              10.3142E+010.0000E+00          0.5000E+00          -.1500E+01
A3  1              10.3142E+010.0000E+00          0.5000E+00          -.2500E+01
A4  1              10.3142E+010.0000E+00          0.5000E+00          -.3500E+01
A5  1              10.3142E+010.0000E+00          0.5000E+00          -.4500E+01
A6  1              10.3142E+010.0000E+00          0.5000E+00          -.5500E+01
A7  1              10.3142E+010.0000E+00          0.5000E+00          -.6500E+01
A8  1              10.3142E+010.0000E+00          0.5000E+00          -.7500E+01
A9  1              10.3142E+010.0000E+00          0.5000E+00          -.8500E+01
AA  1              10.3142E+010.0000E+00          0.5000E+00          -.9500E+01
AB  1              10.3142E+010.0000E+00          0.5000E+00          -.1050E+02
AC  1              10.3142E+010.0000E+00          0.5000E+00          -.1150E+02
AD  1              10.3142E+010.0000E+00          0.5000E+00          -.1250E+02
AE  1              10.3142E+010.0000E+00          0.5000E+00          -.1350E+02
AF  1              10.3142E+010.0000E+00          0.5000E+00          -.1450E+02
AG  1              10.3142E+010.0000E+00          0.5000E+00          -.1550E+02
AH  1              10.3142E+010.0000E+00          0.5000E+00          -.1650E+02
AI  1              10.3142E+010.0000E+00          0.5000E+00          -.1750E+02
```

AJ	1	10.3142E+010.0000E+00	0.5000E+00	-.1850E+02
A2	2	10.9425E+010.0000E+00	0.1500E+01	-.1500E+01
A3	2	10.9425E+010.0000E+00	0.1500E+01	-.2500E+01
A4	2	10.9425E+010.0000E+00	0.1500E+01	-.3500E+01
A5	2	10.9425E+010.0000E+00	0.1500E+01	-.4500E+01
A6	2	10.9425E+010.0000E+00	0.1500E+01	-.5500E+01
A7	2	10.9425E+010.0000E+00	0.1500E+01	-.6500E+01
A8	2	10.9425E+010.0000E+00	0.1500E+01	-.7500E+01
A9	2	10.9425E+010.0000E+00	0.1500E+01	-.8500E+01
AA	2	10.9425E+010.0000E+00	0.1500E+01	-.9500E+01
AB	2	10.9425E+010.0000E+00	0.1500E+01	-.1050E+02
AC	2	10.9425E+010.0000E+00	0.1500E+01	-.1150E+02
AD	2	10.9425E+010.0000E+00	0.1500E+01	-.1250E+02
AE	2	10.9425E+010.0000E+00	0.1500E+01	-.1350E+02
AF	2	10.9425E+010.0000E+00	0.1500E+01	-.1450E+02
AG	2	10.9425E+010.0000E+00	0.1500E+01	-.1550E+02
AH	2	10.9425E+010.0000E+00	0.1500E+01	-.1650E+02
AI	2	10.9425E+010.0000E+00	0.1500E+01	-.1750E+02
AJ	2	10.9425E+010.0000E+00	0.1500E+01	-.1850E+02
A2	3	10.1571E+020.0000E+00	0.2500E+01	-.1500E+01
A3	3	10.1571E+020.0000E+00	0.2500E+01	-.2500E+01
A4	3	10.1571E+020.0000E+00	0.2500E+01	-.3500E+01
A5	3	10.1571E+020.0000E+00	0.2500E+01	-.4500E+01
A6	3	10.1571E+020.0000E+00	0.2500E+01	-.5500E+01
A7	3	10.1571E+020.0000E+00	0.2500E+01	-.6500E+01
A8	3	10.1571E+020.0000E+00	0.2500E+01	-.7500E+01
A9	3	10.1571E+020.0000E+00	0.2500E+01	-.8500E+01
AA	3	10.1571E+020.0000E+00	0.2500E+01	-.9500E+01
AB	3	10.1571E+020.0000E+00	0.2500E+01	-.1050E+02
AC	3	10.1571E+020.0000E+00	0.2500E+01	-.1150E+02
AD	3	10.1571E+020.0000E+00	0.2500E+01	-.1250E+02
AE	3	10.1571E+020.0000E+00	0.2500E+01	-.1350E+02
AF	3	10.1571E+020.0000E+00	0.2500E+01	-.1450E+02
AG	3	10.1571E+020.0000E+00	0.2500E+01	-.1550E+02
AH	3	10.1571E+020.0000E+00	0.2500E+01	-.1650E+02
AI	3	10.1571E+020.0000E+00	0.2500E+01	-.1750E+02
AJ	3	10.1571E+020.0000E+00	0.2500E+01	-.1850E+02
A2	4	10.2199E+020.0000E+00	0.3500E+01	-.1500E+01
A3	4	10.2199E+020.0000E+00	0.3500E+01	-.2500E+01
A4	4	10.2199E+020.0000E+00	0.3500E+01	-.3500E+01
A5	4	10.2199E+020.0000E+00	0.3500E+01	-.4500E+01
A6	4	10.2199E+020.0000E+00	0.3500E+01	-.5500E+01
A7	4	10.2199E+020.0000E+00	0.3500E+01	-.6500E+01
A8	4	10.2199E+020.0000E+00	0.3500E+01	-.7500E+01
A9	4	10.2199E+020.0000E+00	0.3500E+01	-.8500E+01
AA	4	10.2199E+020.0000E+00	0.3500E+01	-.9500E+01
AB	4	10.2199E+020.0000E+00	0.3500E+01	-.1050E+02

AC	4	10.2199E+020.0000E+00	0.3500E+01	-.1150E+02
AD	4	10.2199E+020.0000E+00	0.3500E+01	-.1250E+02
AE	4	10.2199E+020.0000E+00	0.3500E+01	-.1350E+02
AF	4	10.2199E+020.0000E+00	0.3500E+01	-.1450E+02
AG	4	10.2199E+020.0000E+00	0.3500E+01	-.1550E+02
AH	4	10.2199E+020.0000E+00	0.3500E+01	-.1650E+02
AI	4	10.2199E+020.0000E+00	0.3500E+01	-.1750E+02
AJ	4	10.2199E+020.0000E+00	0.3500E+01	-.1850E+02
A2	5	10.2827E+020.0000E+00	0.4500E+01	-.1500E+01
A3	5	10.2827E+020.0000E+00	0.4500E+01	-.2500E+01
A4	5	10.2827E+020.0000E+00	0.4500E+01	-.3500E+01
A5	5	10.2827E+020.0000E+00	0.4500E+01	-.4500E+01
A6	5	10.2827E+020.0000E+00	0.4500E+01	-.5500E+01
A7	5	10.2827E+020.0000E+00	0.4500E+01	-.6500E+01
A8	5	10.2827E+020.0000E+00	0.4500E+01	-.7500E+01
A9	5	10.2827E+020.0000E+00	0.4500E+01	-.8500E+01
AA	5	10.2827E+020.0000E+00	0.4500E+01	-.9500E+01
AB	5	10.2827E+020.0000E+00	0.4500E+01	-.1050E+02
AC	5	10.2827E+020.0000E+00	0.4500E+01	-.1150E+02
AD	5	10.2827E+020.0000E+00	0.4500E+01	-.1250E+02
AE	5	10.2827E+020.0000E+00	0.4500E+01	-.1350E+02
AF	5	10.2827E+020.0000E+00	0.4500E+01	-.1450E+02
AG	5	10.2827E+020.0000E+00	0.4500E+01	-.1550E+02
AH	5	10.2827E+020.0000E+00	0.4500E+01	-.1650E+02
AI	5	10.2827E+020.0000E+00	0.4500E+01	-.1750E+02
AJ	5	10.2827E+020.0000E+00	0.4500E+01	-.1850E+02
A2	6	10.3456E+020.0000E+00	0.5500E+01	-.1500E+01
A3	6	10.3456E+020.0000E+00	0.5500E+01	-.2500E+01
A4	6	10.3456E+020.0000E+00	0.5500E+01	-.3500E+01
A5	6	10.3456E+020.0000E+00	0.5500E+01	-.4500E+01
A6	6	10.3456E+020.0000E+00	0.5500E+01	-.5500E+01
A7	6	10.3456E+020.0000E+00	0.5500E+01	-.6500E+01
A8	6	10.3456E+020.0000E+00	0.5500E+01	-.7500E+01
A9	6	10.3456E+020.0000E+00	0.5500E+01	-.8500E+01
AA	6	10.3456E+020.0000E+00	0.5500E+01	-.9500E+01
AB	6	10.3456E+020.0000E+00	0.5500E+01	-.1050E+02
AC	6	10.3456E+020.0000E+00	0.5500E+01	-.1150E+02
AD	6	10.3456E+020.0000E+00	0.5500E+01	-.1250E+02
AE	6	10.3456E+020.0000E+00	0.5500E+01	-.1350E+02
AF	6	10.3456E+020.0000E+00	0.5500E+01	-.1450E+02
AG	6	10.3456E+020.0000E+00	0.5500E+01	-.1550E+02
AH	6	10.3456E+020.0000E+00	0.5500E+01	-.1650E+02
AI	6	10.3456E+020.0000E+00	0.5500E+01	-.1750E+02
AJ	6	10.3456E+020.0000E+00	0.5500E+01	-.1850E+02
A2	7	10.4084E+020.0000E+00	0.6500E+01	-.1500E+01
A3	7	10.4084E+020.0000E+00	0.6500E+01	-.2500E+01
A4	7	10.4084E+020.0000E+00	0.6500E+01	-.3500E+01

A5	7	10.4084E+020.0000E+00	0.6500E+01	-.4500E+01
A6	7	10.4084E+020.0000E+00	0.6500E+01	-.5500E+01
A7	7	10.4084E+020.0000E+00	0.6500E+01	-.6500E+01
A8	7	10.4084E+020.0000E+00	0.6500E+01	-.7500E+01
A9	7	10.4084E+020.0000E+00	0.6500E+01	-.8500E+01
AA	7	10.4084E+020.0000E+00	0.6500E+01	-.9500E+01
AB	7	10.4084E+020.0000E+00	0.6500E+01	-.1050E+02
AC	7	10.4084E+020.0000E+00	0.6500E+01	-.1150E+02
AD	7	10.4084E+020.0000E+00	0.6500E+01	-.1250E+02
AE	7	10.4084E+020.0000E+00	0.6500E+01	-.1350E+02
AF	7	10.4084E+020.0000E+00	0.6500E+01	-.1450E+02
AG	7	10.4084E+020.0000E+00	0.6500E+01	-.1550E+02
AH	7	10.4084E+020.0000E+00	0.6500E+01	-.1650E+02
AI	7	10.4084E+020.0000E+00	0.6500E+01	-.1750E+02
AJ	7	10.4084E+020.0000E+00	0.6500E+01	-.1850E+02
A2	8	10.4712E+020.0000E+00	0.7500E+01	-.1500E+01
A3	8	10.4712E+020.0000E+00	0.7500E+01	-.2500E+01
A4	8	10.4712E+020.0000E+00	0.7500E+01	-.3500E+01
A5	8	10.4712E+020.0000E+00	0.7500E+01	-.4500E+01
A6	8	10.4712E+020.0000E+00	0.7500E+01	-.5500E+01
A7	8	10.4712E+020.0000E+00	0.7500E+01	-.6500E+01
A8	8	10.4712E+020.0000E+00	0.7500E+01	-.7500E+01
A9	8	10.4712E+020.0000E+00	0.7500E+01	-.8500E+01
AA	8	10.4712E+020.0000E+00	0.7500E+01	-.9500E+01
AB	8	10.4712E+020.0000E+00	0.7500E+01	-.1050E+02
AC	8	10.4712E+020.0000E+00	0.7500E+01	-.1150E+02
AD	8	10.4712E+020.0000E+00	0.7500E+01	-.1250E+02
AE	8	10.4712E+020.0000E+00	0.7500E+01	-.1350E+02
AF	8	10.4712E+020.0000E+00	0.7500E+01	-.1450E+02
AG	8	10.4712E+020.0000E+00	0.7500E+01	-.1550E+02
AH	8	10.4712E+020.0000E+00	0.7500E+01	-.1650E+02
AI	8	10.4712E+020.0000E+00	0.7500E+01	-.1750E+02
AJ	8	10.4712E+020.0000E+00	0.7500E+01	-.1850E+02
A2	9	10.5341E+020.0000E+00	0.8500E+01	-.1500E+01
A3	9	10.5341E+020.0000E+00	0.8500E+01	-.2500E+01
A4	9	10.5341E+020.0000E+00	0.8500E+01	-.3500E+01
A5	9	10.5341E+020.0000E+00	0.8500E+01	-.4500E+01
A6	9	10.5341E+020.0000E+00	0.8500E+01	-.5500E+01
A7	9	10.5341E+020.0000E+00	0.8500E+01	-.6500E+01
A8	9	10.5341E+020.0000E+00	0.8500E+01	-.7500E+01
A9	9	10.5341E+020.0000E+00	0.8500E+01	-.8500E+01
AA	9	10.5341E+020.0000E+00	0.8500E+01	-.9500E+01
AB	9	10.5341E+020.0000E+00	0.8500E+01	-.1050E+02
AC	9	10.5341E+020.0000E+00	0.8500E+01	-.1150E+02
AD	9	10.5341E+020.0000E+00	0.8500E+01	-.1250E+02
AE	9	10.5341E+020.0000E+00	0.8500E+01	-.1350E+02
AF	9	10.5341E+020.0000E+00	0.8500E+01	-.1450E+02

AG 9	10.5341E+020.0000E+00	0.8500E+01	-.1550E+02
AH 9	10.5341E+020.0000E+00	0.8500E+01	-.1650E+02
AI 9	10.5341E+020.0000E+00	0.8500E+01	-.1750E+02
AJ 9	10.5341E+020.0000E+00	0.8500E+01	-.1850E+02
A2 10	10.5969E+020.0000E+00	0.9500E+01	-.1500E+01
A3 10	10.5969E+020.0000E+00	0.9500E+01	-.2500E+01
A4 10	10.5969E+020.0000E+00	0.9500E+01	-.3500E+01
A5 10	10.5969E+020.0000E+00	0.9500E+01	-.4500E+01
A6 10	10.5969E+020.0000E+00	0.9500E+01	-.5500E+01
A7 10	10.5969E+020.0000E+00	0.9500E+01	-.6500E+01
A8 10	10.5969E+020.0000E+00	0.9500E+01	-.7500E+01
A9 10	10.5969E+020.0000E+00	0.9500E+01	-.8500E+01
AA 10	10.5969E+020.0000E+00	0.9500E+01	-.9500E+01
AB 10	10.5969E+020.0000E+00	0.9500E+01	-.1050E+02
AC 10	10.5969E+020.0000E+00	0.9500E+01	-.1150E+02
AD 10	10.5969E+020.0000E+00	0.9500E+01	-.1250E+02
AE 10	10.5969E+020.0000E+00	0.9500E+01	-.1350E+02
AF 10	10.5969E+020.0000E+00	0.9500E+01	-.1450E+02
AG 10	10.5969E+020.0000E+00	0.9500E+01	-.1550E+02
AH 10	10.5969E+020.0000E+00	0.9500E+01	-.1650E+02
AI 10	10.5969E+020.0000E+00	0.9500E+01	-.1750E+02
AJ 10	10.5969E+020.0000E+00	0.9500E+01	-.1850E+02
A2 11	10.6597E+020.0000E+00	0.1050E+02	-.1500E+01
A3 11	10.6597E+020.0000E+00	0.1050E+02	-.2500E+01
A4 11	10.6597E+020.0000E+00	0.1050E+02	-.3500E+01
A5 11	10.6597E+020.0000E+00	0.1050E+02	-.4500E+01
A6 11	10.6597E+020.0000E+00	0.1050E+02	-.5500E+01
A7 11	10.6597E+020.0000E+00	0.1050E+02	-.6500E+01
A8 11	10.6597E+020.0000E+00	0.1050E+02	-.7500E+01
A9 11	10.6597E+020.0000E+00	0.1050E+02	-.8500E+01
AA 11	10.6597E+020.0000E+00	0.1050E+02	-.9500E+01
AB 11	10.6597E+020.0000E+00	0.1050E+02	-.1050E+02
AC 11	10.6597E+020.0000E+00	0.1050E+02	-.1150E+02
AD 11	10.6597E+020.0000E+00	0.1050E+02	-.1250E+02
AE 11	10.6597E+020.0000E+00	0.1050E+02	-.1350E+02
AF 11	10.6597E+020.0000E+00	0.1050E+02	-.1450E+02
AG 11	10.6597E+020.0000E+00	0.1050E+02	-.1550E+02
AH 11	10.6597E+020.0000E+00	0.1050E+02	-.1650E+02
AI 11	10.6597E+020.0000E+00	0.1050E+02	-.1750E+02
AJ 11	10.6597E+020.0000E+00	0.1050E+02	-.1850E+02
A2 12	10.7226E+020.0000E+00	0.1150E+02	-.1500E+01
A3 12	10.7226E+020.0000E+00	0.1150E+02	-.2500E+01
A4 12	10.7226E+020.0000E+00	0.1150E+02	-.3500E+01
A5 12	10.7226E+020.0000E+00	0.1150E+02	-.4500E+01
A6 12	10.7226E+020.0000E+00	0.1150E+02	-.5500E+01
A7 12	10.7226E+020.0000E+00	0.1150E+02	-.6500E+01
A8 12	10.7226E+020.0000E+00	0.1150E+02	-.7500E+01

A9 12	10.7226E+020.0000E+00	0.1150E+02	-.8500E+01
AA 12	10.7226E+020.0000E+00	0.1150E+02	-.9500E+01
AB 12	10.7226E+020.0000E+00	0.1150E+02	-.1050E+02
AC 12	10.7226E+020.0000E+00	0.1150E+02	-.1150E+02
AD 12	10.7226E+020.0000E+00	0.1150E+02	-.1250E+02
AE 12	10.7226E+020.0000E+00	0.1150E+02	-.1350E+02
AF 12	10.7226E+020.0000E+00	0.1150E+02	-.1450E+02
AG 12	10.7226E+020.0000E+00	0.1150E+02	-.1550E+02
AH 12	10.7226E+020.0000E+00	0.1150E+02	-.1650E+02
AI 12	10.7226E+020.0000E+00	0.1150E+02	-.1750E+02
AJ 12	10.7226E+020.0000E+00	0.1150E+02	-.1850E+02
A2 13	10.7854E+020.0000E+00	0.1250E+02	-.1500E+01
A3 13	10.7854E+020.0000E+00	0.1250E+02	-.2500E+01
A4 13	10.7854E+020.0000E+00	0.1250E+02	-.3500E+01
A5 13	10.7854E+020.0000E+00	0.1250E+02	-.4500E+01
A6 13	10.7854E+020.0000E+00	0.1250E+02	-.5500E+01
A7 13	10.7854E+020.0000E+00	0.1250E+02	-.6500E+01
A8 13	10.7854E+020.0000E+00	0.1250E+02	-.7500E+01
A9 13	10.7854E+020.0000E+00	0.1250E+02	-.8500E+01
AA 13	10.7854E+020.0000E+00	0.1250E+02	-.9500E+01
AB 13	10.7854E+020.0000E+00	0.1250E+02	-.1050E+02
AC 13	10.7854E+020.0000E+00	0.1250E+02	-.1150E+02
AD 13	10.7854E+020.0000E+00	0.1250E+02	-.1250E+02
AE 13	10.7854E+020.0000E+00	0.1250E+02	-.1350E+02
AF 13	10.7854E+020.0000E+00	0.1250E+02	-.1450E+02
AG 13	10.7854E+020.0000E+00	0.1250E+02	-.1550E+02
AH 13	10.7854E+020.0000E+00	0.1250E+02	-.1650E+02
AI 13	10.7854E+020.0000E+00	0.1250E+02	-.1750E+02
AJ 13	10.7854E+020.0000E+00	0.1250E+02	-.1850E+02
A2 14	10.8482E+020.0000E+00	0.1350E+02	-.1500E+01
A3 14	10.8482E+020.0000E+00	0.1350E+02	-.2500E+01
A4 14	10.8482E+020.0000E+00	0.1350E+02	-.3500E+01
A5 14	10.8482E+020.0000E+00	0.1350E+02	-.4500E+01
A6 14	10.8482E+020.0000E+00	0.1350E+02	-.5500E+01
A7 14	10.8482E+020.0000E+00	0.1350E+02	-.6500E+01
A8 14	10.8482E+020.0000E+00	0.1350E+02	-.7500E+01
A9 14	10.8482E+020.0000E+00	0.1350E+02	-.8500E+01
AA 14	10.8482E+020.0000E+00	0.1350E+02	-.9500E+01
AB 14	10.8482E+020.0000E+00	0.1350E+02	-.1050E+02
AC 14	10.8482E+020.0000E+00	0.1350E+02	-.1150E+02
AD 14	10.8482E+020.0000E+00	0.1350E+02	-.1250E+02
AE 14	10.8482E+020.0000E+00	0.1350E+02	-.1350E+02
AF 14	10.8482E+020.0000E+00	0.1350E+02	-.1450E+02
AG 14	10.8482E+020.0000E+00	0.1350E+02	-.1550E+02
AH 14	10.8482E+020.0000E+00	0.1350E+02	-.1650E+02
AI 14	10.8482E+020.0000E+00	0.1350E+02	-.1750E+02
AJ 14	10.8482E+020.0000E+00	0.1350E+02	-.1850E+02

A2 15	10.9111E+020.0000E+00	0.1450E+02	-.1500E+01
A3 15	10.9111E+020.0000E+00	0.1450E+02	-.2500E+01
A4 15	10.9111E+020.0000E+00	0.1450E+02	-.3500E+01
A5 15	10.9111E+020.0000E+00	0.1450E+02	-.4500E+01
A6 15	10.9111E+020.0000E+00	0.1450E+02	-.5500E+01
A7 15	10.9111E+020.0000E+00	0.1450E+02	-.6500E+01
A8 15	10.9111E+020.0000E+00	0.1450E+02	-.7500E+01
A9 15	10.9111E+020.0000E+00	0.1450E+02	-.8500E+01
AA 15	10.9111E+020.0000E+00	0.1450E+02	-.9500E+01
AB 15	10.9111E+020.0000E+00	0.1450E+02	-.1050E+02
AC 15	10.9111E+020.0000E+00	0.1450E+02	-.1150E+02
AD 15	10.9111E+020.0000E+00	0.1450E+02	-.1250E+02
AE 15	10.9111E+020.0000E+00	0.1450E+02	-.1350E+02
AF 15	10.9111E+020.0000E+00	0.1450E+02	-.1450E+02
AG 15	10.9111E+020.0000E+00	0.1450E+02	-.1550E+02
AH 15	10.9111E+020.0000E+00	0.1450E+02	-.1650E+02
AI 15	10.9111E+020.0000E+00	0.1450E+02	-.1750E+02
AJ 15	10.9111E+020.0000E+00	0.1450E+02	-.1850E+02
A2 16	10.9739E+020.0000E+00	0.1550E+02	-.1500E+01
A3 16	10.9739E+020.0000E+00	0.1550E+02	-.2500E+01
A4 16	10.9739E+020.0000E+00	0.1550E+02	-.3500E+01
A5 16	10.9739E+020.0000E+00	0.1550E+02	-.4500E+01
A6 16	10.9739E+020.0000E+00	0.1550E+02	-.5500E+01
A7 16	10.9739E+020.0000E+00	0.1550E+02	-.6500E+01
A8 16	10.9739E+020.0000E+00	0.1550E+02	-.7500E+01
A9 16	10.9739E+020.0000E+00	0.1550E+02	-.8500E+01
AA 16	10.9739E+020.0000E+00	0.1550E+02	-.9500E+01
AB 16	10.9739E+020.0000E+00	0.1550E+02	-.1050E+02
AC 16	10.9739E+020.0000E+00	0.1550E+02	-.1150E+02
AD 16	10.9739E+020.0000E+00	0.1550E+02	-.1250E+02
AE 16	10.9739E+020.0000E+00	0.1550E+02	-.1350E+02
AF 16	10.9739E+020.0000E+00	0.1550E+02	-.1450E+02
AG 16	10.9739E+020.0000E+00	0.1550E+02	-.1550E+02
AH 16	10.9739E+020.0000E+00	0.1550E+02	-.1650E+02
AI 16	10.9739E+020.0000E+00	0.1550E+02	-.1750E+02
AJ 16	10.9739E+020.0000E+00	0.1550E+02	-.1850E+02
A2 17	10.1037E+030.0000E+00	0.1650E+02	-.1500E+01
A3 17	10.1037E+030.0000E+00	0.1650E+02	-.2500E+01
A4 17	10.1037E+030.0000E+00	0.1650E+02	-.3500E+01
A5 17	10.1037E+030.0000E+00	0.1650E+02	-.4500E+01
A6 17	10.1037E+030.0000E+00	0.1650E+02	-.5500E+01
A7 17	10.1037E+030.0000E+00	0.1650E+02	-.6500E+01
A8 17	10.1037E+030.0000E+00	0.1650E+02	-.7500E+01
A9 17	10.1037E+030.0000E+00	0.1650E+02	-.8500E+01
AA 17	10.1037E+030.0000E+00	0.1650E+02	-.9500E+01
AB 17	10.1037E+030.0000E+00	0.1650E+02	-.1050E+02
AC 17	10.1037E+030.0000E+00	0.1650E+02	-.1150E+02

AD 17	10.1037E+030.0000E+00	0.1650E+02	-.1250E+02
AE 17	10.1037E+030.0000E+00	0.1650E+02	-.1350E+02
AF 17	10.1037E+030.0000E+00	0.1650E+02	-.1450E+02
AG 17	10.1037E+030.0000E+00	0.1650E+02	-.1550E+02
AH 17	10.1037E+030.0000E+00	0.1650E+02	-.1650E+02
AI 17	10.1037E+030.0000E+00	0.1650E+02	-.1750E+02
AJ 17	10.1037E+030.0000E+00	0.1650E+02	-.1850E+02
A2 18	10.1100E+030.0000E+00	0.1750E+02	-.1500E+01
A3 18	10.1100E+030.0000E+00	0.1750E+02	-.2500E+01
A4 18	10.1100E+030.0000E+00	0.1750E+02	-.3500E+01
A5 18	10.1100E+030.0000E+00	0.1750E+02	-.4500E+01
A6 18	10.1100E+030.0000E+00	0.1750E+02	-.5500E+01
A7 18	10.1100E+030.0000E+00	0.1750E+02	-.6500E+01
A8 18	10.1100E+030.0000E+00	0.1750E+02	-.7500E+01
A9 18	10.1100E+030.0000E+00	0.1750E+02	-.8500E+01
AA 18	10.1100E+030.0000E+00	0.1750E+02	-.9500E+01
AB 18	10.1100E+030.0000E+00	0.1750E+02	-.1050E+02
AC 18	10.1100E+030.0000E+00	0.1750E+02	-.1150E+02
AD 18	10.1100E+030.0000E+00	0.1750E+02	-.1250E+02
AE 18	10.1100E+030.0000E+00	0.1750E+02	-.1350E+02
AF 18	10.1100E+030.0000E+00	0.1750E+02	-.1450E+02
AG 18	10.1100E+030.0000E+00	0.1750E+02	-.1550E+02
AH 18	10.1100E+030.0000E+00	0.1750E+02	-.1650E+02
AI 18	10.1100E+030.0000E+00	0.1750E+02	-.1750E+02
AJ 18	10.1100E+030.0000E+00	0.1750E+02	-.1850E+02
A2 19	10.1162E+030.0000E+00	0.1850E+02	-.1500E+01
A3 19	10.1162E+030.0000E+00	0.1850E+02	-.2500E+01
A4 19	10.1162E+030.0000E+00	0.1850E+02	-.3500E+01
A5 19	10.1162E+030.0000E+00	0.1850E+02	-.4500E+01
A6 19	10.1162E+030.0000E+00	0.1850E+02	-.5500E+01
A7 19	10.1162E+030.0000E+00	0.1850E+02	-.6500E+01
A8 19	10.1162E+030.0000E+00	0.1850E+02	-.7500E+01
A9 19	10.1162E+030.0000E+00	0.1850E+02	-.8500E+01
AA 19	10.1162E+030.0000E+00	0.1850E+02	-.9500E+01
AB 19	10.1162E+030.0000E+00	0.1850E+02	-.1050E+02
AC 19	10.1162E+030.0000E+00	0.1850E+02	-.1150E+02
AD 19	10.1162E+030.0000E+00	0.1850E+02	-.1250E+02
AE 19	10.1162E+030.0000E+00	0.1850E+02	-.1350E+02
AF 19	10.1162E+030.0000E+00	0.1850E+02	-.1450E+02
AG 19	10.1162E+030.0000E+00	0.1850E+02	-.1550E+02
AH 19	10.1162E+030.0000E+00	0.1850E+02	-.1650E+02
AI 19	10.1162E+030.0000E+00	0.1850E+02	-.1750E+02
AJ 19	10.1162E+030.0000E+00	0.1850E+02	-.1850E+02
A2 20	10.0000E+000.0000E+00	0.1950E+02	-.1500E+01
A3 20	10.0000E+000.0000E+00	0.1950E+02	-.2500E+01
A4 20	10.0000E+000.0000E+00	0.1950E+02	-.3500E+01
A5 20	10.0000E+000.0000E+00	0.1950E+02	-.4500E+01

A6 20	10.0000E+000.0000E+00	0.1950E+02	-.5500E+01
A7 20	10.0000E+000.0000E+00	0.1950E+02	-.6500E+01
A8 20	10.0000E+000.0000E+00	0.1950E+02	-.7500E+01
A9 20	10.0000E+000.0000E+00	0.1950E+02	-.8500E+01
AA 20	10.0000E+000.0000E+00	0.1950E+02	-.9500E+01
AB 20	10.0000E+000.0000E+00	0.1950E+02	-.1050E+02
AC 20	10.0000E+000.0000E+00	0.1950E+02	-.1150E+02
AD 20	10.0000E+000.0000E+00	0.1950E+02	-.1250E+02
AE 20	10.0000E+000.0000E+00	0.1950E+02	-.1350E+02
AF 20	10.0000E+000.0000E+00	0.1950E+02	-.1450E+02
AG 20	10.0000E+000.0000E+00	0.1950E+02	-.1550E+02
AH 20	10.0000E+000.0000E+00	0.1950E+02	-.1650E+02
AI 20	10.0000E+000.0000E+00	0.1950E+02	-.1750E+02
AJ 20	10.0000E+000.0000E+00	0.1950E+02	-.1850E+02
A1 1	10.0000E+000.0000E+00	0.5000E+00	-.5000E+00
A1 2	10.0000E+000.0000E+00	0.1500E+01	-.5000E+00
A1 3	10.0000E+000.0000E+00	0.2500E+01	-.5000E+00
A1 4	10.0000E+000.0000E+00	0.3500E+01	-.5000E+00
A1 5	10.0000E+000.0000E+00	0.4500E+01	-.5000E+00
A1 6	10.0000E+000.0000E+00	0.5500E+01	-.5000E+00
A1 7	10.0000E+000.0000E+00	0.6500E+01	-.5000E+00
A1 8	10.0000E+000.0000E+00	0.7500E+01	-.5000E+00
A1 9	10.0000E+000.0000E+00	0.8500E+01	-.5000E+00
A1 10	10.0000E+000.0000E+00	0.9500E+01	-.5000E+00
A1 11	10.0000E+000.0000E+00	0.1050E+02	-.5000E+00
A1 12	10.0000E+000.0000E+00	0.1150E+02	-.5000E+00
A1 13	10.0000E+000.0000E+00	0.1250E+02	-.5000E+00
A1 14	10.0000E+000.0000E+00	0.1350E+02	-.5000E+00
A1 15	10.0000E+000.0000E+00	0.1450E+02	-.5000E+00
A1 16	10.0000E+000.0000E+00	0.1550E+02	-.5000E+00
A1 17	10.0000E+000.0000E+00	0.1650E+02	-.5000E+00
A1 18	10.0000E+000.0000E+00	0.1750E+02	-.5000E+00
A1 19	10.0000E+000.0000E+00	0.1850E+02	-.5000E+00
A1 20	10.0000E+000.0000E+00	0.1950E+02	-.5000E+00
AK 1	10.0000E+000.0000E+00	0.5000E+00	-.1950E+02
AK 2	10.0000E+000.0000E+00	0.1500E+01	-.1950E+02
AK 3	10.0000E+000.0000E+00	0.2500E+01	-.1950E+02
AK 4	10.0000E+000.0000E+00	0.3500E+01	-.1950E+02
AK 5	10.0000E+000.0000E+00	0.4500E+01	-.1950E+02
AK 6	10.0000E+000.0000E+00	0.5500E+01	-.1950E+02
AK 7	10.0000E+000.0000E+00	0.6500E+01	-.1950E+02
AK 8	10.0000E+000.0000E+00	0.7500E+01	-.1950E+02
AK 9	10.0000E+000.0000E+00	0.8500E+01	-.1950E+02
AK 10	10.0000E+000.0000E+00	0.9500E+01	-.1950E+02
AK 11	10.0000E+000.0000E+00	0.1050E+02	-.1950E+02
AK 12	10.0000E+000.0000E+00	0.1150E+02	-.1950E+02
AK 13	10.0000E+000.0000E+00	0.1250E+02	-.1950E+02

```
AK 14              10.0000E+000.0000E+00          0.1350E+02          -.1950E+02
AK 15              10.0000E+000.0000E+00          0.1450E+02          -.1950E+02
AK 16              10.0000E+000.0000E+00          0.1550E+02          -.1950E+02
AK 17              10.0000E+000.0000E+00          0.1650E+02          -.1950E+02
AK 18              10.0000E+000.0000E+00          0.1750E+02          -.1950E+02
AK 19              10.0000E+000.0000E+00          0.1850E+02          -.1950E+02
AK 20              10.0000E+000.0000E+00          0.1950E+02          -.1950E+02

CONNE
A1  1A1  2                  10.5000E+000.5000E+000.6283E+01
A2  1A2  2                  10.5000E+000.5000E+000.6283E+01
A3  1A3  2                  10.5000E+000.5000E+000.6283E+01
A4  1A4  2                  10.5000E+000.5000E+000.6283E+01
A5  1A5  2                  10.5000E+000.5000E+000.6283E+01
A6  1A6  2                  10.5000E+000.5000E+000.6283E+01
A7  1A7  2                  10.5000E+000.5000E+000.6283E+01
A8  1A8  2                  10.5000E+000.5000E+000.6283E+01
A9  1A9  2                  10.5000E+000.5000E+000.6283E+01
AA  1AA  2                  10.5000E+000.5000E+000.6283E+01
AB  1AB  2                  10.5000E+000.5000E+000.6283E+01
AC  1AC  2                  10.5000E+000.5000E+000.6283E+01
AD  1AD  2                  10.5000E+000.5000E+000.6283E+01
AE  1AE  2                  10.5000E+000.5000E+000.6283E+01
AF  1AF  2                  10.5000E+000.5000E+000.6283E+01
AG  1AG  2                  10.5000E+000.5000E+000.6283E+01
AH  1AH  2                  10.5000E+000.5000E+000.6283E+01
AI  1AI  2                  10.5000E+000.5000E+000.6283E+01
AJ  1AJ  2                  10.5000E+000.5000E+000.6283E+01
AK  1AK  2                  10.5000E+000.5000E+000.6283E+01
A1  2A1  3                  10.5000E+000.5000E+000.1257E+02
A2  2A2  3                  10.5000E+000.5000E+000.1257E+02
A3  2A3  3                  10.5000E+000.5000E+000.1257E+02
A4  2A4  3                  10.5000E+000.5000E+000.1257E+02
A5  2A5  3                  10.5000E+000.5000E+000.1257E+02
A6  2A6  3                  10.5000E+000.5000E+000.1257E+02
A7  2A7  3                  10.5000E+000.5000E+000.1257E+02
A8  2A8  3                  10.5000E+000.5000E+000.1257E+02
A9  2A9  3                  10.5000E+000.5000E+000.1257E+02
AA  2AA  3                  10.5000E+000.5000E+000.1257E+02
AB  2AB  3                  10.5000E+000.5000E+000.1257E+02
AC  2AC  3                  10.5000E+000.5000E+000.1257E+02
AD  2AD  3                  10.5000E+000.5000E+000.1257E+02
AE  2AE  3                  10.5000E+000.5000E+000.1257E+02
AF  2AF  3                  10.5000E+000.5000E+000.1257E+02
AG  2AG  3                  10.5000E+000.5000E+000.1257E+02
AH  2AH  3                  10.5000E+000.5000E+000.1257E+02
AI  2AI  3                  10.5000E+000.5000E+000.1257E+02
```

```
AJ  2AJ  3          10.5000E+000.5000E+000.1257E+02
AK  2AK  3          10.5000E+000.5000E+000.1257E+02
A1  3A1  4          10.5000E+000.5000E+000.1885E+02
A2  3A2  4          10.5000E+000.5000E+000.1885E+02
A3  3A3  4          10.5000E+000.5000E+000.1885E+02
A4  3A4  4          10.5000E+000.5000E+000.1885E+02
A5  3A5  4          10.5000E+000.5000E+000.1885E+02
A6  3A6  4          10.5000E+000.5000E+000.1885E+02
A7  3A7  4          10.5000E+000.5000E+000.1885E+02
A8  3A8  4          10.5000E+000.5000E+000.1885E+02
A9  3A9  4          10.5000E+000.5000E+000.1885E+02
AA  3AA  4          10.5000E+000.5000E+000.1885E+02
AB  3AB  4          10.5000E+000.5000E+000.1885E+02
AC  3AC  4          10.5000E+000.5000E+000.1885E+02
AD  3AD  4          10.5000E+000.5000E+000.1885E+02
AE  3AE  4          10.5000E+000.5000E+000.1885E+02
AF  3AF  4          10.5000E+000.5000E+000.1885E+02
AG  3AG  4          10.5000E+000.5000E+000.1885E+02
AH  3AH  4          10.5000E+000.5000E+000.1885E+02
AI  3AI  4          10.5000E+000.5000E+000.1885E+02
AJ  3AJ  4          10.5000E+000.5000E+000.1885E+02
AK  3AK  4          10.5000E+000.5000E+000.1885E+02
A1  4A1  5          10.5000E+000.5000E+000.2513E+02
A2  4A2  5          10.5000E+000.5000E+000.2513E+02
A3  4A3  5          10.5000E+000.5000E+000.2513E+02
A4  4A4  5          10.5000E+000.5000E+000.2513E+02
A5  4A5  5          10.5000E+000.5000E+000.2513E+02
A6  4A6  5          10.5000E+000.5000E+000.2513E+02
A7  4A7  5          10.5000E+000.5000E+000.2513E+02
A8  4A8  5          10.5000E+000.5000E+000.2513E+02
A9  4A9  5          10.5000E+000.5000E+000.2513E+02
AA  4AA  5          10.5000E+000.5000E+000.2513E+02
AB  4AB  5          10.5000E+000.5000E+000.2513E+02
AC  4AC  5          10.5000E+000.5000E+000.2513E+02
AD  4AD  5          10.5000E+000.5000E+000.2513E+02
AE  4AE  5          10.5000E+000.5000E+000.2513E+02
AF  4AF  5          10.5000E+000.5000E+000.2513E+02
AG  4AG  5          10.5000E+000.5000E+000.2513E+02
AH  4AH  5          10.5000E+000.5000E+000.2513E+02
AI  4AI  5          10.5000E+000.5000E+000.2513E+02
AJ  4AJ  5          10.5000E+000.5000E+000.2513E+02
AK  4AK  5          10.5000E+000.5000E+000.2513E+02
A1  5A1  6          10.5000E+000.5000E+000.3142E+02
A2  5A2  6          10.5000E+000.5000E+000.3142E+02
A3  5A3  6          10.5000E+000.5000E+000.3142E+02
A4  5A4  6          10.5000E+000.5000E+000.3142E+02
A5  5A5  6          10.5000E+000.5000E+000.3142E+02
```

A6	5A6	6	10.5000E+000.5000E+000.3142E+02
A7	5A7	6	10.5000E+000.5000E+000.3142E+02
A8	5A8	6	10.5000E+000.5000E+000.3142E+02
A9	5A9	6	10.5000E+000.5000E+000.3142E+02
AA	5AA	6	10.5000E+000.5000E+000.3142E+02
AB	5AB	6	10.5000E+000.5000E+000.3142E+02
AC	5AC	6	10.5000E+000.5000E+000.3142E+02
AD	5AD	6	10.5000E+000.5000E+000.3142E+02
AE	5AE	6	10.5000E+000.5000E+000.3142E+02
AF	5AF	6	10.5000E+000.5000E+000.3142E+02
AG	5AG	6	10.5000E+000.5000E+000.3142E+02
AH	5AH	6	10.5000E+000.5000E+000.3142E+02
AI	5AI	6	10.5000E+000.5000E+000.3142E+02
AJ	5AJ	6	10.5000E+000.5000E+000.3142E+02
AK	5AK	6	10.5000E+000.5000E+000.3142E+02
A1	6A1	7	10.5000E+000.5000E+000.3770E+02
A2	6A2	7	10.5000E+000.5000E+000.3770E+02
A3	6A3	7	10.5000E+000.5000E+000.3770E+02
A4	6A4	7	10.5000E+000.5000E+000.3770E+02
A5	6A5	7	10.5000E+000.5000E+000.3770E+02
A6	6A6	7	10.5000E+000.5000E+000.3770E+02
A7	6A7	7	10.5000E+000.5000E+000.3770E+02
A8	6A8	7	10.5000E+000.5000E+000.3770E+02
A9	6A9	7	10.5000E+000.5000E+000.3770E+02
AA	6AA	7	10.5000E+000.5000E+000.3770E+02
AB	6AB	7	10.5000E+000.5000E+000.3770E+02
AC	6AC	7	10.5000E+000.5000E+000.3770E+02
AD	6AD	7	10.5000E+000.5000E+000.3770E+02
AE	6AE	7	10.5000E+000.5000E+000.3770E+02
AF	6AF	7	10.5000E+000.5000E+000.3770E+02
AG	6AG	7	10.5000E+000.5000E+000.3770E+02
AH	6AH	7	10.5000E+000.5000E+000.3770E+02
AI	6AI	7	10.5000E+000.5000E+000.3770E+02
AJ	6AJ	7	10.5000E+000.5000E+000.3770E+02
AK	6AK	7	10.5000E+000.5000E+000.3770E+02
A1	7A1	8	10.5000E+000.5000E+000.4398E+02
A2	7A2	8	10.5000E+000.5000E+000.4398E+02
A3	7A3	8	10.5000E+000.5000E+000.4398E+02
A4	7A4	8	10.5000E+000.5000E+000.4398E+02
A5	7A5	8	10.5000E+000.5000E+000.4398E+02
A6	7A6	8	10.5000E+000.5000E+000.4398E+02
A7	7A7	8	10.5000E+000.5000E+000.4398E+02
A8	7A8	8	10.5000E+000.5000E+000.4398E+02
A9	7A9	8	10.5000E+000.5000E+000.4398E+02
AA	7AA	8	10.5000E+000.5000E+000.4398E+02
AB	7AB	8	10.5000E+000.5000E+000.4398E+02
AC	7AC	8	10.5000E+000.5000E+000.4398E+02

```
AD   7AD   8          10.5000E+000.5000E+000.4398E+02
AE   7AE   8          10.5000E+000.5000E+000.4398E+02
AF   7AF   8          10.5000E+000.5000E+000.4398E+02
AG   7AG   8          10.5000E+000.5000E+000.4398E+02
AH   7AH   8          10.5000E+000.5000E+000.4398E+02
AI   7AI   8          10.5000E+000.5000E+000.4398E+02
AJ   7AJ   8          10.5000E+000.5000E+000.4398E+02
AK   7AK   8          10.5000E+000.5000E+000.4398E+02
A1   8A1   9          10.5000E+000.5000E+000.5027E+02
A2   8A2   9          10.5000E+000.5000E+000.5027E+02
A3   8A3   9          10.5000E+000.5000E+000.5027E+02
A4   8A4   9          10.5000E+000.5000E+000.5027E+02
A5   8A5   9          10.5000E+000.5000E+000.5027E+02
A6   8A6   9          10.5000E+000.5000E+000.5027E+02
A7   8A7   9          10.5000E+000.5000E+000.5027E+02
A8   8A8   9          10.5000E+000.5000E+000.5027E+02
A9   8A9   9          10.5000E+000.5000E+000.5027E+02
AA   8AA   9          10.5000E+000.5000E+000.5027E+02
AB   8AB   9          10.5000E+000.5000E+000.5027E+02
AC   8AC   9          10.5000E+000.5000E+000.5027E+02
AD   8AD   9          10.5000E+000.5000E+000.5027E+02
AE   8AE   9          10.5000E+000.5000E+000.5027E+02
AF   8AF   9          10.5000E+000.5000E+000.5027E+02
AG   8AG   9          10.5000E+000.5000E+000.5027E+02
AH   8AH   9          10.5000E+000.5000E+000.5027E+02
AI   8AI   9          10.5000E+000.5000E+000.5027E+02
AJ   8AJ   9          10.5000E+000.5000E+000.5027E+02
AK   8AK   9          10.5000E+000.5000E+000.5027E+02
A1   9A1  10          10.5000E+000.5000E+000.5655E+02
A2   9A2  10          10.5000E+000.5000E+000.5655E+02
A3   9A3  10          10.5000E+000.5000E+000.5655E+02
A4   9A4  10          10.5000E+000.5000E+000.5655E+02
A5   9A5  10          10.5000E+000.5000E+000.5655E+02
A6   9A6  10          10.5000E+000.5000E+000.5655E+02
A7   9A7  10          10.5000E+000.5000E+000.5655E+02
A8   9A8  10          10.5000E+000.5000E+000.5655E+02
A9   9A9  10          10.5000E+000.5000E+000.5655E+02
AA   9AA  10          10.5000E+000.5000E+000.5655E+02
AB   9AB  10          10.5000E+000.5000E+000.5655E+02
AC   9AC  10          10.5000E+000.5000E+000.5655E+02
AD   9AD  10          10.5000E+000.5000E+000.5655E+02
AE   9AE  10          10.5000E+000.5000E+000.5655E+02
AF   9AF  10          10.5000E+000.5000E+000.5655E+02
AG   9AG  10          10.5000E+000.5000E+000.5655E+02
AH   9AH  10          10.5000E+000.5000E+000.5655E+02
AI   9AI  10          10.5000E+000.5000E+000.5655E+02
AJ   9AJ  10          10.5000E+000.5000E+000.5655E+02
```

```
AK  9AK 10                    10.5000E+000.5000E+000.5655E+02
A1 10A1 11                    10.5000E+000.5000E+000.6283E+02
A2 10A2 11                    10.5000E+000.5000E+000.6283E+02
A3 10A3 11                    10.5000E+000.5000E+000.6283E+02
A4 10A4 11                    10.5000E+000.5000E+000.6283E+02
A5 10A5 11                    10.5000E+000.5000E+000.6283E+02
A6 10A6 11                    10.5000E+000.5000E+000.6283E+02
A7 10A7 11                    10.5000E+000.5000E+000.6283E+02
A8 10A8 11                    10.5000E+000.5000E+000.6283E+02
A9 10A9 11                    10.5000E+000.5000E+000.6283E+02
AA 10AA 11                    10.5000E+000.5000E+000.6283E+02
AB 10AB 11                    10.5000E+000.5000E+000.6283E+02
AC 10AC 11                    10.5000E+000.5000E+000.6283E+02
AD 10AD 11                    10.5000E+000.5000E+000.6283E+02
AE 10AE 11                    10.5000E+000.5000E+000.6283E+02
AF 10AF 11                    10.5000E+000.5000E+000.6283E+02
AG 10AG 11                    10.5000E+000.5000E+000.6283E+02
AH 10AH 11                    10.5000E+000.5000E+000.6283E+02
AI 10AI 11                    10.5000E+000.5000E+000.6283E+02
AJ 10AJ 11                    10.5000E+000.5000E+000.6283E+02
AK 10AK 11                    10.5000E+000.5000E+000.6283E+02
A1 11A1 12                    10.5000E+000.5000E+000.6912E+02
A2 11A2 12                    10.5000E+000.5000E+000.6912E+02
A3 11A3 12                    10.5000E+000.5000E+000.6912E+02
A4 11A4 12                    10.5000E+000.5000E+000.6912E+02
A5 11A5 12                    10.5000E+000.5000E+000.6912E+02
A6 11A6 12                    10.5000E+000.5000E+000.6912E+02
A7 11A7 12                    10.5000E+000.5000E+000.6912E+02
A8 11A8 12                    10.5000E+000.5000E+000.6912E+02
A9 11A9 12                    10.5000E+000.5000E+000.6912E+02
AA 11AA 12                    10.5000E+000.5000E+000.6912E+02
AB 11AB 12                    10.5000E+000.5000E+000.6912E+02
AC 11AC 12                    10.5000E+000.5000E+000.6912E+02
AD 11AD 12                    10.5000E+000.5000E+000.6912E+02
AE 11AE 12                    10.5000E+000.5000E+000.6912E+02
AF 11AF 12                    10.5000E+000.5000E+000.6912E+02
AG 11AG 12                    10.5000E+000.5000E+000.6912E+02
AH 11AH 12                    10.5000E+000.5000E+000.6912E+02
AI 11AI 12                    10.5000E+000.5000E+000.6912E+02
AJ 11AJ 12                    10.5000E+000.5000E+000.6912E+02
AK 11AK 12                    10.5000E+000.5000E+000.6912E+02
A1 12A1 13                    10.5000E+000.5000E+000.7540E+02
A2 12A2 13                    10.5000E+000.5000E+000.7540E+02
A3 12A3 13                    10.5000E+000.5000E+000.7540E+02
A4 12A4 13                    10.5000E+000.5000E+000.7540E+02
A5 12A5 13                    10.5000E+000.5000E+000.7540E+02
A6 12A6 13                    10.5000E+000.5000E+000.7540E+02
```

```
A7 12A7 13                    10.5000E+000.5000E+000.7540E+02
A8 12A8 13                    10.5000E+000.5000E+000.7540E+02
A9 12A9 13                    10.5000E+000.5000E+000.7540E+02
AA 12AA 13                    10.5000E+000.5000E+000.7540E+02
AB 12AB 13                    10.5000E+000.5000E+000.7540E+02
AC 12AC 13                    10.5000E+000.5000E+000.7540E+02
AD 12AD 13                    10.5000E+000.5000E+000.7540E+02
AE 12AE 13                    10.5000E+000.5000E+000.7540E+02
AF 12AF 13                    10.5000E+000.5000E+000.7540E+02
AG 12AG 13                    10.5000E+000.5000E+000.7540E+02
AH 12AH 13                    10.5000E+000.5000E+000.7540E+02
AI 12AI 13                    10.5000E+000.5000E+000.7540E+02
AJ 12AJ 13                    10.5000E+000.5000E+000.7540E+02
AK 12AK 13                    10.5000E+000.5000E+000.7540E+02
A1 13A1 14                    10.5000E+000.5000E+000.8168E+02
A2 13A2 14                    10.5000E+000.5000E+000.8168E+02
A3 13A3 14                    10.5000E+000.5000E+000.8168E+02
A4 13A4 14                    10.5000E+000.5000E+000.8168E+02
A5 13A5 14                    10.5000E+000.5000E+000.8168E+02
A6 13A6 14                    10.5000E+000.5000E+000.8168E+02
A7 13A7 14                    10.5000E+000.5000E+000.8168E+02
A8 13A8 14                    10.5000E+000.5000E+000.8168E+02
A9 13A9 14                    10.5000E+000.5000E+000.8168E+02
AA 13AA 14                    10.5000E+000.5000E+000.8168E+02
AB 13AB 14                    10.5000E+000.5000E+000.8168E+02
AC 13AC 14                    10.5000E+000.5000E+000.8168E+02
AD 13AD 14                    10.5000E+000.5000E+000.8168E+02
AE 13AE 14                    10.5000E+000.5000E+000.8168E+02
AF 13AF 14                    10.5000E+000.5000E+000.8168E+02
AG 13AG 14                    10.5000E+000.5000E+000.8168E+02
AH 13AH 14                    10.5000E+000.5000E+000.8168E+02
AI 13AI 14                    10.5000E+000.5000E+000.8168E+02
AJ 13AJ 14                    10.5000E+000.5000E+000.8168E+02
AK 13AK 14                    10.5000E+000.5000E+000.8168E+02
A1 14A1 15                    10.5000E+000.5000E+000.8796E+02
A2 14A2 15                    10.5000E+000.5000E+000.8796E+02
A3 14A3 15                    10.5000E+000.5000E+000.8796E+02
A4 14A4 15                    10.5000E+000.5000E+000.8796E+02
A5 14A5 15                    10.5000E+000.5000E+000.8796E+02
A6 14A6 15                    10.5000E+000.5000E+000.8796E+02
A7 14A7 15                    10.5000E+000.5000E+000.8796E+02
A8 14A8 15                    10.5000E+000.5000E+000.8796E+02
A9 14A9 15                    10.5000E+000.5000E+000.8796E+02
AA 14AA 15                    10.5000E+000.5000E+000.8796E+02
AB 14AB 15                    10.5000E+000.5000E+000.8796E+02
AC 14AC 15                    10.5000E+000.5000E+000.8796E+02
AD 14AD 15                    10.5000E+000.5000E+000.8796E+02
```

```
AE 14AE 15                    10.5000E+000.5000E+000.8796E+02
AF 14AF 15                    10.5000E+000.5000E+000.8796E+02
AG 14AG 15                    10.5000E+000.5000E+000.8796E+02
AH 14AH 15                    10.5000E+000.5000E+000.8796E+02
AI 14AI 15                    10.5000E+000.5000E+000.8796E+02
AJ 14AJ 15                    10.5000E+000.5000E+000.8796E+02
AK 14AK 15                    10.5000E+000.5000E+000.8796E+02
A1 15A1 16                    10.5000E+000.5000E+000.9425E+02
A2 15A2 16                    10.5000E+000.5000E+000.9425E+02
A3 15A3 16                    10.5000E+000.5000E+000.9425E+02
A4 15A4 16                    10.5000E+000.5000E+000.9425E+02
A5 15A5 16                    10.5000E+000.5000E+000.9425E+02
A6 15A6 16                    10.5000E+000.5000E+000.9425E+02
A7 15A7 16                    10.5000E+000.5000E+000.9425E+02
A8 15A8 16                    10.5000E+000.5000E+000.9425E+02
A9 15A9 16                    10.5000E+000.5000E+000.9425E+02
AA 15AA 16                    10.5000E+000.5000E+000.9425E+02
AB 15AB 16                    10.5000E+000.5000E+000.9425E+02
AC 15AC 16                    10.5000E+000.5000E+000.9425E+02
AD 15AD 16                    10.5000E+000.5000E+000.9425E+02
AE 15AE 16                    10.5000E+000.5000E+000.9425E+02
AF 15AF 16                    10.5000E+000.5000E+000.9425E+02
AG 15AG 16                    10.5000E+000.5000E+000.9425E+02
AH 15AH 16                    10.5000E+000.5000E+000.9425E+02
AI 15AI 16                    10.5000E+000.5000E+000.9425E+02
AJ 15AJ 16                    10.5000E+000.5000E+000.9425E+02
AK 15AK 16                    10.5000E+000.5000E+000.9425E+02
A1 16A1 17                    10.5000E+000.5000E+000.1005E+03
A2 16A2 17                    10.5000E+000.5000E+000.1005E+03
A3 16A3 17                    10.5000E+000.5000E+000.1005E+03
A4 16A4 17                    10.5000E+000.5000E+000.1005E+03
A5 16A5 17                    10.5000E+000.5000E+000.1005E+03
A6 16A6 17                    10.5000E+000.5000E+000.1005E+03
A7 16A7 17                    10.5000E+000.5000E+000.1005E+03
A8 16A8 17                    10.5000E+000.5000E+000.1005E+03
A9 16A9 17                    10.5000E+000.5000E+000.1005E+03
AA 16AA 17                    10.5000E+000.5000E+000.1005E+03
AB 16AB 17                    10.5000E+000.5000E+000.1005E+03
AC 16AC 17                    10.5000E+000.5000E+000.1005E+03
AD 16AD 17                    10.5000E+000.5000E+000.1005E+03
AE 16AE 17                    10.5000E+000.5000E+000.1005E+03
AF 16AF 17                    10.5000E+000.5000E+000.1005E+03
AG 16AG 17                    10.5000E+000.5000E+000.1005E+03
AH 16AH 17                    10.5000E+000.5000E+000.1005E+03
AI 16AI 17                    10.5000E+000.5000E+000.1005E+03
AJ 16AJ 17                    10.5000E+000.5000E+000.1005E+03
AK 16AK 17                    10.5000E+000.5000E+000.1005E+03
```

```
A1 17A1 18                    10.5000E+000.5000E+000.1068E+03
A2 17A2 18                    10.5000E+000.5000E+000.1068E+03
A3 17A3 18                    10.5000E+000.5000E+000.1068E+03
A4 17A4 18                    10.5000E+000.5000E+000.1068E+03
A5 17A5 18                    10.5000E+000.5000E+000.1068E+03
A6 17A6 18                    10.5000E+000.5000E+000.1068E+03
A7 17A7 18                    10.5000E+000.5000E+000.1068E+03
A8 17A8 18                    10.5000E+000.5000E+000.1068E+03
A9 17A9 18                    10.5000E+000.5000E+000.1068E+03
AA 17AA 18                    10.5000E+000.5000E+000.1068E+03
AB 17AB 18                    10.5000E+000.5000E+000.1068E+03
AC 17AC 18                    10.5000E+000.5000E+000.1068E+03
AD 17AD 18                    10.5000E+000.5000E+000.1068E+03
AE 17AE 18                    10.5000E+000.5000E+000.1068E+03
AF 17AF 18                    10.5000E+000.5000E+000.1068E+03
AG 17AG 18                    10.5000E+000.5000E+000.1068E+03
AH 17AH 18                    10.5000E+000.5000E+000.1068E+03
AI 17AI 18                    10.5000E+000.5000E+000.1068E+03
AJ 17AJ 18                    10.5000E+000.5000E+000.1068E+03
AK 17AK 18                    10.5000E+000.5000E+000.1068E+03
A1 18A1 19                    10.5000E+000.5000E+000.1131E+03
A2 18A2 19                    10.5000E+000.5000E+000.1131E+03
A3 18A3 19                    10.5000E+000.5000E+000.1131E+03
A4 18A4 19                    10.5000E+000.5000E+000.1131E+03
A5 18A5 19                    10.5000E+000.5000E+000.1131E+03
A6 18A6 19                    10.5000E+000.5000E+000.1131E+03
A7 18A7 19                    10.5000E+000.5000E+000.1131E+03
A8 18A8 19                    10.5000E+000.5000E+000.1131E+03
A9 18A9 19                    10.5000E+000.5000E+000.1131E+03
AA 18AA 19                    10.5000E+000.5000E+000.1131E+03
AB 18AB 19                    10.5000E+000.5000E+000.1131E+03
AC 18AC 19                    10.5000E+000.5000E+000.1131E+03
AD 18AD 19                    10.5000E+000.5000E+000.1131E+03
AE 18AE 19                    10.5000E+000.5000E+000.1131E+03
AF 18AF 19                    10.5000E+000.5000E+000.1131E+03
AG 18AG 19                    10.5000E+000.5000E+000.1131E+03
AH 18AH 19                    10.5000E+000.5000E+000.1131E+03
AI 18AI 19                    10.5000E+000.5000E+000.1131E+03
AJ 18AJ 19                    10.5000E+000.5000E+000.1131E+03
AK 18AK 19                    10.5000E+000.5000E+000.1131E+03
A1 19A1 20                    10.5000E+000.5000E+000.1194E+03
A2 19A2 20                    10.5000E+000.5000E+000.1194E+03
A3 19A3 20                    10.5000E+000.5000E+000.1194E+03
A4 19A4 20                    10.5000E+000.5000E+000.1194E+03
A5 19A5 20                    10.5000E+000.5000E+000.1194E+03
A6 19A6 20                    10.5000E+000.5000E+000.1194E+03
A7 19A7 20                    10.5000E+000.5000E+000.1194E+03
```

```
A8 19A8 20                    10.5000E+000.5000E+000.1194E+03
A9 19A9 20                    10.5000E+000.5000E+000.1194E+03
AA 19AA 20                    10.5000E+000.5000E+000.1194E+03
AB 19AB 20                    10.5000E+000.5000E+000.1194E+03
AC 19AC 20                    10.5000E+000.5000E+000.1194E+03
AD 19AD 20                    10.5000E+000.5000E+000.1194E+03
AE 19AE 20                    10.5000E+000.5000E+000.1194E+03
AF 19AF 20                    10.5000E+000.5000E+000.1194E+03
AG 19AG 20                    10.5000E+000.5000E+000.1194E+03
AH 19AH 20                    10.5000E+000.5000E+000.1194E+03
AI 19AI 20                    10.5000E+000.5000E+000.1194E+03
AJ 19AJ 20                    10.5000E+000.5000E+000.1194E+03
AK 19AK 20                    10.5000E+000.5000E+000.1194E+03
A1  1A2  1                    30.5000E+000.5000E+000.3142E+011.
A2  1A3  1                    30.5000E+000.5000E+000.3142E+011.
A3  1A4  1                    30.5000E+000.5000E+000.3142E+011.
A4  1A5  1                    30.5000E+000.5000E+000.3142E+011.
A5  1A6  1                    30.5000E+000.5000E+000.3142E+011.
A6  1A7  1                    30.5000E+000.5000E+000.3142E+011.
A7  1A8  1                    30.5000E+000.5000E+000.3142E+011.
A8  1A9  1                    30.5000E+000.5000E+000.3142E+011.
A9  1AA  1                    30.5000E+000.5000E+000.3142E+011.
AA  1AB  1                    30.5000E+000.5000E+000.3142E+011.
AB  1AC  1                    30.5000E+000.5000E+000.3142E+011.
AC  1AD  1                    30.5000E+000.5000E+000.3142E+011.
AD  1AE  1                    30.5000E+000.5000E+000.3142E+011.
AE  1AF  1                    30.5000E+000.5000E+000.3142E+011.
AF  1AG  1                    30.5000E+000.5000E+000.3142E+011.
AG  1AH  1                    30.5000E+000.5000E+000.3142E+011.
AH  1AI  1                    30.5000E+000.5000E+000.3142E+011.
AI  1AJ  1                    30.5000E+000.5000E+000.3142E+011.
AJ  1AK  1                    30.5000E+000.5000E+000.3142E+011.
A1  2A2  2                    30.5000E+000.5000E+000.9425E+011.
A2  2A3  2                    30.5000E+000.5000E+000.9425E+011.
A3  2A4  2                    30.5000E+000.5000E+000.9425E+011.
A4  2A5  2                    30.5000E+000.5000E+000.9425E+011.
A5  2A6  2                    30.5000E+000.5000E+000.9425E+011.
A6  2A7  2                    30.5000E+000.5000E+000.9425E+011.
A7  2A8  2                    30.5000E+000.5000E+000.9425E+011.
A8  2A9  2                    30.5000E+000.5000E+000.9425E+011.
A9  2AA  2                    30.5000E+000.5000E+000.9425E+011.
AA  2AB  2                    30.5000E+000.5000E+000.9425E+011.
AB  2AC  2                    30.5000E+000.5000E+000.9425E+011.
AC  2AD  2                    30.5000E+000.5000E+000.9425E+011.
AD  2AE  2                    30.5000E+000.5000E+000.9425E+011.
AE  2AF  2                    30.5000E+000.5000E+000.9425E+011.
AF  2AG  2                    30.5000E+000.5000E+000.9425E+011.
```

```
AG  2AH  2                30.5000E+000.5000E+000.9425E+011.
AH  2AI  2                30.5000E+000.5000E+000.9425E+011.
AI  2AJ  2                30.5000E+000.5000E+000.9425E+011.
AJ  2AK  2                30.5000E+000.5000E+000.9425E+011.
A1  3A2  3                30.5000E+000.5000E+000.1571E+021.
A2  3A3  3                30.5000E+000.5000E+000.1571E+021.
A3  3A4  3                30.5000E+000.5000E+000.1571E+021.
A4  3A5  3                30.5000E+000.5000E+000.1571E+021.
A5  3A6  3                30.5000E+000.5000E+000.1571E+021.
A6  3A7  3                30.5000E+000.5000E+000.1571E+021.
A7  3A8  3                30.5000E+000.5000E+000.1571E+021.
A8  3A9  3                30.5000E+000.5000E+000.1571E+021.
A9  3AA  3                30.5000E+000.5000E+000.1571E+021.
AA  3AB  3                30.5000E+000.5000E+000.1571E+021.
AB  3AC  3                30.5000E+000.5000E+000.1571E+021.
AC  3AD  3                30.5000E+000.5000E+000.1571E+021.
AD  3AE  3                30.5000E+000.5000E+000.1571E+021.
AE  3AF  3                30.5000E+000.5000E+000.1571E+021.
AF  3AG  3                30.5000E+000.5000E+000.1571E+021.
AG  3AH  3                30.5000E+000.5000E+000.1571E+021.
AH  3AI  3                30.5000E+000.5000E+000.1571E+021.
AI  3AJ  3                30.5000E+000.5000E+000.1571E+021.
AJ  3AK  3                30.5000E+000.5000E+000.1571E+021.
A1  4A2  4                30.5000E+000.5000E+000.2199E+021.
A2  4A3  4                30.5000E+000.5000E+000.2199E+021.
A3  4A4  4                30.5000E+000.5000E+000.2199E+021.
A4  4A5  4                30.5000E+000.5000E+000.2199E+021.
A5  4A6  4                30.5000E+000.5000E+000.2199E+021.
A6  4A7  4                30.5000E+000.5000E+000.2199E+021.
A7  4A8  4                30.5000E+000.5000E+000.2199E+021.
A8  4A9  4                30.5000E+000.5000E+000.2199E+021.
A9  4AA  4                30.5000E+000.5000E+000.2199E+021.
AA  4AB  4                30.5000E+000.5000E+000.2199E+021.
AB  4AC  4                30.5000E+000.5000E+000.2199E+021.
AC  4AD  4                30.5000E+000.5000E+000.2199E+021.
AD  4AE  4                30.5000E+000.5000E+000.2199E+021.
AE  4AF  4                30.5000E+000.5000E+000.2199E+021.
AF  4AG  4                30.5000E+000.5000E+000.2199E+021.
AG  4AH  4                30.5000E+000.5000E+000.2199E+021.
AH  4AI  4                30.5000E+000.5000E+000.2199E+021.
AI  4AJ  4                30.5000E+000.5000E+000.2199E+021.
AJ  4AK  4                30.5000E+000.5000E+000.2199E+021.
A1  5A2  5                30.5000E+000.5000E+000.2827E+021.
A2  5A3  5                30.5000E+000.5000E+000.2827E+021.
A3  5A4  5                30.5000E+000.5000E+000.2827E+021.
A4  5A5  5                30.5000E+000.5000E+000.2827E+021.
A5  5A6  5                30.5000E+000.5000E+000.2827E+021.
```

```
A6  5A7  5                30.5000E+000.5000E+000.2827E+021.
A7  5A8  5                30.5000E+000.5000E+000.2827E+021.
A8  5A9  5                30.5000E+000.5000E+000.2827E+021.
A9  5AA  5                30.5000E+000.5000E+000.2827E+021.
AA  5AB  5                30.5000E+000.5000E+000.2827E+021.
AB  5AC  5                30.5000E+000.5000E+000.2827E+021.
AC  5AD  5                30.5000E+000.5000E+000.2827E+021.
AD  5AE  5                30.5000E+000.5000E+000.2827E+021.
AE  5AF  5                30.5000E+000.5000E+000.2827E+021.
AF  5AG  5                30.5000E+000.5000E+000.2827E+021.
AG  5AH  5                30.5000E+000.5000E+000.2827E+021.
AH  5AI  5                30.5000E+000.5000E+000.2827E+021.
AI  5AJ  5                30.5000E+000.5000E+000.2827E+021.
AJ  5AK  5                30.5000E+000.5000E+000.2827E+021.
A1  6A2  6                30.5000E+000.5000E+000.3456E+021.
A2  6A3  6                30.5000E+000.5000E+000.3456E+021.
A3  6A4  6                30.5000E+000.5000E+000.3456E+021.
A4  6A5  6                30.5000E+000.5000E+000.3456E+021.
A5  6A6  6                30.5000E+000.5000E+000.3456E+021.
A6  6A7  6                30.5000E+000.5000E+000.3456E+021.
A7  6A8  6                30.5000E+000.5000E+000.3456E+021.
A8  6A9  6                30.5000E+000.5000E+000.3456E+021.
A9  6AA  6                30.5000E+000.5000E+000.3456E+021.
AA  6AB  6                30.5000E+000.5000E+000.3456E+021.
AB  6AC  6                30.5000E+000.5000E+000.3456E+021.
AC  6AD  6                30.5000E+000.5000E+000.3456E+021.
AD  6AE  6                30.5000E+000.5000E+000.3456E+021.
AE  6AF  6                30.5000E+000.5000E+000.3456E+021.
AF  6AG  6                30.5000E+000.5000E+000.3456E+021.
AG  6AH  6                30.5000E+000.5000E+000.3456E+021.
AH  6AI  6                30.5000E+000.5000E+000.3456E+021.
AI  6AJ  6                30.5000E+000.5000E+000.3456E+021.
AJ  6AK  6                30.5000E+000.5000E+000.3456E+021.
A1  7A2  7                30.5000E+000.5000E+000.4084E+021.
A2  7A3  7                30.5000E+000.5000E+000.4084E+021.
A3  7A4  7                30.5000E+000.5000E+000.4084E+021.
A4  7A5  7                30.5000E+000.5000E+000.4084E+021.
A5  7A6  7                30.5000E+000.5000E+000.4084E+021.
A6  7A7  7                30.5000E+000.5000E+000.4084E+021.
A7  7A8  7                30.5000E+000.5000E+000.4084E+021.
A8  7A9  7                30.5000E+000.5000E+000.4084E+021.
A9  7AA  7                30.5000E+000.5000E+000.4084E+021.
AA  7AB  7                30.5000E+000.5000E+000.4084E+021.
AB  7AC  7                30.5000E+000.5000E+000.4084E+021.
AC  7AD  7                30.5000E+000.5000E+000.4084E+021.
AD  7AE  7                30.5000E+000.5000E+000.4084E+021.
AE  7AF  7                30.5000E+000.5000E+000.4084E+021.
```

```
AF   7AG   7          30.5000E+000.5000E+000.4084E+021.
AG   7AH   7          30.5000E+000.5000E+000.4084E+021.
AH   7AI   7          30.5000E+000.5000E+000.4084E+021.
AI   7AJ   7          30.5000E+000.5000E+000.4084E+021.
AJ   7AK   7          30.5000E+000.5000E+000.4084E+021.
A1   8A2   8          30.5000E+000.5000E+000.4712E+021.
A2   8A3   8          30.5000E+000.5000E+000.4712E+021.
A3   8A4   8          30.5000E+000.5000E+000.4712E+021.
A4   8A5   8          30.5000E+000.5000E+000.4712E+021.
A5   8A6   8          30.5000E+000.5000E+000.4712E+021.
A6   8A7   8          30.5000E+000.5000E+000.4712E+021.
A7   8A8   8          30.5000E+000.5000E+000.4712E+021.
A8   8A9   8          30.5000E+000.5000E+000.4712E+021.
A9   8AA   8          30.5000E+000.5000E+000.4712E+021.
AA   8AB   8          30.5000E+000.5000E+000.4712E+021.
AB   8AC   8          30.5000E+000.5000E+000.4712E+021.
AC   8AD   8          30.5000E+000.5000E+000.4712E+021.
AD   8AE   8          30.5000E+000.5000E+000.4712E+021.
AE   8AF   8          30.5000E+000.5000E+000.4712E+021.
AF   8AG   8          30.5000E+000.5000E+000.4712E+021.
AG   8AH   8          30.5000E+000.5000E+000.4712E+021.
AH   8AI   8          30.5000E+000.5000E+000.4712E+021.
AI   8AJ   8          30.5000E+000.5000E+000.4712E+021.
AJ   8AK   8          30.5000E+000.5000E+000.4712E+021.
A1   9A2   9          30.5000E+000.5000E+000.5341E+021.
A2   9A3   9          30.5000E+000.5000E+000.5341E+021.
A3   9A4   9          30.5000E+000.5000E+000.5341E+021.
A4   9A5   9          30.5000E+000.5000E+000.5341E+021.
A5   9A6   9          30.5000E+000.5000E+000.5341E+021.
A6   9A7   9          30.5000E+000.5000E+000.5341E+021.
A7   9A8   9          30.5000E+000.5000E+000.5341E+021.
A8   9A9   9          30.5000E+000.5000E+000.5341E+021.
A9   9AA   9          30.5000E+000.5000E+000.5341E+021.
AA   9AB   9          30.5000E+000.5000E+000.5341E+021.
AB   9AC   9          30.5000E+000.5000E+000.5341E+021.
AC   9AD   9          30.5000E+000.5000E+000.5341E+021.
AD   9AE   9          30.5000E+000.5000E+000.5341E+021.
AE   9AF   9          30.5000E+000.5000E+000.5341E+021.
AF   9AG   9          30.5000E+000.5000E+000.5341E+021.
AG   9AH   9          30.5000E+000.5000E+000.5341E+021.
AH   9AI   9          30.5000E+000.5000E+000.5341E+021.
AI   9AJ   9          30.5000E+000.5000E+000.5341E+021.
AJ   9AK   9          30.5000E+000.5000E+000.5341E+021.
A1  10A2  10          30.5000E+000.5000E+000.5969E+021.
A2  10A3  10          30.5000E+000.5000E+000.5969E+021.
A3  10A4  10          30.5000E+000.5000E+000.5969E+021.
A4  10A5  10          30.5000E+000.5000E+000.5969E+021.
```

```
A5 10A6 10                    30.5000E+000.5000E+000.5969E+021.
A6 10A7 10                    30.5000E+000.5000E+000.5969E+021.
A7 10A8 10                    30.5000E+000.5000E+000.5969E+021.
A8 10A9 10                    30.5000E+000.5000E+000.5969E+021.
A9 10AA 10                    30.5000E+000.5000E+000.5969E+021.
AA 10AB 10                    30.5000E+000.5000E+000.5969E+021.
AB 10AC 10                    30.5000E+000.5000E+000.5969E+021.
AC 10AD 10                    30.5000E+000.5000E+000.5969E+021.
AD 10AE 10                    30.5000E+000.5000E+000.5969E+021.
AE 10AF 10                    30.5000E+000.5000E+000.5969E+021.
AF 10AG 10                    30.5000E+000.5000E+000.5969E+021.
AG 10AH 10                    30.5000E+000.5000E+000.5969E+021.
AH 10AI 10                    30.5000E+000.5000E+000.5969E+021.
AI 10AJ 10                    30.5000E+000.5000E+000.5969E+021.
AJ 10AK 10                    30.5000E+000.5000E+000.5969E+021.
A1 11A2 11                    30.5000E+000.5000E+000.6597E+021.
A2 11A3 11                    30.5000E+000.5000E+000.6597E+021.
A3 11A4 11                    30.5000E+000.5000E+000.6597E+021.
A4 11A5 11                    30.5000E+000.5000E+000.6597E+021.
A5 11A6 11                    30.5000E+000.5000E+000.6597E+021.
A6 11A7 11                    30.5000E+000.5000E+000.6597E+021.
A7 11A8 11                    30.5000E+000.5000E+000.6597E+021.
A8 11A9 11                    30.5000E+000.5000E+000.6597E+021.
A9 11AA 11                    30.5000E+000.5000E+000.6597E+021.
AA 11AB 11                    30.5000E+000.5000E+000.6597E+021.
AB 11AC 11                    30.5000E+000.5000E+000.6597E+021.
AC 11AD 11                    30.5000E+000.5000E+000.6597E+021.
AD 11AE 11                    30.5000E+000.5000E+000.6597E+021.
AE 11AF 11                    30.5000E+000.5000E+000.6597E+021.
AF 11AG 11                    30.5000E+000.5000E+000.6597E+021.
AG 11AH 11                    30.5000E+000.5000E+000.6597E+021.
AH 11AI 11                    30.5000E+000.5000E+000.6597E+021.
AI 11AJ 11                    30.5000E+000.5000E+000.6597E+021.
AJ 11AK 11                    30.5000E+000.5000E+000.6597E+021.
A1 12A2 12                    30.5000E+000.5000E+000.7226E+021.
A2 12A3 12                    30.5000E+000.5000E+000.7226E+021.
A3 12A4 12                    30.5000E+000.5000E+000.7226E+021.
A4 12A5 12                    30.5000E+000.5000E+000.7226E+021.
A5 12A6 12                    30.5000E+000.5000E+000.7226E+021.
A6 12A7 12                    30.5000E+000.5000E+000.7226E+021.
A7 12A8 12                    30.5000E+000.5000E+000.7226E+021.
A8 12A9 12                    30.5000E+000.5000E+000.7226E+021.
A9 12AA 12                    30.5000E+000.5000E+000.7226E+021.
AA 12AB 12                    30.5000E+000.5000E+000.7226E+021.
AB 12AC 12                    30.5000E+000.5000E+000.7226E+021.
AC 12AD 12                    30.5000E+000.5000E+000.7226E+021.
AD 12AE 12                    30.5000E+000.5000E+000.7226E+021.
```

```
AE 12AF 12                    30.5000E+000.5000E+000.7226E+021.
AF 12AG 12                    30.5000E+000.5000E+000.7226E+021.
AG 12AH 12                    30.5000E+000.5000E+000.7226E+021.
AH 12AI 12                    30.5000E+000.5000E+000.7226E+021.
AI 12AJ 12                    30.5000E+000.5000E+000.7226E+021.
AJ 12AK 12                    30.5000E+000.5000E+000.7226E+021.
A1 13A2 13                    30.5000E+000.5000E+000.7854E+021.
A2 13A3 13                    30.5000E+000.5000E+000.7854E+021.
A3 13A4 13                    30.5000E+000.5000E+000.7854E+021.
A4 13A5 13                    30.5000E+000.5000E+000.7854E+021.
A5 13A6 13                    30.5000E+000.5000E+000.7854E+021.
A6 13A7 13                    30.5000E+000.5000E+000.7854E+021.
A7 13A8 13                    30.5000E+000.5000E+000.7854E+021.
A8 13A9 13                    30.5000E+000.5000E+000.7854E+021.
A9 13AA 13                    30.5000E+000.5000E+000.7854E+021.
AA 13AB 13                    30.5000E+000.5000E+000.7854E+021.
AB 13AC 13                    30.5000E+000.5000E+000.7854E+021.
AC 13AD 13                    30.5000E+000.5000E+000.7854E+021.
AD 13AE 13                    30.5000E+000.5000E+000.7854E+021.
AE 13AF 13                    30.5000E+000.5000E+000.7854E+021.
AF 13AG 13                    30.5000E+000.5000E+000.7854E+021.
AG 13AH 13                    30.5000E+000.5000E+000.7854E+021.
AH 13AI 13                    30.5000E+000.5000E+000.7854E+021.
AI 13AJ 13                    30.5000E+000.5000E+000.7854E+021.
AJ 13AK 13                    30.5000E+000.5000E+000.7854E+021.
A1 14A2 14                    30.5000E+000.5000E+000.8482E+021.
A2 14A3 14                    30.5000E+000.5000E+000.8482E+021.
A3 14A4 14                    30.5000E+000.5000E+000.8482E+021.
A4 14A5 14                    30.5000E+000.5000E+000.8482E+021.
A5 14A6 14                    30.5000E+000.5000E+000.8482E+021.
A6 14A7 14                    30.5000E+000.5000E+000.8482E+021.
A7 14A8 14                    30.5000E+000.5000E+000.8482E+021.
A8 14A9 14                    30.5000E+000.5000E+000.8482E+021.
A9 14AA 14                    30.5000E+000.5000E+000.8482E+021.
AA 14AB 14                    30.5000E+000.5000E+000.8482E+021.
AB 14AC 14                    30.5000E+000.5000E+000.8482E+021.
AC 14AD 14                    30.5000E+000.5000E+000.8482E+021.
AD 14AE 14                    30.5000E+000.5000E+000.8482E+021.
AE 14AF 14                    30.5000E+000.5000E+000.8482E+021.
AF 14AG 14                    30.5000E+000.5000E+000.8482E+021.
AG 14AH 14                    30.5000E+000.5000E+000.8482E+021.
AH 14AI 14                    30.5000E+000.5000E+000.8482E+021.
AI 14AJ 14                    30.5000E+000.5000E+000.8482E+021.
AJ 14AK 14                    30.5000E+000.5000E+000.8482E+021.
A1 15A2 15                    30.5000E+000.5000E+000.9111E+021.
A2 15A3 15                    30.5000E+000.5000E+000.9111E+021.
A3 15A4 15                    30.5000E+000.5000E+000.9111E+021.
```

```
A4 15A5 15                    30.5000E+000.5000E+000.9111E+021.
A5 15A6 15                    30.5000E+000.5000E+000.9111E+021.
A6 15A7 15                    30.5000E+000.5000E+000.9111E+021.
A7 15A8 15                    30.5000E+000.5000E+000.9111E+021.
A8 15A9 15                    30.5000E+000.5000E+000.9111E+021.
A9 15AA 15                    30.5000E+000.5000E+000.9111E+021.
AA 15AB 15                    30.5000E+000.5000E+000.9111E+021.
AB 15AC 15                    30.5000E+000.5000E+000.9111E+021.
AC 15AD 15                    30.5000E+000.5000E+000.9111E+021.
AD 15AE 15                    30.5000E+000.5000E+000.9111E+021.
AE 15AF 15                    30.5000E+000.5000E+000.9111E+021.
AF 15AG 15                    30.5000E+000.5000E+000.9111E+021.
AG 15AH 15                    30.5000E+000.5000E+000.9111E+021.
AH 15AI 15                    30.5000E+000.5000E+000.9111E+021.
AI 15AJ 15                    30.5000E+000.5000E+000.9111E+021.
AJ 15AK 15                    30.5000E+000.5000E+000.9111E+021.
A1 16A2 16                    30.5000E+000.5000E+000.9739E+021.
A2 16A3 16                    30.5000E+000.5000E+000.9739E+021.
A3 16A4 16                    30.5000E+000.5000E+000.9739E+021.
A4 16A5 16                    30.5000E+000.5000E+000.9739E+021.
A5 16A6 16                    30.5000E+000.5000E+000.9739E+021.
A6 16A7 16                    30.5000E+000.5000E+000.9739E+021.
A7 16A8 16                    30.5000E+000.5000E+000.9739E+021.
A8 16A9 16                    30.5000E+000.5000E+000.9739E+021.
A9 16AA 16                    30.5000E+000.5000E+000.9739E+021.
AA 16AB 16                    30.5000E+000.5000E+000.9739E+021.
AB 16AC 16                    30.5000E+000.5000E+000.9739E+021.
AC 16AD 16                    30.5000E+000.5000E+000.9739E+021.
AD 16AE 16                    30.5000E+000.5000E+000.9739E+021.
AE 16AF 16                    30.5000E+000.5000E+000.9739E+021.
AF 16AG 16                    30.5000E+000.5000E+000.9739E+021.
AG 16AH 16                    30.5000E+000.5000E+000.9739E+021.
AH 16AI 16                    30.5000E+000.5000E+000.9739E+021.
AI 16AJ 16                    30.5000E+000.5000E+000.9739E+021.
AJ 16AK 16                    30.5000E+000.5000E+000.9739E+021.
A1 17A2 17                    30.5000E+000.5000E+000.1037E+031.
A2 17A3 17                    30.5000E+000.5000E+000.1037E+031.
A3 17A4 17                    30.5000E+000.5000E+000.1037E+031.
A4 17A5 17                    30.5000E+000.5000E+000.1037E+031.
A5 17A6 17                    30.5000E+000.5000E+000.1037E+031.
A6 17A7 17                    30.5000E+000.5000E+000.1037E+031.
A7 17A8 17                    30.5000E+000.5000E+000.1037E+031.
A8 17A9 17                    30.5000E+000.5000E+000.1037E+031.
A9 17AA 17                    30.5000E+000.5000E+000.1037E+031.
AA 17AB 17                    30.5000E+000.5000E+000.1037E+031.
AB 17AC 17                    30.5000E+000.5000E+000.1037E+031.
AC 17AD 17                    30.5000E+000.5000E+000.1037E+031.
```

```
AD 17AE 17                    30.5000E+000.5000E+000.1037E+031.
AE 17AF 17                    30.5000E+000.5000E+000.1037E+031.
AF 17AG 17                    30.5000E+000.5000E+000.1037E+031.
AG 17AH 17                    30.5000E+000.5000E+000.1037E+031.
AH 17AI 17                    30.5000E+000.5000E+000.1037E+031.
AI 17AJ 17                    30.5000E+000.5000E+000.1037E+031.
AJ 17AK 17                    30.5000E+000.5000E+000.1037E+031.
A1 18A2 18                    30.5000E+000.5000E+000.1100E+031.
A2 18A3 18                    30.5000E+000.5000E+000.1100E+031.
A3 18A4 18                    30.5000E+000.5000E+000.1100E+031.
A4 18A5 18                    30.5000E+000.5000E+000.1100E+031.
A5 18A6 18                    30.5000E+000.5000E+000.1100E+031.
A6 18A7 18                    30.5000E+000.5000E+000.1100E+031.
A7 18A8 18                    30.5000E+000.5000E+000.1100E+031.
A8 18A9 18                    30.5000E+000.5000E+000.1100E+031.
A9 18AA 18                    30.5000E+000.5000E+000.1100E+031.
AA 18AB 18                    30.5000E+000.5000E+000.1100E+031.
AB 18AC 18                    30.5000E+000.5000E+000.1100E+031.
AC 18AD 18                    30.5000E+000.5000E+000.1100E+031.
AD 18AE 18                    30.5000E+000.5000E+000.1100E+031.
AE 18AF 18                    30.5000E+000.5000E+000.1100E+031.
AF 18AG 18                    30.5000E+000.5000E+000.1100E+031.
AG 18AH 18                    30.5000E+000.5000E+000.1100E+031.
AH 18AI 18                    30.5000E+000.5000E+000.1100E+031.
AI 18AJ 18                    30.5000E+000.5000E+000.1100E+031.
AJ 18AK 18                    30.5000E+000.5000E+000.1100E+031.
A1 19A2 19                    30.5000E+000.5000E+000.1162E+031.
A2 19A3 19                    30.5000E+000.5000E+000.1162E+031.
A3 19A4 19                    30.5000E+000.5000E+000.1162E+031.
A4 19A5 19                    30.5000E+000.5000E+000.1162E+031.
A5 19A6 19                    30.5000E+000.5000E+000.1162E+031.
A6 19A7 19                    30.5000E+000.5000E+000.1162E+031.
A7 19A8 19                    30.5000E+000.5000E+000.1162E+031.
A8 19A9 19                    30.5000E+000.5000E+000.1162E+031.
A9 19AA 19                    30.5000E+000.5000E+000.1162E+031.
AA 19AB 19                    30.5000E+000.5000E+000.1162E+031.
AB 19AC 19                    30.5000E+000.5000E+000.1162E+031.
AC 19AD 19                    30.5000E+000.5000E+000.1162E+031.
AD 19AE 19                    30.5000E+000.5000E+000.1162E+031.
AE 19AF 19                    30.5000E+000.5000E+000.1162E+031.
AF 19AG 19                    30.5000E+000.5000E+000.1162E+031.
AG 19AH 19                    30.5000E+000.5000E+000.1162E+031.
AH 19AI 19                    30.5000E+000.5000E+000.1162E+031.
AI 19AJ 19                    30.5000E+000.5000E+000.1162E+031.
AJ 19AK 19                    30.5000E+000.5000E+000.1162E+031.
A1 20A2 20                    30.5000E+000.5000E+000.1225E+031.
A2 20A3 20                    30.5000E+000.5000E+000.1225E+031.
```

```
A3 20A4 20                    30.5000E+000.5000E+000.1225E+031.
A4 20A5 20                    30.5000E+000.5000E+000.1225E+031.
A5 20A6 20                    30.5000E+000.5000E+000.1225E+031.
A6 20A7 20                    30.5000E+000.5000E+000.1225E+031.
A7 20A8 20                    30.5000E+000.5000E+000.1225E+031.
A8 20A9 20                    30.5000E+000.5000E+000.1225E+031.
A9 20AA 20                    30.5000E+000.5000E+000.1225E+031.
AA 20AB 20                    30.5000E+000.5000E+000.1225E+031.
AB 20AC 20                    30.5000E+000.5000E+000.1225E+031.
AC 20AD 20                    30.5000E+000.5000E+000.1225E+031.
AD 20AE 20                    30.5000E+000.5000E+000.1225E+031.
AE 20AF 20                    30.5000E+000.5000E+000.1225E+031.
AF 20AG 20                    30.5000E+000.5000E+000.1225E+031.
AG 20AH 20                    30.5000E+000.5000E+000.1225E+031.
AH 20AI 20                    30.5000E+000.5000E+000.1225E+031.
AI 20AJ 20                    30.5000E+000.5000E+000.1225E+031.
AJ 20AK 20                    30.5000E+000.5000E+000.1225E+031.

GENER----1----*----2----*----3----*----4----*----5----*----6----*----7----*----8'

INCON----1----*----2----*----3----*----4----*----5----*----6----*----7----*----8'
A2 0100018000013.000000000E-01
1.01325000000000E+055.00000000000000E-024.80000000000000E-021.00000000000000E+01
A3 0100018000013.000000000E-01
1.01325000000000E+055.00000000000000E-024.80000000000000E-021.00000000000000E+01
A4 0100018000013.000000000E-01
1.01325000000000E+055.00000000000000E-024.80000000000000E-021.00000000000000E+01
A5 0100018000013.000000000E-01
1.01325000000000E+055.00000000000000E-024.80000000000000E-021.00000000000000E+01
A6 0100018000013.000000000E-01
1.01325000000000E+055.00000000000000E-024.80000000000000E-021.00000000000000E+01
A7 0100018000013.000000000E-01
1.01325000000000E+055.00000000000000E-024.80000000000000E-021.00000000000000E+01
A8 0100018000013.000000000E-01
1.01325000000000E+055.00000000000000E-024.80000000000000E-021.00000000000000E+01
A9 0100018000013.000000000E-01
1.01325000000000E+055.00000000000000E-024.80000000000000E-021.00000000000000E+01
AA 0100018000013.000000000E-01
1.01325000000000E+055.00000000000000E-024.80000000000000E-021.00000000000000E+01
AB 0100018000013.000000000E-01
1.01325000000000E+055.00000000000000E-024.80000000000000E-021.00000000000000E+01
AC 0100018000013.000000000E-01
1.01325000000000E+055.00000000000000E-024.80000000000000E-021.00000000000000E+01
AD 0100018000013.000000000E-01
1.01325000000000E+055.00000000000000E-024.80000000000000E-021.00000000000000E+01
AE 0100018000013.000000000E-01
1.01325000000000E+055.00000000000000E-024.80000000000000E-021.00000000000000E+01
```

```
AF 0100018000013.000000000E-01
1.01325000000000E+055.00000000000000E-024.80000000000000E-021.00000000000000E+01
AG 0100018000013.000000000E-01
1.01325000000000E+055.00000000000000E-024.80000000000000E-021.00000000000000E+01
AH 0100018000013.000000000E-01
1.01325000000000E+055.00000000000000E-024.80000000000000E-021.00000000000000E+01
AI 0100018000013.000000000E-01
1.01325000000000E+055.00000000000000E-024.80000000000000E-021.00000000000000E+01
AJ 0100018000013.000000000E-01
1.01325000000000E+055.00000000000000E-024.80000000000000E-021.00000000000000E+01

START
ENDCY
```

Intentionally Left Blank

APPENDIX C: Description of the prototype SEAtrace™ inversion code design

The code was written in C++ using the Borland C++ compiler, version 4.5. The code uses standard C++ constructs so that it can be used on any state-of-the art C++ compiler.

The code consists of two modules: barrier.cpp and leak.cpp. The driver code is barrier.cpp, while leak.cpp is the implementation code for a class called Leak. The specification for LEAK is contained in the header file leak.h.

The class Leak has four public member functions: Leak, Search, Erfc, and ~Leak. Leak is the default constructor for the class. Search is the calculational engine that implements the algorithm developed by Walsh. Erfc is a function that calculates the complementary error function to within a fractional error of less than 1.2×10^{-7} using a Chebyshev polynomial fit. [Press, Numerical Recipes] Erfc is called by Search. ~Leak is the class destructor which cleans up the heap; this is necessary because the code uses dynamic allocation of arrays.

The class Leak has one private data member, data, of type BarrierData. BarrierData is a structure with the following public data members:

- numberMonitors — the number of monitors
- measTimes — the maximum number of measurement times for any of the monitors
- error — a pointer to a dynamically allocated single dimensional array that contains the fractional errors for each monitor
- xLocation — a pointer to a dynamically allocated single dimension array that contains the 'x' locations of the monitors
- yLocation — a pointer to a dynamically allocated single dimension array that contains the 'y' locations of the monitors
- zLocation — a pointer to a dynamically allocated single dimension array that contains the 'z' locations of the monitors
- time — a pointer to a dynamically allocated double dimension array that contains the measurement times for each monitor
- E0 — the search criterion
- p[6] — the array of the six unknown parameter
- limit[6][2] — the array of the upper and lower bounds on the six unknown parameters
- a,b, and y — the values for the y coordinate of the vertical wall specified by $y = ax + b$

A front-end code, barr_dat.cpp was written to create a file of input data for the actual code. The input data file created is barr_dat.dat. With this input file, barrier,cpp performs the calculation and stores the results in an output file barr_p.dat. Also, barrier,cpp creates an output file, debug.dat, that can be used for printing results of calculations with small N values.

Intentionally Left Blank

APPENDIX D: History of the monitoring well array emplacement

The small scale field experiment was located east of the eastern fence of the CWL, by the western fence of the drum disposal pit. An array of nine Geoprobe wells was installed and instrumented in February 1994. Figure D-1 shows a best estimate of sample locations for ports used in this experiment, based on observations made during installation. Dotted lines depict wells that were either abandoned because of their inability to remain open to depth long enough to instrument the well, or because of a drilling problem. Abandoned wells were backfilled with dry Voclay (a bentonite high solids grout).

Two of the wells are multipoint sample wells, 2 inches in diameter. The desired total depth was not reached in either well. The injection well #5 was punched to 23 feet, the drill stem removed and the well tagged to approximately 10 feet. PVC rod was inserted and used to try and break through what was felt to be a bridge at that elevation, with no success. The well was then water filled to the surface. After several minutes the bridge broke and the well was tagged to 19 1/2 feet. The membrane was inserted with a flexible PVC rod (not inverted) to a depth of 18 1/2 feet, leaving six inches of the membrane protruding above ground surface. Dirt was bermed up around the membrane, the basepipe was tied to a stake, and the system was water filled. The second multiport sampling well (#3) suffered similar difficulties. This well was originally punched to 18 1/2 feet, tagged just less than 15 feet, re-punched to 21 feet, and then tagged at 17'2". The membrane length was adjusted (the membrane was cut and rewelded) to this shorter length. However, upon insertion of the system, a depth of only 15 feet could be reached, leaving 21 inches of the system protruding above ground surface. Soil was built up around the membrane, the basepipe was tied to a stake, and the membrane was water filled. Subsequent checks showed that some leakage of water was occurring in this well. Bentonite was added (calculated to fill approximately half of the membrane) to minimize or eliminate the leak. Initially this was thought to be successful (several days showed no change in the water level), then the water level begin to drop again. Further investigation showed a blockage in the membrane very close to ground surface, possibly caused by collapse of the borehole. Initial work performed at the site was completed in April 1994. The well was capped and sat untouched until November 1995. At this time, the water level in the well was unchanged indicating any initial leakage from the membrane had been successfully blocked. The water level in well #5 was low by several feet, indicating a small leak in the membrane. Bentonite was added to the water and the leak was stopped.

The membranes used in both multipoint sampling wells were of typical construction for a SEAMIST™ gas sampling system. The membrane material used was a 4.5-oz/yd^2 urethane-coated polyester, with a lap welded and taped seam construction. Stainless steel elbow fittings were used as ports and 1/8 x 1/16-inch polyethylene sample pressure tubing connects each port to the surface. Additionally, each membrane was fitted with a second port (1/4 x 3/16 PVC tubing to the surface) at the centermost sampling elevation to allow in-situ permeability measurements to be taken.

The remaining seven Geoprobe wells in the experimental array were completed as standard gas sampling wells. They are all 1-inch in diameter having a 6-inch screened sample region at the bottom of the well, with 1/4 x 3/16-inch polyethylene tubing to the surface. The holes were back-filled using standard procedures.

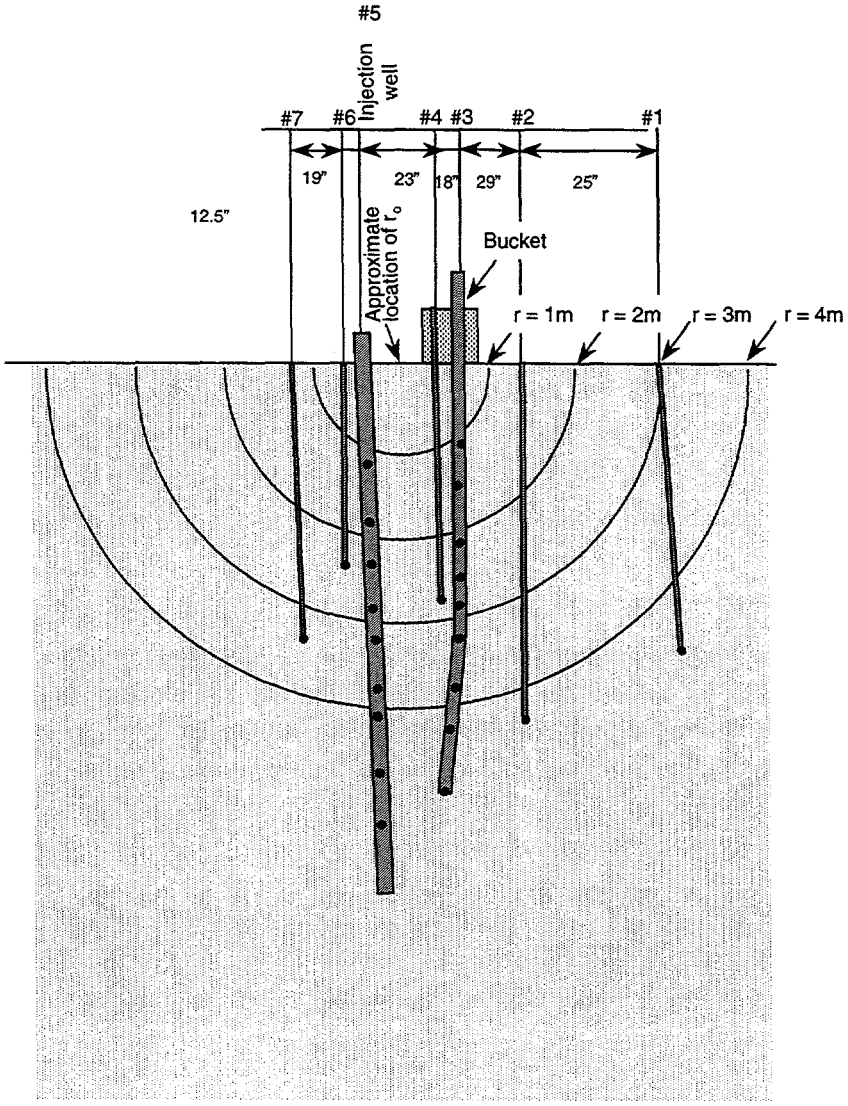

Figure D-1: Estimated locations of Geoprobe wells used in the field tests.

DISTRIBUTION

1 John Heiser
Brookhaven National Laboratory
Bldg. 830
34 North Railroad Ave.
Upton, NY 11973

1 Kevin Kostelnick
Idaho National Engineering &
Environmental Lab
P.O. Box 1625
Idaho Falls, ID 83415-3710

1 Bruce Erdal
Los Alamos National Laboratory
EM-TD, MS J591
Los Alamos, NM 87545

1 Andrea Hart
MSE Technology Applications, Inc.
P.O. Box 4078
Butte, MT 59702

1 Robert Andrews, Ph.D.
National Research Council
Board of Radioactive Waste
Management
2001 Wisconsin Ave., N.W.
Washington, DC 20007

1 J. Espinosa
NM Environment Department
1190 St. Francis Drive
Santa Fe, NM 87503-0968

1 New Mexico Junior College
Lovington Highway
Hobbs, NM 88240

1 New Mexico State Library
325 Don Gaspar
Santa Fe, NM 87503

1 New Mexico Tech
Campus Street
Socorro, NM 87810

1 Tom Early
Oak Ridge National Laboratory
P.O. Box 2008
Oak Ridge, TN 37831-6317

1 Cindy Kendrick
Oak Ridge National Laboratory
P.O. Box 2001, EW-923
Oak Ridge, TN 37831

7 Sandra Dalvit Dunn
Science & Engineering Associates
3205 Richards Lane
Suite A
Santa Fe, NM 87505

1 D. Dresp
Thomas Branigan Library
106 W. Hadley St.
Las Cruces, NM 88003

1 Kim Abott
U.S. Department of Energy
Room 700 N
1301 Clay Street
Oakland, CA 94612-5208

1 Richard Baker
U.S. Department of Energy
9800 South Cass Ave.
Argonne, IL 60439

1 Paul Beam
U.S. Department of Energy
Cloverleaf Building
19901 Germantown Rd.
Germantown, MD 20874-1290

1 Bob Bedick
U.S. Department of Energy
3610 Collins Ferry Rd.
Morgantown, WV 26507-0880

1 Skip Chamberlain
U.S. Department of Energy
Cloverleaf Building
19901 Germantown Rd.
Germantown, MD 20874-1290

1 Douglas Denham
U.S. Department of Energy
P.O. Box 5400
Albuquerque, NM 87185

1 Gillian Eaton
U.S. Department of Energy
Tech Site, Bldg. T124A
P.O. Box 928
Golden, CO 80402-0928

1 John Geiger
U.S. Department of Energy
P.O. Box A
Aiken, SC 29802

1 Dennis Green
U.S. Department of Energy
850 Energy Drive
Idaho Falls, ID 83401-1563

1 Marvin Gross
U.S. Department of Energy
P.O. Box 538704
Cincinnati, OH 45253-8704

1 Gary Huffman
U.S. Department of Energy
Highway 93rd & Cactus St.
Golden, CO 80402

1 Scott McMullin
U.S. Department of Energy
Bldg. 703-46A
P.O. Box A
Aiken, SC 29802

1 Charles Nalezny
U.S. Department of Energy
Cloverleaf Bldg.
19901 Germantown Rd.
Germantown, MD 20874-1290

1 James Paulson
U.S. Department of Energy
9800 South Cass Ave.
Argonne, IL 60439

1 Michael Serrato
U.S. Department of Energy
Environmental Sciences Section
P.O. Box 616 / 773-42A
Aiken, SC 29802

1 Mel Shupe
U.S. Department of Energy
Industrial Park
P.O. Box 3462
Butte, MT 59702

1 Jef Walker
U.S. Department of Energy
Cloverleaf Bldg.
19901 Germantown Rd.
Germantown, MD 20874-1290

1 Bill Wilborn
U.S. Department of Energy
2753 S Highland Rd.
Las Vegas, NV 89109

1 James Wright
U.S. Department of Energy
Bldg. 703-46A
P.O. Box A
Aiken, SC 29803

1 Paul Zielinski
U.S. Department of Energy
Cloverleaf Bldg.
19901 Germantown Rd.
Germantown, MD 20874-1290

1	Arturo Palomares U.S. Environmental Protection Agency 999 18th Street Suite 500 Denver, CO 80202	
1	Government Publications Department University of New Mexico Albuquerque, NM 87131	
1	MS 0701	R.W. Lynch, 6100
5	0706	C.V. Williams, 6113
1	0719	G.C. Allen, 6131
1	0719	J.D. Betsill, 6131
2	0719	T.D. Burford, 6131
2	0719	D.A. Padilla, 6131
1	1132	W. Cox, 6100
1	1132	D. Fate, 6132
1	1147	F. Nimick, 6133
1	9018	Central Technical Files, 8940-2
2	0899	Technical Library, 4916
2	0619	Review & Approval Desk, 12690 for DOE/OSTI